Syracuse University

SURFACE

June 2018

The balance of poly(U) polymerase activity ensures germline identity, survival, and development in Caenorhabditis elegans

Yini Li
Syracuse University

Follow this and additional works at: https://surface.syr.edu/etd

 Part of the Life Sciences Commons

Recommended Citation

Abstract

Uridylation of RNAs has been found to be highly prevalent and conserved among eukaryotes. The untemplated addition of uridines to the 3' end of RNA molecules is catalyzed by poly (U) polymerase (PUP). Uridylation has a fundamental role in RNA decay. The emerging discoveries regarding uridylation emphasize a new layer of gene regulation, and therefore we were curious about the developmental consequences of such gene regulation. Here, we investigated the roles of three *Caenorhabditis elegans* proteins, with in vitro PUP activity, in germline development. PUP-1/CDE-1 and PUP-2 are known to target certain classes of small non-coding RNA, and the function of PUP-3 remains unknown. We examined the developmental phenotypes of *pup* mutants and evaluated the expression of PUP proteins in the germ line. We show that PUP-1 and PUP-2 function together to maintain germline identity and ensure germline survival and development under conditions of stress. PUP-1 and PUP-2 have distinct expression patterns within the germ line and localize to distinct subcellular compartments. In contrast, PUP-3 has a distinct role in germline development. PUP-3 abundance is elevated in the *pup-1/-2* double mutant germline, and the loss of PUP-3 activity largely suppresses the *pup-1/-2* germline phenotype. We propose that germline survival, identity, and development require the correct balance of PUP activity.

The balance of poly(U) polymerase activity ensures germline identity, survival, and

development in *Caenorhabditis elegans*

By

Yini Li

B.S. East China University of Science and Technology, 2012

DISSERTATION

Submitted in partial fulfillment of the requirements for the degree of

Doctor of Philosophy in Biology

Syracuse University

June 2018

Acknowledgement

This thesis would not be possible without the support from many people.

First, I would like to thank my advisor, Eleanor Maine, for being an amazing mentor who teaches me how to think, act, speak and write as an independent scientist. I am extremely grateful for your constant support and encouragement. You are always there whenever I need advice.

I thank all the members of my committee for their valuable suggestions. I would especially like to thank Sarah Hall. Without your constructive suggestions, I would not be able to obtain my *pup-1/-2* double mutant in such an easy way. I would also like to thank Dave Pruyne for his willingness to answer my questions and share reagents.

I want to express my gratitude to the previous and current members of Maine lab for creating a "life-friendly" environment. Special thanks to Bing Yang, Yiqing Guo and Xia Xu. You all motivate me to be a better thinker and researcher.

I thank my dear friends back home for always asking me when to graduate, although it was one of the hardest questions. I thank all the awesome friends I met at SU. Thank you for bringing so much fun into my life. Especially Ying, thank you for being a listener, a cheerleader and an irreplaceable friend.

Finally, my deepest appreciation goes out to my family. Thank mom and dad for your unconditional support. You are the best. You are the ones that make me fearless on my way pursuing my dreams.

Contents

Chapter I. Introduction

1.1 The germ line

The germ line is a lineage of cells that give rise to sperm and oocytes. The germ line is important in development because it is capable of providing the continuity of life and responsible for passing genetic and epigenetic information on to subsequent generations. Cells of the germ line (called "germ cells") are specified as distinct from somatic cells in early development, e.g., as early as early embryogenesis in *Caenorhabditis elegans* (Strome and Updike, 2015). In contrast to somatic cells that normally undergo replicative aging and cell death, germ cells do not undergo the physiological and structural changes associated with replicative aging. In this sense, the germ line is sometimes considered an immortal cell lineage. The immortal feature of the germ line highlights the significance of the studies regarding germline abnormality and relevant disorders. For example, if there is a disease-linked gene mutation in the soma, it does not affect the next generation in most cases (if we disregard the soma-to-germline communication (Devanapally et al., 2015)). On the contrary, mutations that arise in the germ line can be passed onto the next generation. Through forward genetic analysis, defects that break the immortality of the germ line may help identify mechanisms that limit replicative aging *per se.*

We use the nematode, *Caenorhabditis elegans* as a model organism for the study of the germ line due to its many advantages, including: ~40% of *C. elegans* genes encode proteins closely related to human proteins, 50% of the adult *C. elegans* cells are germ cells, and the

species can be genetically manipulated in numerous ways (Pazdernik and Schedl, 2013). Genetic studies using *C. elegans* have identified multiple physiological processes critical for germline maintenance. In the following sub-sections, I will briefly review *C. elegans* germline basics and germline regulation in terms of suppressing somatic gene expression in germ cells and epigenetic regulation during germline development.

1.1.1 The *C. elegans* germline development

C. elegans has two sexes: hermaphrodite (XX) and male (XO). Hermaphrodites contain two U-shaped gonad arms; produce both oocytes and sperm, and can fertilize their own oocytes with their own sperm to create offspring. Males have a J-shaped gonad, produce only sperm, and are rare in nature. Males are generated by spontaneous non-disjunction of the X chromosome during meiosis in the germ line (Hodgkin et al., 1979). In the laboratory, males are propagated by either crossing the spontaneously appearing males with hermaphrodites or by introducing mutations that lead to high incidence of males, such as a *him-8* mutation (Pazdernik and Schedl, 2013). The *him-8* mutation perturbs X chromosome segregation, which leads to increased frequency of X-chromosome non-disjunction in the hermaphrodite germ line (Hodgkin et al., 1979).

Regardless of the sex differences in morphology and gene regulation, the hermaphrodite and male have a generally similar progression of germline development, with nuclei organized in a temporal-spatial gradient controlled by both physical forces between cells and internal signal transduction (Hubbard and Greenstein, 2005). The most distal end is the proliferative zone where germ cell nuclei undergo mitotic divisions and pre-meiotic S-phase. As cells move farther from the distal end, they enter early meiosis and progress through leptotene and zygotene stages.

Leptotene and zygotene are quick developmental stages in the gonad. In leptotene, chromosomes polarize to the side of the nuclus to form a crescent-shaped arrangement. This organization is proposed to bring chromosomes in close vicinity and thereby to facilitate the search between homologous chromosomes (Hirsh et al., 1976). In zygotene stage, synapsis and recombination initiate. Synapsis starts from the pairing center at the end of the chromosome and progresses along the aligned chromosomes in concert with synaptonemal complex (SC) component loading (Hillers et al., 2015). The SC is composed of a group of proteins (REC-8, HIM-3, HTP-3 as axial elements) that localize between sister chromatids and SYP proteins (SYP-1/2/3/4 as central elements) that localize between synapsed homologs. Pachytene is a protracted phase characterized by a nuclear morphology known as "bowl of spaghetti", in which chromosomes re-disperse throughout the nucleus (Lui and Colaiácovo, 2013). Synapsis is completed at early pachytene, which provides the context for the crossover recombination events in mid-pachytene. From late-pachytene to diplotene, the SC disassembles and chromosomes undergo dramatic condensation to form diakinesis bivalents in the hermaphrodite and karyosomes in the male (Lui and Colaiácovo, 2013).

1.1.2. Factors that prevent somatic gene expression in the germ line

P granules are found in the *C. elegans* germline cytoplasm and are essential for germline identity, maintenance, and fertility. P granules are named due to their segregation to the P lineage. Maternally contributed P granules are progressively partitioned from the 1-cell zygote to the P1 cell, P2 cell, P3 cell and P4 cell through four asymmetric cell division (Fig. 1.1). P1, P2, P3 and P4 are the germline blastomeres; P4 is considered to be the primordial germ cell (PGC) that later gives rise to all germ cells (Hubbard and Greenstein, 2005). P granules are

dispersed throughout the zygote and P1 cytoplasm. P granules start to attach to the nuclear periphery in P2. In P4 and its descendants, P granules associate with the nuclear envelope, sitting on nuclear pores (Updike and Strome, 2010). P granules are ribonucleoprotein particles, composed of RNAs and proteins. Vasa DEAD-box helicase proteins, GLH-1/2/3/4 (germline helicase) and RGG domain proteins PGL-1/2/3 (P-granule abnormality), are the constitutive P granule proteins and are commonly used as P granule markers (Kuznicki et al., 2000). PGLs and GLHs show segregation to the germline blastomeres from somatic blastomeres during embryogenesis (Kawasaki et al., 2004). In addition, P granules also contain many other proteins that are associated with small RNA machinery (Updike and Strome, 2010).

Germ cells and somatic cells are two distinct cell types. Somatic cells are mortal as they undergo senescence and death in each generation. In contrast, germ line is an immortal cell lineage, capable of giving rise to each subsequent generation. Maintaining the germ line-soma distinction is important for animal fitness and propagation. Perturbing the germ line-soma distinction in germ cells may lead to sterility or germ cell mortality, while disrupting the distinction in somatic cells may lead to improper cell proliferation and cancer. In order to maintain the germline identity, germ cells adopt multiple robust mechanisms to protect against transformation into somatic cells. In *C. elegans,* there are two general levels of protection – one is at the specification of PGCs and the other is in post-hatching germ lines (Strome and Updike, 2015).

The first level of germ cell fate protection against somatic gene expression is accomplished by transcriptional inhibition and chromatin repression of somatic genes in germline blastomeres during embryogenesis. Four MES (maternal-effect sterility) proteins are involved in this mechanism. Maternal loss of any MES protein leads to PGC death and sterility

in progeny (Bender et al., 2004; Xu et al., 2001). MES-2/3/6 form a complex that is the *C. elegans* homolog of the polycomb repressive complex 2 (PRC2). MES-2 is a homolog of the PRC2 subunit, EZH2, containing a SET domain responsible for histone lysine methyltransferase activity (Strome, 2005). MES-6 is a homolog of the PRC2 subunit, ESC, containing a WD40 domain possibly acting as protein interaction scaffold (Schapira et al., 2017). MES-3 is a novel protein with no recognizable motifs (Xu et al., 2001). The MES-2/3/6 complex generates the repressive histone modification H3K27me2 (Bender et al., 2004; Xu et al., 2001). MES-4 is a nuclear SET domain (NSD) - containing protein that generates active histone modifications, H3K36me2/3 (Furuhashi et al., 2010; Rechtsteiner et al., 2010). Chromatin immunoprecipitation assays revealed the targets of these histone modifiers. In adult germ lines and early embryos, MES-2/3/6-mediated H3K27me2 highly associates with soma-specific genes on autosomes and the X chromosome, whereas MES-4-mediated H3K36 methylation is enriched on germ-line expressed genes primarily located on autosomes (Bender et al., 2004; Fong et al., 2002). Accordingly, an attractive model is that MES proteins ensure the inheritance of germline memory from parental germ line to early embryos by promoting germline gene expression and suppressing somatic gene interference (Gaydos et al., 2012; Gaydos et al., 2014).

In PGCs, transcription is prohibited by inhibition of CDK9 (cyclin-dependent kinase 9), a positive transcription elongation factor (Sano et al., 2004). CDK9 phosphorylates serine 2 of the RNA polymerase II C-terminal domain (CTD) to activate transcription elongation (Sano et al., 2004). *C. elegans* PIE-1 (pharynx intestine in excess 1) protein is expressed in oocytes and 1-cell stage embryos and partitions into germline blastomeres. PIE-1 prevents CDK9 from interacting with RNA Pol II via a competitive CTD-like domain (Zhang et al., 2003). Loss of maternally-provided PIE-1acitivity causes P3 to adopt a somatic MS-like cell fate (Mello et al.,

1992). MEX-1 has been found to be required for partitioning PIE-1 to germline blastomeres. Loss of MEX-1 results in a reduced level of PIE-1 in germline blastomeres and mislocalization of PIE-1 to E and MS blastomeres. Consequently, loss of MEX-1 activity leads P3 to adopt a somatic MS-like cell fate (Guedes and Priess, 1997). PIE-1 is degraded upon division of P4 to form Z2 and Z3 (Mello et al., 1996). At that point, a chromatin-based mechanism succeeds PIE-1 repression. As observed, active histone modifications H3K4 methylation and H4K8 acetylation are globally lost coincident with more condensed DNA in Z2 and Z3 (Schaner et al., 2003). NANOS (NOS-1/-2), homologous to *Drosophila* Nanos which is required for embryonic patterning and PGC development, activity is required to maintain this unique chromatin architecture in the germline (Schaner et al., 2003).

The second level of protecting germ cell fate occurs post hatching. Several studies have shown that germline identity in the adult is maintained through chromatin modulators and RNA regulators. Loss of P granules, ectopic expression of P granule components, presence of cells with somatic morphology, and/or detection of somatic gene expression in the germ line is observed in strains with perturbed chromatin state or RNA regulation in the germ line. Examples include: MES-2/3/6 complex mutants, where H3K27me2/3 is removed (Tursun et al., 2011); mutations that influence MES-2/3/6 activity, such as mutants of histone chaperone protein LIN-53 (abnormal cell lineage) and MES-4 (Patel et al., 2012); and mutations that impact H3K4 methylation, such as simultaneous loss of two chromatin factors, SPR-5 (suppressor of presenilin defect) and LET-418 (lethal) (Käser-Pébernard et al., 2014) or SET-2 and its cofactor WDR-5.1 (Robert et al., 2014). In addition, RNA regulators, e.g., the germline-specific Argonaute HRDE-1 and RNA-binding translational regulators MEX-3 and GLD-1, are required for maintaining germ cell identity. PGLs were used as marker proteins to define cells with germline fate in all of
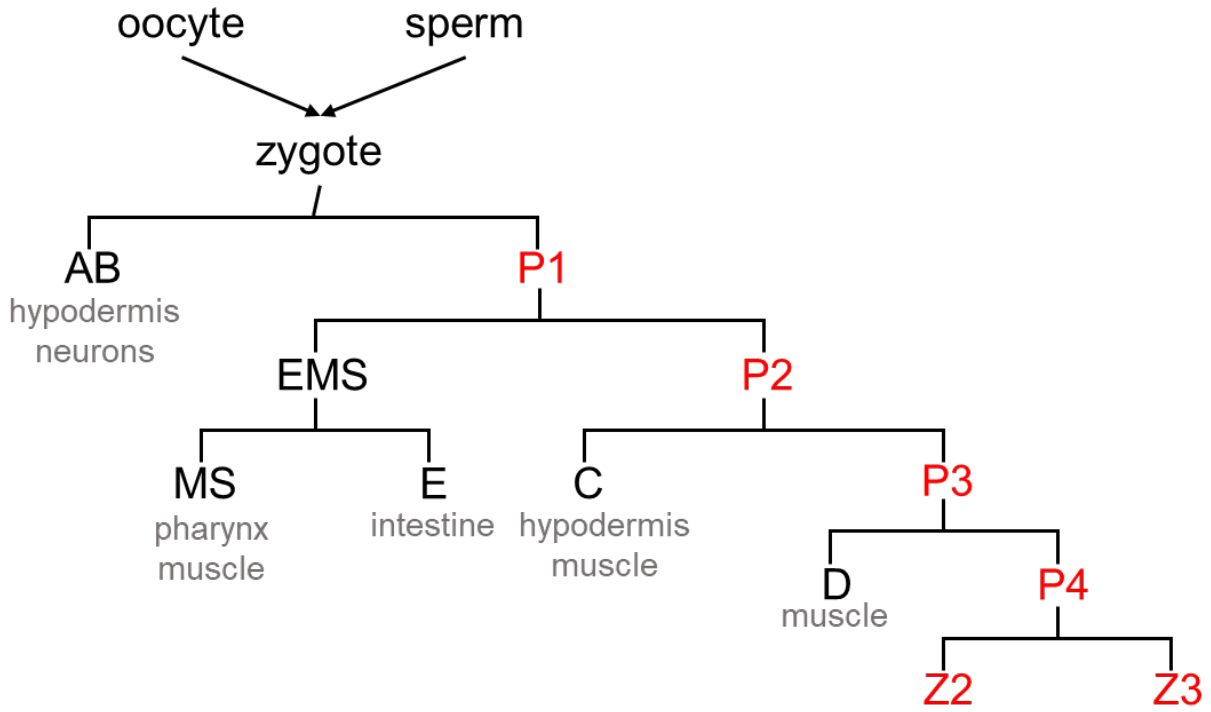
Figure 1.1 Early blastomere fates. Oocytes and sperm fuse and initiate embryonic development. The lineal relationships and names of embryonic blastomeres are shown. Germ lineage is depicted in red.

these studies. Somatic transformation in those mutants is linked with abnormal P granule distribution or expression (Ciosk et al., 2006; Robert et al., 2014). A study by Updike et al (2014) reports that germ cells depleted of P-granule factors express pan-neuronal genes and appear to have neurite-like projections (Updike et al., 2014). The study emphasizes a correlation between P granules and germline fate protection.

1.1.3. Epigenetic regulation in germ lines

Epigenetic regulation is important for germline development. There are three types of epigenetic regulation: histone modification, small RNA regulation and DNA methylation. In *C. elegans,* no canonical DNA methylation is observed; instead, *C. elegans* utilizes histone modifications and small RNA regulation to moderate gene transcription and chromatin state. Here, I concentrate on histone modifications (see small RNA section for small RNA regulation).

The DNA is wrapped around histone octamers to form a nucleosome. Each nucleosomal unit is composed of a pair of each core histone, H2A, H2B, H3 and H4, with ~145 bp of DNA wound around it (Lawrence et al., 2016). Rather than simply "gluing" DNA together as chromosomes, histones carry many post-transcriptional modifications on their N-terminal "tails," and these modifications can influence chromatin compaction and transcription factor accessibility (ALLFREY et al., 1964). Some of the modifications on these tails have been shown to reduce chromatin compaction and promote transcription, e.g., H3K4 methylation, H3K36me2/3 and H3K9 acetylation. Some of the modifications have been found to compact chromatin and/or repress transcription, e.g., H3K27 methylation and H3K9 methylation.

In the zygote, chromosomes from sperm and oocyte, respectively, arrive with different epigenetic states that reflect their different developmental histories. The epigenetic pattern of maternal and paternal chromosomes is reprogrammed in the zygote to ensure the correct initiation of embryonic gene expression (Morgan et al., 2005). In all stages before the division of P4 cell into Z2/Z3 cells, chromatin regulation is similar in germline blastomeres and their somatic neighbors (Schaner et al., 2003). After formation of the Z2/Z3, chromatin regulation starts to differentiate between germ lineage and somatic lineages (Schaner and Kelly, 2006). Transcriptional repression mechanisms, including loss of active histone marks, H4K8 acetylation/H4K4 methylation, and slight enhancement of repressive histone marks, H3K27 methylation, are engaged upon the birth of Z2/Z3 cells (Van Wynsberghe and Maine, 2013). In contrast, epigenetic regulation stays relative the same in somatic blastomeres (Schaner and Kelly, 2006). After completion of embryogenesis, germline transcription is active from L1, coinciding with germ cell expansion (Van Wynsberghe and Maine, 2013). In contrast, transcription is active in somatic lineages as early as the eight-cell stage of embryogenesis (Wang et al., 2011).

In the adult germ line, histone modification is observed during different stages of meiosis when assayed via indirect immunofluorescence; moreover, X chromosome regulation is different from autosome regulation. On autosomes, active histone marks, H3K4 methylation and H3K9 acetylation, are detected at high abundance in both males and hermaphrodites beginning in mitosis and extending through sperm/oocyte development (Bean et al., 2004; Kelly et al., 2002). Correspondingly, repressive histone marks H3K27me3/H3K9me2 are present at fairly low levels on autosomes throughout these stages (Bean et al., 2004; Kelly et al., 2002). The X chromosome, in contrast, associates with low active histone marks (e.g., H3K4 methylation and H3K9 acetylation) and high repressive histone marks (e.g., H3K27me3) throughout meiotic

stages (Bean et al., 2004; Kelly et al., 2002). Consistent with the repression-biased histone modifications, activated (serine 2-phosphorylated) RNA polymerase II is also largely absent from the X chromosome (Van Wynsberghe and Maine, 2013). Overall, these observations imply a global inactivation of genes on the X chromosome (Bean et al., 2004). The histone modification data demonstrating active autosomes and an inactive X chromosome are consistent with the gene expression data which revealed that germline genes are enriched on autosomes while absent on the X chromosome (Reinke et al., 2004; Reinke et al., 2000).

Of note, X chromosome regulation is not identical in the hermaphrodite versus male. The adult male germ line accumulates high H3K9me2 signal on the X chromosome during pachytene, as detected via immunofluorescence imaging, and this modification is observed until the beginning of spermatogenesis; however, the hermaphrodite does not exhibit such enrichment on the X chromosomes (Van Wynsberghe and Maine, 2013). Studies have indicated that such enrichment of H3K9me2 on the male X chromosome is probably due to it entering meiosis without a pairing partner, rather than sex-specific or X chromosome-specific mechanisms: disruption of X chromosome pairing in the hermaphrodite and introduction of unpaired autosomal fragments are also enriched with H3K9me2 in pachytene nuclei (Bean et al., 2004; Kelly et al., 2002; Maine et al., 2005; Strome et al., 2014). One hypothesis proposed by McKee and Handel is that such silencing of the X chromosome and the structural condensation of the X chromosome via chromatin regulation are likely to prevent loss of a single chromosome lacking a pairing partner, as in XO males (McKee and Handel, 1993).

1.2 Small RNA networks

Around 60 years ago, Alexander Rich, an origin-of-life researcher, proposed the RNA world hypothesis, attempting to provide an adequate answer to how life got started. The RNA world described a hypothetical stage approximately 4 billion years ago when RNA was the first genetic material and catalyst for the emergence of the modern cellular system that is composed of DNA and proteins (Alberts B, 2002). We still have no clue today about whether this theoretical world was ever bona fide present, but a myriad of findings from RNA biologists suggest the presence of an "RNA world" inside cells across organisms. An army of small RNAs that are less than 100nt in length, but with distinct duties, are found to be the key players in this "RNA world". Small RNAs regulate both mRNAs (translation) and chromatin (transcription), which thereby form an elaborate surveillance net within our cells against foreign genetic materials, transposons, and aberrant transcripts and meanwhile protect and control the expression of endogenous genes (Cech and Steitz, 2014).

The use of the term "small RNAs" varies widely. The "small RNAs" I refer to here are those eukaryotic Argonaute-associated RNAs that are limited to 20-30nt long. It should be noted, however, that bacterial small RNAs, transfer RNAs (tRNA) and small nucleolar RNA (snoRNA) are also cited as small RNAs sometimes (Cech and Steitz, 2014). Based on the Argonaute proteins they associate with, three classes of endogenous small RNAs are currently studied in depth. They are endogenous small interfering RNAs (endo-siRNAs), microRNAs (miRNAs) and Piwi-interacting RNAs (piRNAs). In the following sub-sections, I attempt to summarize our current knowledge of each class of small RNAs from the aspects of their biogenesis, interacting pathways, and putative functions.

1.2.1 Small interfering RNAs

siRNAs are single-stranded RNAs about 21-26nt in length. *C. elegans* is currently found

to possess two species of siRNAs that are 26G siRNAs and 22G siRNAs, respectively. 26G

siRNAs are considered to be the primary siRNAs which are 26nt in length, a guanosine at the

first nucleotide position of 5'end, and generated by Dicer from double-stranded RNAs (dsRNAs)

(Billi et al., 2014). As a product of Dicer processing, 26G RNAs possess a 5' monophosphate

signature. In contrast, 22G siRNAs are considered to be the secondary siRNAs which are 22nt in

length, a 5' guanosine bias, and generated independently from Dicer by RNA-dependent RNA

polymerases (RdRPs); their production relies on 26G siRNAs (Billi et al., 2014). Depletion of

26G siRNAs or the components important for 26G siRNA biogenesis leads to the loss of the

corresponding 22G siRNAs (Billi et al., 2014). As products of RNA polymerases, 22G siRNAs

are triphosphorylated at the 5' terminus.

26G siRNAs were early considered to be germline-specific, as northern blot data shows

absence of 26G siRNAs in germline-depleted mutants (Han et al., 2009). However, a later study

revealed an appreciable number of 26G siRNAs are synthesized in soma (Gent et al., 2010).

Within the 26G siRNA species, there are two subclasses based on the Argonaute they associate

with later. One is ERGO-1-associated 26G siRNAs, and the other subclass is ALG-3/-4 -

associated 26G siRNAs (Conine et al., 2010; Conine et al., 2013; Vasale et al., 2010). Curiously,

the two subclasses of 26G RNAs exhibit distinct expression patterns and mutually exclusive

targeting preferences. In contrast, 22G siRNAs are more diversely expressed in that 22G

siRNAs are detected in both soma and germ line (Gu et al., 2009). There are also two subclasss

of 22G siRNAs based on their associated Argonautes. One is CSR-1-associated 22G siRNAs,

and the other is WAGO-associated 22G siRNAs (Claycomb et al., 2009; Duchaine et al., 2006).

1.2.1.1 ERGO-1-associated 26G siRNAs

ERGO-1-associated 26G siRNAs are highly enriched in oocytes and embryos (Fig. 1.2). The ERGO-1 26G siRNAs are antisense, perfectly complementary to their targets. By mapping to the genome, it was revealed that ERGO-1 26G siRNAs, though generated in oogenesis, do not target germline-expressed genes (Han et al., 2009). Instead, among ~180 loci that are intensively targeted by ERGO-1 siRNAs, half are coding genes and half are unannotated clusters on the genome; many of the target loci appear to be homologous or tandem repeats, duplicated genes and pseudogenes (Vasale et al., 2010). Therefore, a hypothetical role for ERGO-1 is to buffer against deleterious consequences arising from expression of the noncoding sequences which are recently duplicated or acquired (Fischer et al., 2011; Vasale et al., 2010).

The essential proteins required for the biogenesis and maturation of ERGO-1-associated 26G siRNAs are DCR-1 (Dicer), RRF-3 (RNA-dependent RNA polymerase, RdRp), ERI-1 (exonuclease), RDE-4 (RNA-binding protein), DRH-3 (Dicer-related DExD/H box helicase), ERI-3 (unknown), ERI-5 (Tudor-domain protein), HENN-1 (RNA 3'end methyltransferase), and ERGO-1 (Argonaute). They are considered to be essential components due to the fact that their mutations can directly cause the loss of some or all ERGO-1-class 26G siRNAs (Billi et al., 2014; Duchaine et al., 2006; Gu et al., 2009; Han et al., 2009; Pavelec et al., 2009; Vasale et al., 2010). According to current findings, it is considered that ERI-3/5 tether all the essential components (except ERI-6/7) together to form a complex (Pavelec et al., 2009). Within the complex, RRF-3 synthesizes antisense strand with its RdRP activity, RDE-4 binds to the synthesized double-stranded RNAs with its high affinity to dsRNAs, DRH-3 as a distantly related ortholog of DCR-1 couples with DCR-1 to calibrate the lengths of target RNA duplexes, DCR-1 cleaves long dsRNAs to 26nt (sometimes 27nt) duplexes with its RNase III nuclease

activity, and ERGO-1 assists the maturation of RNA duplexes to become 26G siRNAs and guide their targeting (Billi et al., 2014; Duchaine et al., 2006; Gu et al., 2009; Han et al., 2009; Pavelec et al., 2009; Vasale et al., 2010). During the maturation of ERGO-1 associated 26G, a terminal 2'-O-methylation is involved to prevent the siRNAs from degradation possibly via uridylation (Ruby et al., 2006). HENN-1 has been found to be required for methylation of this particular subclass of siRNAs and the recruitment of HENN-1 seems to be dictated by the Argonaute ERGO-1 (Billi et al., 2012; Kamminga et al., 2012). In *henn-1* mutant, 26G siRNAs show significant decrease in abundance and increased 3' uridylation frequency. This suggests that non-methylated 26G siRNAs are more prone to uridylation and less stable (Kamminga et al., 2012).

In addition to the essential proteins above, there are multiple factors that play lesser roles in accumulating ERGO-1-associated 26G siRNAs. For example, ERI-6/7 encodes a helicase protein, associating with a special subclass of ERGO-1 26G siRNAs that have a ~19nt passenger strand possibly cleaved via ERI-1 endonucleolytic cleavage (Fischer et al., 2008; Fischer et al., 2011). In addition, a group of mutator proteins, especially MUT-16, are involved in accumulation of ERGO-1-associated 26G siRNAs (Zhang et al., 2011).

In oocytes and embryos

Duplicated genes, noncoding loci

Transcription & splicing

mature mRNA

5'cap

AAAAAAAAAAAA

AAAAAAAAAA

5'cap

RRF-3
+ERI complex

AAAAAAAAAA

ERGO-1-associated 26G siRNA

5' G ERGO-1 3'
2-O-me

Serves as primers
to propagate 22G siRNAs ?

5'cap

RRF-1
EGO-1
+DRH-3 & EKL-1

AAAAAAAAAA

A subset

A subset

WAGO-associated 22G siRNA

5' G HRDE 3'

WAGO-associated 22G siRNA

5' G WAGO-1 3'

5'cap
3' WAGO-1
G 5'

AAAAAAAAAA

Shuttle outside P granules

Degradadation of target mRNAs

15

Figure 1.2 ERGO-1-associated siRNA pathway. ERGO-1-associated 26G siRNAs are enriched in oocytes and embryos. The templates for ERGO-1-associated 26G siRNAs are duplicated genes and non-coding loci. The ERI complex containing RRF-3 (RdRp) generates 26G siRNAs (dark green line). These 26G siRNAs load onto Argonaute ERGO-1. ERGO-1-associated 26G siRNAs are modified with 2-O-methylation. ERGO-1-associated 26G siRNAs are required for the propagation 22G siRNAs (light green line), maybe acting as primers for 22G siRNA biogenesis. The generation of 22G siRNAs requires EGO-1 and RRF-1 (RdRps) and co-factors (e.g., DRH-3 and EKL-1). A subset of these 22G siRNAs associate with cytoplasmic WAGO-1 Argonaute and target mRNAs for degradation. Another subset of these 22G siRNAs associate with nuclear HRDE RNAi pathway and trigger deposition of repressive H3K9me3 marks to the corresponding genomic loci.

1.2.1.2 ALG-3/-4-associated 26G siRNAs

ALG-3/-4-associated 26G siRNAs are present in spermatogenesis cells while absent from mature sperm, and their expression occurs in a relatively narrow window during development when spermatogenesis happens (Han et al., 2009) (Fig. 1.3). The ALG-3/-4- associated 26G siRNAs are antisense to spermatogenesis-enriched transcripts (Conine et al., 2010; Gent et al., 2009). Data from deep sequencing and phenotypic analysis of *alg-3/-4* mutant suggest that ALG-3/-4- associated 26G siRNAs are required for robust spermatogenic gene expression during spermatogenesis, especially indirectly influencing the transformation of spermatids into polarized motile spermatozoa (Conine et al., 2013).

The essential proteins required for the biogenesis and maturation of ALG-3/-4-associated 26G siRNAs are mostly the same as for ERGO-1-associated 26G siRNAs. However, many of the accessory factors are not found to be required for ALG-3/-4-associated 26G siRNA accumulation (Billi et al., 2014). For example, mutation of ERI-6/7 does not cause decrease of ALG-3/-4-associated 26G siRNA level. Similar observations were made with mutations of most *Mutator* proteins (Fischer et al., 2011). Only loss of *mut-7* leads to a modest decrease of ALG-3/-4-associated 26G siRNAs (Fischer et al., 2011). In addition, distinct from ERGO-1-associated 26G siRNAs, ALG-3/-4-associated 26G siRNAs are not protected with 2'-O-methylation (Billi et al., 2012; Kamminga et al., 2012). The mechanism and advantage of such differential 26G siRNA methylation are still unclear. However, a favorable explanation so far is that methylation of ERGO-1 associated 26G siRNAs may ensure robust inheritance and perdurance of those siRNAs in the ooctyes and zygotes, whereas ALG-3/-4-associated 26G siRNAs are present only for a short period of developmental window and therefore do not need to be maintained for long-term usage (Billi et al., 2012).

In developing sperm

Spermatogenesis genes

Transcription & splicing

mature mRNA

5' cap

AAAAAAAAAAAA

5' cap

RRF-3
+ERI complex

5' cap

AAAAAAAAAA

ALG-3/4-associated 26G siRNA

5' G
ALG-3/4
3'

RRF-1
EGO-1
+DRH-3 & EKL-1

5' cap

AAAAAAAAAA

A majority (85%)

A minority

CSR-1-associated 22G siRNA

5' G
CSR-1
3'

CSR-1-associated 22G siRNA

5' G
CSR-1
UUU 3'

Degradation of CSR-1-associated 22G siRNAs

WAGO-associated 22G siRNA

5' G
WAGO-1
3'

5' cap
3'
WAGO-1
G 5'

AAAAAAAAAA

Shuttle outside P granules

Degradation of target mRNAs

18

Figure 1.3 ALG-3/-4 siRNA pathway. ALG-3/-4-associated 26G siRNAs (dark blue lines) are enriched in developing sperm. The templates for ALG-3/-4-associated 26G siRNAs are mRNAs of spermatogenesis genes. Similar to ERGO-1-associated 26G siRNAs, ERI complex containing RRF-3 generates 26G siRNAs. These 26G siRNAs associate with ALG-3/-4 Argonaute. ALG-3/-4-associated 26G siRNAs are not 2-O-methylation protected. The production of 22G siRNAs (light blue lines) requires RRF-1, EGO-1, DRH-3 and EKL-1. A majority (~85%) of these 22G siRNAs associate with CSR-1 Argonaute. Some of these CSR-1-bound 22G siRNAs are degraded via 3'uridylation-mediated RNA decay machinery. Some of those promote transcription of spermatogenesis genes and form a positive feedback loop with ALG-3/-4 26G siRNA pathway. A minority of these ALG-3/-4 26G-derived 22G siRNAs associate with WAGO-1-mediated silencing pathway.

1.2.1.3 CSR-1-associated 22G siRNAs

CSR-1-associated 22G siRNAs majorly target germline genes, with ~40% of total CSR-1 22G siRNAs having non-template uridine extension (Claycomb et al., 2009). CSR-1-associated 22G siRNAs are antisense to 4191 protein-coding genes (~80% of them are germline-expressed genes), seven families of repetitive elements (~1% of all the CSR-1 siRNA targets) and 23 pseudogene loci (Claycomb et al., 2009). ChIP-qPCR analysis at particular 22G siRNA target loci found that CSR-1 was never enriched at the target loci of another germline-expressed Argonaute, WAGO-1, which implies that CSR-1-associated 22G siRNAs may have distinct territories on chromosomes from WAGO-1(Claycomb et al., 2009).

The essential factors required for the biogenesis and maturation of CSR-1-associated 22G siRNAs in the germ line are EGO-1 (an RNA-directed RNA polymerase, RdRp), DRH-3 (a helicase) and EKL-1 (a Tudor domain protein). In the mutants of *ego-1, drh-3, ekl-1* and *csr-1,* a subset of identified CSR-1-associated 22G siRNAs showed altered abundance. In the germ line, EGO-1, DRH-3, EKL-1 and CSR-1 localize to P granules (Claycomb et al., 2009; Gu et al., 2009; Smardon et al., 2000). However, those proteins are not restricted to the germ line. The absence of a germ line does not lead to complete loss of *ego-1* transcripts (Smardon et al., 2000). Protein blot shows that DRH-3, EKL-1 and CSR-1 can still be detected in a mutant lacking a germ line (Claycomb et al., 2009). These results suggest that the CSR-1 pathway does also have a role in somatic tissues. In support of the somatic function of the CSR-1 pathway, it is found that CSR-1 is required for dauer formation under different stress conditions, especially functioning in sensory neurons (Bharadwaj and Hall, 2017).

As secondary siRNAs, CSR-1 IP-enriched small RNAs were found antisense to 85% of all ALG-3/-4-associated siRNA targets. This finding indicated that CSR-1 and ALG-3/-4 are in the same pathway. In addition, the relationship of CSR-1 and ALG-3/-4 pathways are not linear. Instead, CSR-1 functions with ALG-3/-4 via a small RNA feedback loop (Conine et al., 2010; Conine et al., 2013) (Fig. 1.3). Unlike conventional small RNA pathways, CSR-1-associated 22G siRNAs do not downregulate their targets (Claycomb et al., 2009). In the male germ line, CSR-1-associated 22G siRNAs are found to promote the transcription of genes. Those target genes are not only spermatogenesis-specific genes, but also a repertoire of oogenesis-specific genes (Conine et al., 2010) (Fig. 1.3). In the hermaphrodite germ line, the CSR-1-associated 22G pathway promotes genome-wide sense-oriented RNA polymerase II transcription and is suggested to prevent antisense transcription and ectopic transcription of silent chromatin domains (Cecere et al., 2014). At present, we still lack a clear mechanistic understanding of how CSR-1 regulates transcription. It is known that CSR-1 interacts with nascent transcripts and the RNA Pol II machinery, and both of those interactions depend on 22G RNAs. With respect to the observation of a global increase in antisense RNA Pol II transcription and ectopic transcription in *csr-1* mutants, one explanation is that mutation of *csr-1* may lead to an increased availability of free RNA Pol II, which causes elevated transcriptional events all over the genome, including antisense transcription and ectopic transcription at normally silent domains (Cecere et al., 2014).

The CSR-1-associated 22G siRNA pathway also functions with the piRNA surveillance pathway (Seth et al., 2013; Wedeles et al., 2013). It is demonstrated that CSR-1-associated 22G siRNAs bind to active transgenes (e.g., active allele with GFP tag) and can propagate the activation of an active transgene in *trans*. In addition, the activated status is also found to be transmitted to normally silent transgenes (e.g., silent allele with GFP tag); in this case, a

Germline-expressed coding genes, or self RNAs

Transcription & splicing

mature mRNA

5'cap AAAAAAAAAA

In hermaphrodite germ line

5'cap RRF-1 EGO-1 AAAAAAAAAA

CSR-1-associated 22G siRNA

CSR-1 3' G 5'   CSR-1 3' G 5'   CSR-1 3' G 5' ⊣ PRG-1

CSR-1-associated 22G siRNA

5'cap CSR-1 3' G 5' AAAAAAAAAA

5'cap CSR-1 3' G 5' AAAAAAAAAA

Self protection

22
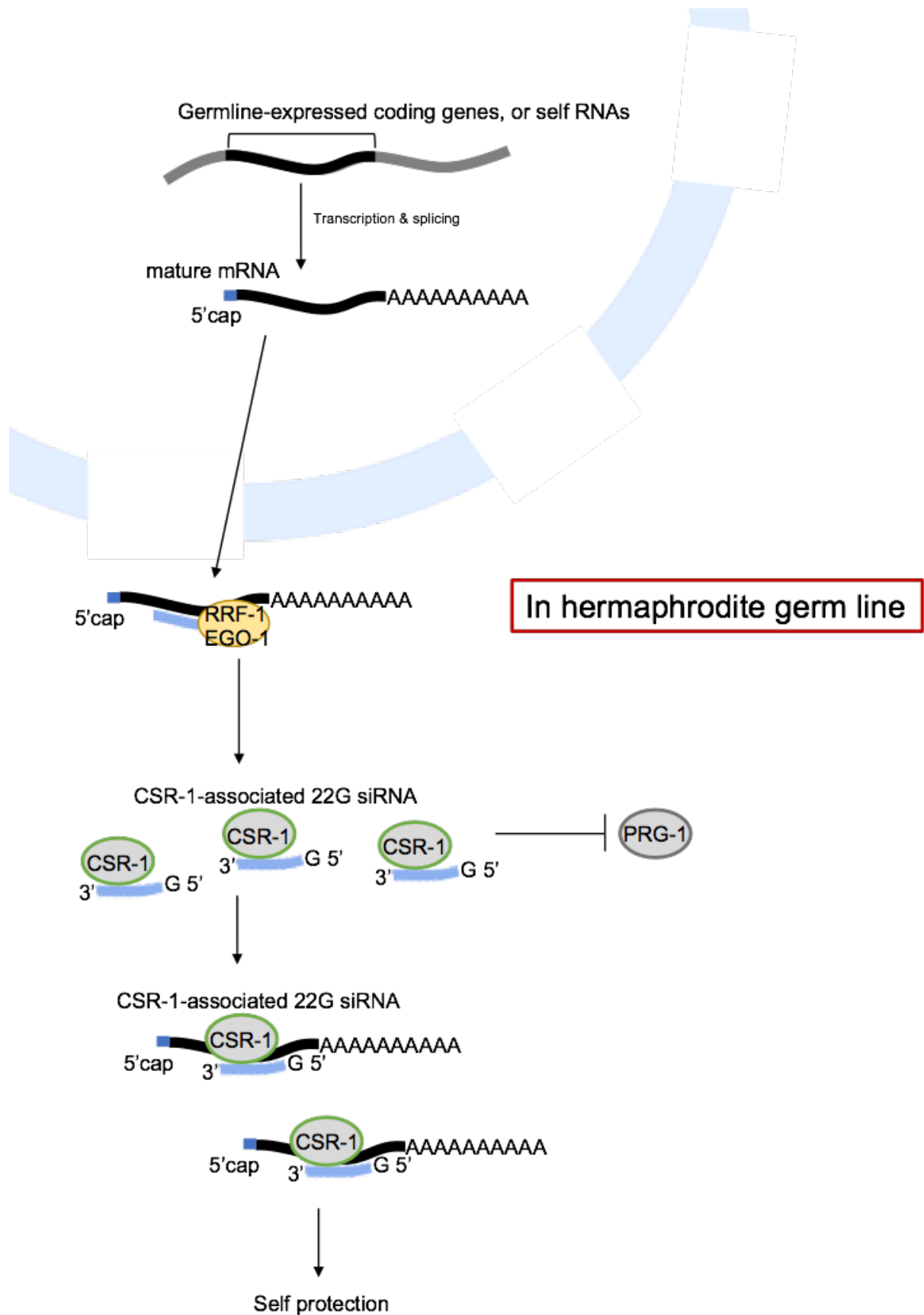
Figure 1.4 CSR-1-associated 22G siRNA pathway. The template for CSR-1-associated 22G

siRNAs are mRNAs of germline-expressed coding genes, or "self" RNAs. CSR-1-associated

22G siRNA pathway functions to license "self" transcripts, and prevent "self" transcripts from

associating with PRG-1 Argonaute.

transgene that is normally silenced will be gradually licensed to express after multigenerational exposure to transactivation from an active transgene (Seth et al., 2013; Wedeles et al., 2013). This phenomenon may occur because the activated transgene starts to produce its own CSR-1-associated 22G siRNAs. However, the activated transgene will be re-silenced eventually via the piRNA silencing mechanism (Seth et al., 2013). These findings raise a notion of a small RNA-regulated surveillance mechanism to identify self *vs.* non-self transcripts, and the CSR-1-associated 22G siRNA pathway is considered to function in licensing of "self" transcripts (Seth et al., 2013) (Fig. 1.4). However, this model has only been tested on transgenes, or partially examined through the Conine et al (2014) study on endogenous ALG-3/-4 targets. Endogenous ALG-3/-4 targets are "self" transcripts and consistently they are found to promote CSR-1-associated 22G siRNA expression.

1.2.1.4 WAGO-associated 22G siRNAs

WAGO refers to a clade of 12 <u>w</u>orm-specific <u>Argo</u>naute proteins. Some WAGOs are imported into the nucleus whereas other WAGOs localize in the cytoplasm. Moreover, some *wago* transcripts are classified as germline-intrinsic, others as oogenesis/spermatogenesis-enriched, and still others as somatic (Billi et al., 2014). WAGO-associated 22G siRNAs target both somatic and germline genes. To date, only WAGO-4-associated 22G siRNAs have been examined with uridine extension (Xu et al., 2018). The production of WAGO-associated 22G siRNAs can be triggered multiple ways including by 26G siRNA pathway, exogenous siRNA pathway, and piRNA pathway activity (Billi et al., 2014). Therefore, depletion of any primary pathway will not cause complete loss of the WAGO-associated 22G siRNAs.

In the germ line, the biogenesis of WAGO-associated and CSR-1-associated 22G siRNAs share several essential factors, such as DRH-3, EKL-1 and EGO-1 (Billi et al., 2014). However, in addition to EGO-1, the biogenesis of WAGO-associated 22G siRNAs collaboratively required another RdRp, RRF-1. RRF-1 and EGO-1 have high sequence similarity and two genes localize adjacent to each other on the genome in an operon (Mangone et al., 2010; Smardon et al., 2000). Germline WAGO-associated 22G siRNAs are amplified by six mutator proteins in a perinuclear mutator focus before loading onto WAGO Argonautes (Billi et al., 2014). It is not surprising to find that 22G siRNAs are three-fold more abundant than 26G siRNAs (Gu et al., 2012a), considering the fact that WAGO-associated siRNAs are generated and amplified by multiple different mechanisms.

Multiple pathways require WAGO-associated 22G siRNAs to effect target silencing. In the male germline, a proportion of ALG-3/-4 26G-derived 22G siRNAs are loaded onto WAGO Argonautes, which leads to post-transcriptional silencing of their target mRNAs (Conine et al., 2013). In oocytes and embryos, ERGO-1-associated 26G siRNAs are hypothesized to serve as a guide for the production of 22G siRNAs via RdRps (i.e., RRF-1 and EGO-1), and these 22G siRNAs are then loaded onto WAGO Argonautes to execute silencing of ERGO-1 targets such as genomic duplications and non-coding sequences (Vasale et al., 2010) (Fig. 1.2). Exogenous RNAi also requires the cytoplasmic WAGO-associated 22G siRNA pathway to mediate post-transcriptional gene silencing for a short term (<4 generations) (Zhang and Ruvkun, 2012). For long-term silencing (>30 generations), two particular WAGO-associated 22G siRNA-mediated nuclear RNAi pathway are required: HRDE pathway and NRDE pathway (Zhang and Ruvkun, 2012). The nuclear RNAi pathways regulate gene silencing at a transcriptional level. In these pathways, both WAGO-9/HRDE-1 and WAGO-12/NRDE-3 are capable of carrying 22G

siRNAs to enter the nucleus where they associate with nascent pre-mRNA targets and recruit

NRDE-2 and a number of chromatin factors, including H3K9me3-binding proteins and several

histone methyltransferases, to deposit the repressive chromatin mark H3K9me3 (Ashe et al.,

2012; Shirayama et al., 2012). In addition, there also is evidence that the nuclear RNAi

machinery mediates inhibition of RNA Pol II during transcription elongation (Guang et al.,

2010). The two Argonautes seem to share silencing mechanisms and factors, but they act in

different tissue types. WAGO-9/HRDE-1 is expressed in germ cells, while WAGO-12/NRDE-3

is expressed in somatic cells (Buckley et al., 2012; Guang et al., 2010; Reinke et al., 2004). In

addition, WAGO-9/HRDE-1 has been found to participate in the piRNA-mediated self vs. non-

self-surveillance machinery (as described in the CSR-1 22G siRNA section; Fig. 1.4). WAGO-

9/HRDE-1 binds to piRNA-derived 22G siRNAs and silences non-self RNAs (e.g., transgenes)

by recruiting H3K9me3 and preventing transcription (Seth et al., 2013; Shirayama et al., 2012;

Wedeles et al., 2013). On the other hand, P granule-localized WAGO-1 has been found to

associate with both piRNA-dependent and -independent surveillance machinery to target

endogenous transcripts such as silence transposons, pseudogenes, aberrant transcripts and many

coding genes (Gu et al., 2009; Lee et al., 2012).

1.2.2. MicroRNAs

        miRNAs are a class of endogenous small RNAs, of ~22nt in length, commonly acting as

guide molecules in post-transcriptional gene silencing via base-pairing with target mRNAs (Kim

et al., 2009). In different organisms, miRNAs lead to different consequential outcomes. In

plants, miRNAs make nearly perfect matches to their target mRNAs and lead to mRNA cleavage

(Carrington and Ambros, 2003). In animals, miRNAs make imperfect matches to their target

26

mRNAs, especially the 3' UTR, and lead to mRNA decay or translational repression. miRNA target specificity relies on a seed sequence located 2-8 nt from the 5' end of each miRNA (Bartel, 2009). In animals, usually each individual miRNA can target hundreds of mRNAs via the seed sequence. Animals contain hundreds of miRNA genes. *C. elegans, Drosophila*, and *Arabidopsis* each have ~150 known miRNA genes, and the human genome contains ~700 known miRNA genes (Ha and Kim, 2014). ~55% of *C. elegans* miRNAs show homology to human miRNAs, indicating a conserved role of miRNAs and miRNA mechanism across species. In addition, miRNAs usually show tissue-specific expression, which makes them candidate targets for therapeutic treatments.

The biogenesis of miRNA begins with the transcription of the primary miRNA (pri-miRNA) by RNA Pol II from a miRNA gene in the nucleus (Bartel, 2009). Pri-miRNAs are several kilobase in length and form a hairpin secondary structure (Bartel, 2009). Next, the pri-miRNA is cleaved by a nuclear RNase III-type protein, Drosha, at the base of the hairpin structure to generate a short haripin structure called precusor-miRNA (pre-miRNA) (Bartel, 2009). This step also requires a cofactor, known as Pasha in *C. elegans* and DGCR8 in humans, to form a microprocessor complex with Drosha. Pasha acts as a molecular ruler to measure the distance from the base of the flanking ssRNA segment to the stem of pri-miRNA and guide Drosha processing (Yeom et al., 2006). The pre-miRNAs are exported to the cytoplasm and further processed by Dicer to release the miRNA duplex of ~22 nt. The strands of the miRNA duplex are unwound from each other by Argonaute. The less-stable passenger strand is then degraded and the guide strand becomes the mature miRNA (Bartel, 2009).

Many factors have been found to regulate different aspects in miRNA biogenesis and processing. A number of regulatory proteins have been described to relate to expression patterns

of miRNAs in pathological conditions. For example, LIN28 physically interacts with *let-7* at pri-miRNA and block further miRNA processing (Lehrbach et al., 2009). Overexpression of LIN28 and reduced level of *let-7* expression occur most frequently in over 20 types of human cancers (Balzeau et al., 2017). In addition, terminal uridyltransferases/poly(U) polymerases act on pre-miRNAs of *let-7* to induce their decay in a LIN28-dependent manner (see the Poly(U) polymerases section) (Newman et al., 2008). RNA editing on the miRNA transcripts via adenosine deaminases acting on RNA (ADARs) and polymorphisms in a miRNA gene have also been found to alter miRNA processing of particular miRNA clusters (Luciano et al., 2004; Slezak-Prochazka et al., 2010).

1.2.3 PIWI-interacting RNAs (piRNAs)

PiRNAs are ssRNAs that are highly enriched in germ lines of different organisms. However, piRNA sequences and biogenesis are diverse among organisms. In *Drosophila* and mice, piRNAs are ~26 to 30 nt long with 5' uracil preference and 3' terminal ribose 2'-O-methylation modification (Siomi et al., 2011). In *C. elegans,* piRNAs are 21nt long but share the same 5' and 3' features, and therefore *C. elegans* piRNAs are also referred as 21U RNAs (Weick and Miska, 2014). According to the findings to date, no conserved factors for piRNA biogenesis, other than the Argonaute PIWI, have been discovered between *C. elegans* and other organisms. In addition, *C. elegans* seems to utilize a unique signal amplification mechanism that involves siRNAs, rather than the ping-pong mechanism in *Drosophila* and mice where solely piRNAs participate in the amplification loop (Weick and Miska, 2014). *C. elegans* has been estimated to contain 12,000-16,000 piRNA genes (Ruby et al., 2006). The vast majority of the piRNA genes map to two distinct clusters on chromosome IV. Another set of piRNAs are not

derived from the chromosome IV clusters, but instead map to transcription start sites, contributing ~5% of total piRNAs (Gu et al., 2012b; Ruby et al., 2006). piRNAs have been linked with transcriptional silencing of transposons and protein-coding targets (Lee et al., 2012). In addition, piRNAs have been found to silence "non-self" transgenes for many generations (Lee et al., 2012).

In *C. elegans,* several factors have been discovered to be essential at different steps of piRNA biogenesis. First, precursor piRNAs are bi-directionally transcribed from piRNA genes by RNA Pol II. At the transcription step, a bipartite sequence motif located upstream of most piRNA genes is found to serve as an autonomous promoter for the transcription of precursor piRNAs (Ruby et al., 2006). In addition, transcription from this motif has been shown to be regulated by a group of transcription factors known as Forkhead proteins (i.e., FKH-3/4/5 and UNC-130). Depletion of them leads to a decreased level of piRNAs (Cecere et al., 2012). FKH-3/5 have been demonstrated to interact with the bipartite sequence motif in vitro, and UNC-130 has been shown to interact both in vitro and in vivo (Cecere et al., 2012). In addition to the transcription factors, PRDE-1 (pi<u>R</u>NA-<u>d</u>efective 1), a nuclear germline-expressed protein, is required for the production of precursor piRNA from the genomic loci with the motif (Weick et al., 2014). In *prde-1* mutants, mature piRNAs are absent and there is an appreciable decrease in precursor piRNAs (Weick et al., 2014). In addition, the Hannon lab has identified several genes important for piRNA production, termed TOFU (Twenty-One-u Fouled Ups). Among them, *tofu-3/4/5* are required for precursor piRNA production (Goh et al., 2014). After transcription, precursor piRNAs will go through shortening process to become mature piRNAs. Mature piRNAs are 21nt long with removed 5' 2-nt extension and 3' shortening. The factors required for this step are still a mystery, but perhaps some exonucleases in other small RNA pathways might

be shared here. Several factors have been found to function during piRNA maturation. *tofu-1/-2*

mutants exhibit an accumulation of precursor piRNA and a deficit of mature piRNAs, suggesting

TOFU-1/-2 participate in precusor piRNA processing (Goh et al., 2014). Similar observations

were made in a mutant of a cytoplasmic factor PID-1 (de Albuquerque et al., 2014). Notably, the

same as ERGO-1-associated siRNAs, 2'-O-methylation via HENN-1 is detected at the 3' end of

piRNAs. However, loss of methylation only causes a mild decrease of the piRNA population

(Kamminga et al., 2012).

The biological significance of piRNAs are mostly discussed in two aspects:

transcriptional gene silencing of transposon elements and protein coding genes (Bagijn et al.,

2012; Lee et al., 2012) and transgenerational gene silencing of exotic genes (Seth et al., 2013).

piRNA pathway is found to feed into downstream WAGO-associated 22G siRNA pathways for

signal amplification and transcriptional silencing of transposons (de Albuquerque et al., 2015)

(Fig. 1.5). For brevity (see WAGO-associated siRNAs section for details), in the soma, piRNAs

engage into the biogenesis of secondary 22G siRNAs via RdRps EGO-1/RRF-3 and the

amplified 22G siRNAs load onto the somatic NRDE nuclear RNAi pathway for transcriptional

silencing, whereas in the germ line, piRNAs link to HRDE nuclear RNAi pathway (Phillips et

al., 2015) (Fig. 1.5). However, not all piRNAs discovered in *C. elegans* map to transposon

regions, instead, a subset of piRNAs map to protein-coding regions. A number of protein-coding

genes are silenced via piRNA-mediated mechanism. However there is no clear effector pathway

characterized yet, perhaps via the HRDE pathway. Another aspect of piRNAs that has been

under extensive study is its function in transgenerational gene silencing. As stated in the

WAGO-associated siRNA section, HRDE-mediated nuclear RNAi can be inherited for many

generations (Buckley et al., 2012; Spracklin et al., 2017). This silencing requires piRNAs to

piRNA gene clusters

Non-self RNA

Transcription

5'cap AAAAAAAAAA

piRNA precusor

5'cap+extension

U

Shortening

mature piRNA

U

Transcriptional repression

PRG-1-associated piRNA

PRG-1

PRG-1 3' U 5'

PRG-1 3' U 5'

3' U 5'

WAGO-associated 22G siRNA

HRDE/NRDE HRDE/NRDE HRDE/NRDE

RRF-1 EGO-1

5'cap AAAAAAAAAA

WAGO-associated 22G siRNA

WAGO WAGO WAGO

WAGO transposon genes or non-self RNAs

5'cap AAAAAAAAAA

Post-transcriptional gene silencing

31

Figure 1.5 The piRNA pathway. piRNA precusors are generated from piRNA gene cluster loci. piRNA precusors go through a shortening process to become mature piRNAs with 5'U preference. piRNAs associate with PRG-1 Argonaute and trigger secondary 22G siRNA production. These 22G siRNAs are loaded onto either WAGO-class silencing pathway or HRDE-mediated nuclear RNAi pathway.

generate secondary 22G siRNAs to take effect, however piRNAs are found to be essential for the initial establishment of silencing but not for subsequent maintenance of the silencing status.

1.2.4. Summary

Research on the discovery and characterization of endogenous small RNA has flourished in the past decade. We have become clearer on questions of where, when and how small RNAs are expressed. Many different small RNA pathways were found to share factors for their biogenesis or in the effector complex. Therefore, it would be interesting to know how small RNAs are sorted into specific Argonaute complexes. Possibly, some factors may act as "writers." "Writers" may mark particular small RNAs so that they are recognized by specific classes of Argonaute "readers." In addition, lines of evidence show that the small RNA circuits correlate with certain histone modifications to shape complex genomes. Understanding chromatin diversity can help better predict the outcomes of any given small RNA pathway. On the other hand, the epigenetic landscape of the genome may in turn affect the biogenesis of small RNAs and perhaps thereby finetune the expression of genes according to the needs of the developmental moment. Some small RNA pathways and small RNA species exhibit preferential enrichment in germ line or somatic tissues or a particular cell type. It would be interesting to consider whether there is a correlation between cell identity and certain small RNA pathways. This hypothesis is supported by a recent finding in *Drosophila* showed that oncogenic transformation of somatic cells was able to induce a functional piRNA pathway that is typically suppressed in the somatic cells and active only in germ cells (Fagegaltier et al., 2016). With the basic knowledge of small RNA biogenesis, expression and targeting, more sophisticated questions can now be asked to explore the biological significance of those small RNAs. The

findings to date hint at three general roles for small RNAs: piRNAs serve as guardians of the genome, siRNAs are protectors that prevent deleterious consequences of harmful or inappropriate gene expression, and miRNAs are immediate executors who block translation or clear the target transcript instantly.

1.3 Poly (U) polymerases

RNAs receive extra nucleotides at their 3' end after transcription. These nucleotides are *de novo,* not templated from DNA. The 3' tailing of RNAs is intriguingly described as the wagging "tail" of RNA molecules (like that for dogs) because the modifications at 3' end are highly active. The wagging "tail" can be as short as a mono-nucleotide or as long as hundreds of nucleotides. Evidence shows that the wagging "tail" is able to determine the fate of RNAs – to stabilize an RNA or recruit RNA decay machinery to destablize an RNA. There are four types of 3' modifications, including adenylation, uridylation, cytidylation and guanylation. Adenylation of mRNA is the most well-documented 3' modification; it stabilizes mRNAs and aids export of mRNAs from the nucleus in eukaryotes (Tian and Manley, 2013). Relatively recent studies with less biased sequencing methods uncovered a widespread phenomenon of 3' uridylation on diverse RNA species among eukaryotes. Uridylation catalyzes the transfer of UMP residues to the 3' hydroxyl group of RNA. In the standard human fibroblast cell line, ~80% of mRNA species that encode functional proteins are found to have U-tails at a frequency of more than 2% (Chang et al., 2014). In contrast, RNA cytidylation and guanylation are much less frequently detected (Chang et al., 2014; Morozov et al., 2010).

34

Enzymes that catalyze 3' uridylation belong to the superfamily of DNA polymerase β-like nucleotidyl transferases. Members of this superfamily contain an upstream nucleotidyl transferase domain, downstream poly(A) polymerase (PAP)-associated domain, and various numbers of RNA-binding domains. The superfamily is conserved among diverse divisions of life from archaea and bacteria to eukaryotes (Martin and Keller, 2007). The superfamily harbors a branch of canonical poly(A) polymerases, including *C. elegans* GLD-2 and human PAPD4 (Martin and Keller, 2007). Apart from canonical poly(A) polymerases (PAP), other members of the superfamily are referred as non-canonical PAPs due to their missing one or two conserved domains (Martin and Keller, 2007). Among the non-canonical PAPs, a branch of them are predicted, and many of them have already been characterized, to have uridyl transferase [or poly(U) polymerase] activity (Martin and Keller, 2007). Based on the distribution pattern of branches in the DNA polymerase β-like nucleotidyl transferase superfamily, Aravind and Koonin hypothesized from a phylogenetic point of view that the members may have independently diverged from a common ancestor with a general and non-specific nucleotidyl transferase activity to acquire distinct functional domains and therefore to occupy vacant evolutionary niches (Aravind and Koonin, 1999).

In this section, I will focus on the branch of validated cytoplasmic poly(U) polymerases (PUPs) in different organisms, and I will summarize recent findings of their biological significance. However, it should be noted that one class of nuclear PUP has also been reported (Munoz-Tello et al., 2015; Rüegger et al., 2015). This class of enzyme uridylates U6 small nuclear RNAs specifically in the nucleus, which allows the proper production of splicing-competent U6 snRNPs (Munoz-Tello et al., 2015). In human, there are 7 predicted PUPs, typically called terminal uridyl transferases (TUTases) (Kwak and Wickens, 2007; Wickens and

Kwak, 2008). However, only three TUTases are cytoplasmic and have been characterized with functional PUP activity in more detail. Considering the technical advantages and manipulation convenience of human cell lines, human TUTases are extensively studied from the biochemical and structural aspects (Kwak and Wickens, 2007; Wickens and Kwak, 2008). In mouse and zebrafish, two TUTases have been studied hitherto. In *C. elegans,* there are four validated PUPs – two of them have been investigated in some detail (PUP-1 and PUP-2), one has not been characterized previously (PUP-3), and one regulates U6 small nuclear RNA (USIP-1) (Kwak and Wickens, 2007; Wickens and Kwak, 2008). In yeast, although it is the system where the first PUP has been identified, there is only one PUP well-characterized (Wang et al., 2000).

1.3.1 Human TUTase1/MTPAP/PAPD1/Hs4

TUTase1 is exclusively expressed in the cytoplasm in HeLa cells (Mullen and Marzluff, 2008). *In vitro* assay by Kwak and Wicken et al (2007) did not find TUTase1 to exhibit either PAP or PUP activity (Kwak and Wickens, 2007; Wickens and Kwak, 2008). However, later studies showed that there are some correlations between TUTase1 and uridylation of histone mRNAs (Mullen and Marzluff, 2008) (Fig. 1.6). In the study, degradation intermediates of histone H3 mRNAs were detected with oligouridine on the 3'end, and knocking down TUTase1 reduced the rate of histone mRNA degradation (Mullen and Marzluff, 2008). Histone mRNAs, as the only mRNAs that are not poly-adenylated, have a stem-loop sequence at the 3' end, and they are rapidly degraded at the end of S phase or when DNA replication is inhibited [e.g. by hydroxyurea(HU) treatment] in order to adapt to the rapid change of DNA synthesis rate at this stage (Pandey and Marzluff, 1987). *In vivo* mRNAs of *hist2h3d* and *hist2h3a/c* and their identified degradation intermediates were detected with heterogeneous lengths of non-templated

U at the 3' ends (Mullen and Marzluff, 2008). Knocking down TUTase1 reduced the rate of degradation of these histone gene mRNAs (Mullen and Marzluff, 2008). TUTase1 does not show strong activity on other types of mRNA or on histone mRNAs at other point in the cell cycle (Lim et al., 2014). In *in vitro* uridylation experiments, TUTase1 is immunoprecipitated with pre-*let-7* miRNA (Heo et al., 2012), though the detailed function of TUTase1 on pre-*let-7* has not been characterized yet. TUTase1 is not required for uridylating the products of *let-7* miRNA-targeted mRNA cleavage (Xu et al., 2016).

1.3.2 Human TUTase4/ZCCHC11/PAPD3/Hs3 and TUTase7/ZCCHC6

TUTase4 is exclusively expressed in the cytoplasm of human cells (Heo et al., 2012; Schmidt et al., 2011). The PUP activity of TUTase4 was identified by Kwak and Wickens through in vitro assay (Kwak and Wickens, 2007). Studies have demonstrated TUTase4 targets different RNA species – histone mRNAs, mRNAs with poly(A) tails, and miRNAs (Fig. 1.6). Schmidt et al 2011 reported immunoprecipitation data showing that TUTase4 binds to histone mRNA, *hist2h3,* in vivo (Schmidt et al., 2011). In addition, they found TUTase4 associated with histone mRNAs for uridylation-induced degradation.

Another important role of TUTase4 is linked to the regulation of mRNA with poly(A) tails (Fig. 1.6). TUTase4 is found to function redundantly in mRNA regulation with its paralog, TUTase7. TUTase7 is also a cytoplasmic PUP. In most studies about mRNA stability, TUTase4 and TUTase7 are usually studied together. Double knockout of TUTase4 and TUTase7 is lethal, therefore all the relevant studies utilized double knockdown as an alternative approach (Lim et al., 2014). Double knockdown of TUTase4/7 led to a significant increase of human mRNAs

(Lim et al., 2014). In addition, it was noted that TUTase4/7 tend to oligo-uridylate mRNAs with short A-tails (5-25nt) in vivo. In vitro, consistent with its in vivo preference for short A-tails, TUTase4 was able efficiently oligo-uridylate mRNA substrates without a poly(A) tail or with a poly(A)$_{10}$ tail, but was less efficient at modifying mRNA substrates with poly(A)$_{25}$ or poly(A)$_{50}$ (Lim et al., 2014). Phenotypically, TUTase4/7 double knockdown cells proliferate relatively slowly compared to wildtype (Lim et al., 2014).

TUTase4/7 also function redundantly in different steps during miRNA regulation. Excitingly, TUTase4/7, when regulating miRNAs, is able to switch between two modes of activity that occur in different cellular contexts and lead to opposite outcomes; they either oligo-uridylate the pre-*let-7* miRNA for decay or mono-uridylate it to promote its expression. Five aspects of TUTase4/7 activity are described here (Fig. 1.6).

(i) *oligo-uridylation on let-7 pre-miRNA:* In embryonic stem cells and multiple cancer cells where LIN28 is expressed, TUTase4 and TUTase7 are recruited to the LIN28-bound pre-*let-7* and oligo-uridylate the pre-*let-7*, adding 10-30 nts; this modification leads to turnover of the pre-*let-7* (Heo et al., 2012; Thornton et al., 2012; Thornton et al., 2014). Structural analysis uncovered that TUTase4/7 contain two multidomain modules: a catalytic module responsible for addition of Us, and a LIN28-interacting module (LIM). During the oligo-uridylation, LIN28, pre-*let-7*, and the TUTase LIM domain form a stable ternary complex, which facilitates the addition and growth of oligoU tails (Faehnle et al., 2014). In addition, the CCHC zinc knuckle domain of TUTase 4/7 is indispensable for oligo-uridylation (Wang et al., 2017).

(ii) *oligo-uridylation on 3' trimmed pre-miRNAs:* A study by Kim et al (2015) noted a special group of pre-miRNAs with 3' trimmed ends where the 3' end is recessed into the stem by 10-20nt. TUTase7 is thought to generate oligo-U tails on those 3' trimmed pre-miRNAs to target

them for degradation (Kim et al., 2015). It is hypothesized that oligo-uridylation at the 3' hairpin of pre-miRNAs disguises the pre-miRNAs from being recognized by Dicer and therefore prevents further processing.

(iii) *oligo-uridylation on mature miRNAs:* Human TUTase4 is implicated in targeting mature miRNAs, particularly *let-7* family miRNAs and miRNAs regulating Homeobox (Hox) genes. In vitro, human TUTase4/7 show a preference for the *let-7* guide strand over the *let-7* passenger strand and other synthetic non-*let-7* small RNAs, and recognize ssRNA over dsRNA. In addition, TUTase4/7 are predicted to recognize their uridylation targets by the presence of a GUAG sequence motif present in *let-7* miRNA family members and miRNA regulators of Homeobox (Hox) genes (Thornton et al., 2014).

(iv) *mono-uridylation on pre-miRNAs:* Conversely, in differentiated cells lacking LIN28, TUTase4/7 add mono-Us to pre-miRNA that acquires a shorter (1nt) 3' overhang (termed group II pre-miRNAs), which promote pre-miRNA maturation rather than RNA decay (Heo et al., 2012). Often, pre-miRNAs yield a 2 nt 3' overhang after Drosha processing. The structure of 2 nt 3' overhang is essential for subsequent Dicer recognition and processing. It is noted that TUTase4/7, together with TUTase2, act specifically on the group II pre-miRNAs (most belonging to the *let-7* miRNA family) and create a 2 nt 3' overhang by adding a mono-U to the overhang (Kim et al., 2015). Recognition by Dicer requires the 2 nt 3' overhang. By doing so, the group II pre-miRNAs are able to favor the Dicer processing. Knocking down TUTase2, 4 and 7 alone or in combination leads to reduced mature *let-7* miRNA level (Heo et al., 2012). Structural analysis demonstrates that the catalytic domain of TUTase7 forms a duplex-RNA-binding pocket that favors group II pre-miRNAs to transiently interact and acquire mono-U addition.
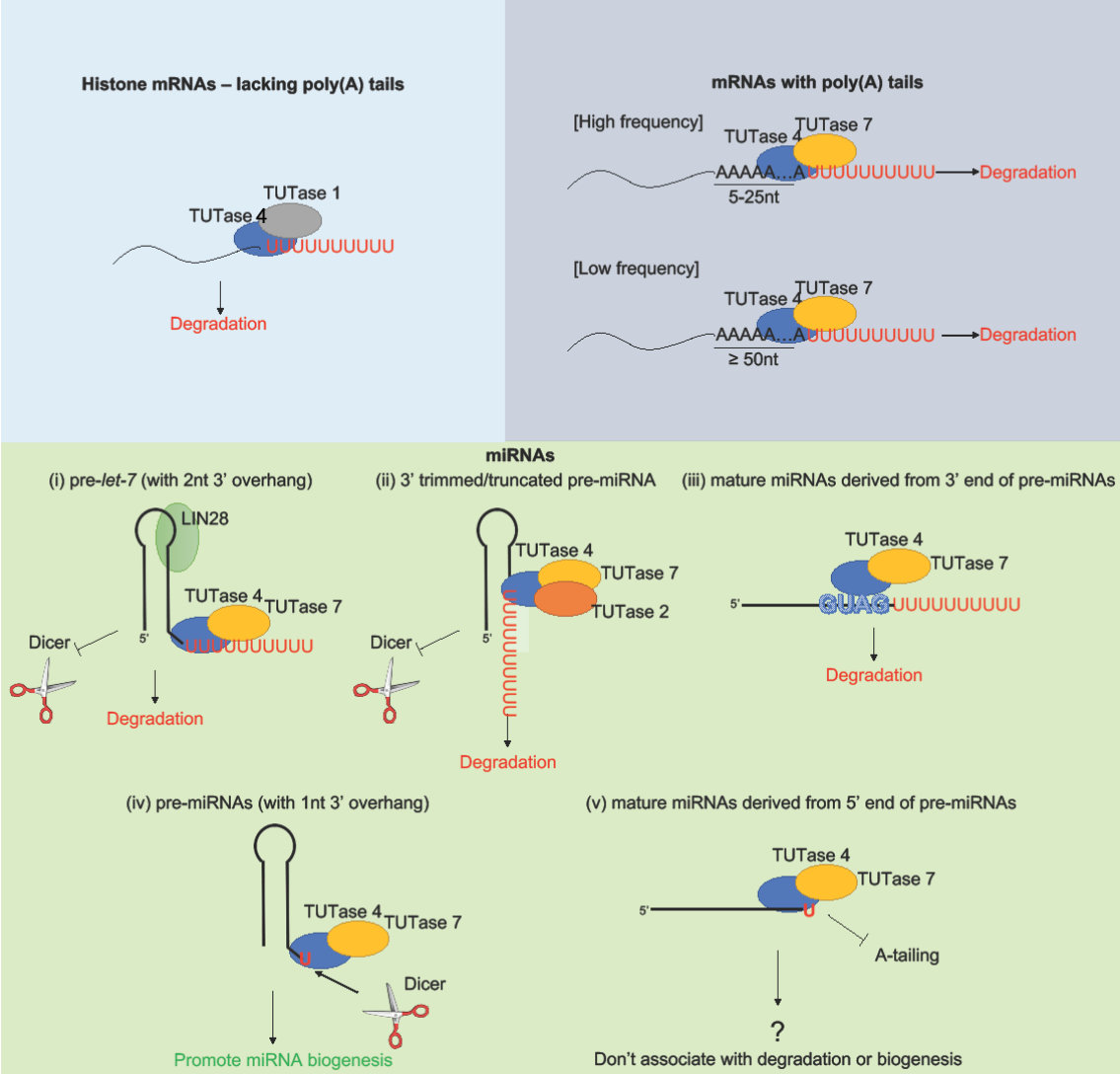
Figure 1.6 A summary of the known functions of human TUTases. TUTase1 and TUTase4 oligo-uridylate histone mRNA for degradation. TUTase4 and TUTase7 preferentially oligo-uridylate mRNAs with long poly(A) tails for degradation. TUTases also target miRNAs: (i) with the presence of LIN28, TUTase4 and TUTase7 are recruited by LIN28 and oligo-uridylate pre-*let-7* for degradation; (ii) TUTase 2, TUTase4 and TUTase7 oligo-uridylate 3' trimmed pre-miRNAs for degradation; (iii) TUTase4 and TUTase7 recognize GUAG motif on the mature miRNAs that are derived from the 3'end of pre-miRNAs and oligo-uridylate them for degradation; (iv) TUTase4 and TUTase7 mono-uridylate pre-miRNAs with 1-nt 3' overhang. The addition of mono-U to the 1nt 3' overhang facilitates Dicer recognition; (v) TUTase4 and TUTase7 mono-uridylate the mature miRNAs that are derived from the 5' end of pre-miRNAs. The addition of mono-U prevents poly(A) polymerase association to these mature miRNAs. In addition, mono-U addition in this case does neither associate with degradation nor promote miRNA biogenesis.

(v) mono-uridylation on mature miRNAs: By evaluating particular miRNAs in HeLa cells, a cell type that does not express LIN28, mature miRNAs derived from the 5' arm of the pre-miRNA hairpin were detected being mono-uridylated. Depletion of TUTase4/7 leads to substantial loss of miRNA mono-uridylation and a concomitant increase in 3' adenylation (Thornton et al., 2014). Notably, TUTase4/7 depletion does not show an effect on miRNA levels, suggesting that the mono-uridylation of the 5'-derived miRNA does not promote RNA decay (Thornton et al., 2014). Taken together, oligo-uridylation generally correlates with RNA decay, in opposition to mono-uridylation that seems to stabilize/promote the biogenesis of miRNAs.

1.3.3 Mouse TUTase4 (mTUTase4) and TUTase7 (mTUTase7)

mTUTase4 and mTUTase7 are both expressed from the primordial to the late antral stages of oogenesis in mouse (Morgan et al., 2017). Like their human orthologs, mTUTase4 and mTUTase7 function redundantly, and therefore they are often studied in combination. *tutase4/7* germinal vesicle (GV) conditional knockout mice produce a generally normal number of oocytes, but the animals are infertile due to failure to complete meiosis I. In mouse GV, maternal transcripts with short A-tails are found to be most affected by the presence/absence of TUT4/7 activities. In addition, the impact of TUT4/7 on mRNAs is quite specific to oocytes. In somatic cells where miRNA pathway functions, TUT4/7 have only minor impacts on the miRNA population (Morgan et al., 2017).

In somatic tissues, *mtutase4/7* mRNA are detected in diverse tissues, including spleen, thymus, skin muscle, heart, brain, kidney, liver and lung (Kozlowski et al., 2017). Among them,

murine lungs exhibited the most enriched expression, followed by liver. The relative mRNA

expression of *mtutase4* and *mtutase7* varies among tissues, e.g., *mtutase7* mRNA expression was

~4 fold more abundant in lungs than *mtutase4*, whereas their levels are the same in brain, heart

and muscle tissues. The difference of *mtutase4* and *mtutase7* expression suggests a possible

tissue-specific function of mTUTase4 and mTUTase7. In addition, mTUTase7 is noted to play a

role in innate immunity. Loss of mTUTase7 leads to over-expression of multiple cytokines in

response to bacterial stimulation (Kozlowski et al., 2017).

1.3.4 Zebrafish TUTase4/drTUTase4/Zcchc11 and TUTase7/drTUTase7/Zcchc6 (zTUTase4/7)

The expression patterns of zTUTase4 and zTUTase7 are unclear to date. Evidence from

in situ hybridization assays shows that their mRNAs are expressed in germ cells of the zebrafish

ovary, most prominently in mid oocyte stages while lacking in early and late stage oocytes

(Kamminga et al., 2010). In addition, zTUTase4/7 are implicated in regulating a subset of

miRNAs in embryos (Thornton et al., 2014). Therefore, according to the distribution of their

substrate, zTUTase4/7 are likely to express in zebrafish germ line and early embryogenesis.

Phenotypic analysis using morpholino knockdown of TUTase7 in the zygote resulted in multiple

developmental defects, including developmental delay, degeneration of somites, tail elongation

failure, and abnormal pericardial cavity morphology during embryogenesis. After

embryogenesis, a majority of fish died during mid-larval development (5 dpf) (Thornton et al.,

2014). Consistent with the finding that human TUTase4/7 regulates miRNAs that target *Hox*

genes, mRNAs of certain *Hox* genes were significantly downregulated in the TUTase7-depleted

embryos (Thornton et al., 2014). Additionally, zTUTase4/7 are speculated to be responsible for

piRNA uridylation in the zebrafish germ line. A study conducted by Ketting and colleagues

43

revealed that piRNAs lacking a 2'-O-methyl modification became uridylated and adenylated (Kamminga et al., 2010). Uridylation was highly detected on piRNAs that are derived from retro-transposons, which correlates with a decrease in piRNA abundance and mild de-repression of transposon transcripts (Kamminga et al., 2010). Since piRNAs are germline-specific small RNAs, three candidate zTUTases (i.e., zTUTase2/4/7) are proposed to function in germ cells (Kamminga et al., 2010).

1.3.5 *C. elegans* PUP-1/CDE-1/CID-1

The *pup-1* transcript is detected throughout the entire gonad via in situ hybridization (van Wolfswinkel et al., 2009). By using anti-PUP-1 antiserum, PUP-1 was reported to localize to perinuclear germ granules in maturing sperm of males and L4 hermaphrodites, and in the P-cell lineage of embryos (van Wolfswinkel et al., 2009). Although anti-PUP-1 antibody did not detect PUP-1 on P granules in the mitotic or early meiotic germ line (van Wolfswinkel et al., 2009), our epitope-tagged endogenous PUP-1 clearly co-localizes with P granule components (See Chapter II).

The poly(U) polymerase activity of *C. elegans* PUP-1 was first identified by the Wickens lab survey (Kwak and Wickens, 2007). Later, small RNA deep sequencing results from van Wolfswinkel et al (2009) revealed that PUP-1 activity correlates with U-tails of various lengths ranging from 1 nt to 6 nt *in vivo* (van Wolfswinkel et al., 2009). Comparison between the small RNA libraries of wildtype and the *pup-1(tm1021)* mutant discovered that siRNA species are influenced by loss of PUP-1 activity. In addition, loss of PUP-1 activity impacts miRNAs, as well (van Wolfswinkel et al., 2009). SiRNA reads with increased

abundance in the *pup-1* mutant significantly match CSR-1-associated siRNAs. Further

comparison between CSR-1-siRNA IP libraries from wildtype and the *pup-1* mutant supports

the conclusion that PUP-1 uridylates CSR-1-bound siRNAs for decay (van Wolfswinkel et al.,

2009).

Some interesting observations of the van Wolfswinkel et al study are worth further

discussion. For example, loss of PUP-1 activity does not completely abolish uridylation at the

3' end of siRNAs, which suggest that other activities may be redundant with PUP-1 (van

Wolfswinkel et al., 2009). Also, almost equivalent percentages of reads are detected with

either mono-uridylation or oligo-uridylation (van Wolfswinkel et al., 2009). Oligo-uridylated

siRNAs have been demonstrated to bind to CSR-1 and subsequently be degraded (van

Wolfswinkel et al., 2009). However, if mono-uridylated siRNAs are not intermediate products

of oligo-uridylation, then they may have a different fate as mono-uridylated siRNAs may bind

to other Argonautes and may be degraded. For example, human TUTases that mono-/oligo-

uridylate can result in different outcomes (Heo et al., 2012).   In addition, *pup-1* is found to be

required for RNAi inheritance in that *pup-1(gg519)* mutants are sensitive to *gfp* RNAi, but *gfp*

silencing is not inherited in subsequent generations (Spracklin et al., 2017). Phenotypically,

pup-1(tm1021) mutants exhibit a mortal germline phenotype at stressful temperature (Spracklin

et al., 2017) and chromosome segregation defects visible as univalents in maturing oocytes,

mislocalization of centromeric proteins in the embryo, and increased non-disjunction (van

Wolfswinkel et al., 2009).

1.3.6 *C. elegans* PUP-2

By CRISPR epitope tag knock-in, we found that PUP-2 is present in both female and male germ lines. PUP-2 strongly expresses in the cytoplasm of diakinesis oocytes and sharply drops in late oocytes undergoing maturation. In the male germ line, PUP-2 expression is relatively weak and is detected in the cytoplasm of pachytene cells and condensing spermatocytes. Lehrbach et al investigated the post-transcriptional regulation of *let-7* miRNA by using a transgenic *let-7* expression under the control of a heterologous promoter. They found that LIN28 binds to pre-*let-7*, which prevents Dicer processing; PUP-2 contributes to this LIN28 regulation of *let-7*. *In vitro* assay shows that PUP-2 physically interacts with LIN28 and uridylates pre-*let-7* for degradation in a LIN28-dependent manner (Lehrbach et al., 2009). *let-7* miRNA is known to express in the hypodermal seam cells in *C. elegans* (Vella et al., 2004). Therefore, PUP-2 is likely to express in somatic tissues as well, although no one has examined so far. A later study demonstrated that, during late stages of *C. elegans* development when LIN28 expression is diminished, partial knockdown or loss of PUP-2 activity *in vivo* has no appreciable impact on the abundance of endogenous pre-*let-7* or endogenous mature *let-7* (Van Wynsberghe et al., 2011). This observation supports the notion that in the soma, PUP-2-mediated uridylation of *let-7* during its biogenesis is largely LIN28-dependent. The *let-7* family miRNAs are found to be targeted by uridylation in both *C. elegans* and human, which suggests a conserved function of PUPs in regulating *let-7* miRNAs.

1.3.7 Yeast Cid1

Cid1 was the first PUP to be identified. Cid1 was identified in fission yeast through its

involvement in the yeast S-M checkpoint (also known as the replication checkpoint): overexpressing Cid1 made the cells less sensitive to hydroxyurea or caffeine treatment (Wang et al., 1999). Later, careful *in vitro* analysis revealed that Cid1 has robust PUP activity, especially as a component of native multiprotein complexes containing multiple RNA binding proteins (Rissland et al., 2007). Cid1-dependent uridylation of polyadenylated mRNAs leads to RNA decay. Although the researchers only evaluated a handful of transcripts (i.e., *act1, adh1,* and *urg1*), all of the tested transcripts were found to carry short U-tails, which suggests that uridylation may be a widespread phenomenon in fission yeast (Rissland and Norbury, 2009). In addition, the study uncovered an additional RNA decay pathway that is independent of deadenylation and is mediated by uridylation-promoted RNA decapping (Rissland and Norbury, 2009).

1.3.8 Summary

In the last couple of years, extensive attention has been drawn to this RNA modification, RNA 3' uridylation, which has been hidden from people's view for so many years. Study of PUPs, the enzymes that catalyze uridylation, is evidently important for deciphering the mechanism and function of this modification. As our knowledge expands, we begin to appreciate their multiple roles in gene regulation. For example, the same set of PUPs can regulate more than one RNA species, the same PUP can lead to different RNA fates in different cellular localizations/environments, and multiple PUPs are usually required redundantly to achieve the same goal. Perhaps investigating the expression or subcellular localization of different PUPs will provide us some clues about their local function. For example, location in P-bodies may lead to RNA decay, in stress granules may lead to translational inhibition, and on P

granules or in cytosol may regulate different processes during RNA metabolism. Perhaps identifying the PUP interactors in different cells may also help us understand the diverse outcomes of uridylation. Furthermore, as our knowledge expands on the biochemical roles of the PUPs, we start to be curious about the developmental consequences of uridylation for controlling RNA stability or maybe even on marking RNAs for targeting (no evidence has been shown so far). Some PUPs have been found to have restricted expression patterns in either somatic tissues or germ lines (Kozlowski et al., 2017). Understanding the *in vivo* impacts of uridylation during development of different tissues is a large field of investigation, and it may be especially challenging due to the complexity of target RNA species. In this sense, using relative simple but still complex enough organisms such as *C. elegans* may be a good way to start coupling the uridylated target RNA with phenotypes.

1.4 Projects

In this thesis, I explore the role of poly (U) polymerases as critical regulators at different aspects of germline development in *C. elegans*. I show a role for PUPs in germline viability, germ cell identity, gamete formation, and meiotic H3K9me2 distribution. In Chapter II, I present data showing that PUP-1 and PUP-2 are required redundantly under conditions of temperature stress to ensure germline survival, identity as distinct from soma, and gamete formation, whereas PUP-3 activity is antagonistic to PUP-1 and PUP-2 in these aspects. In Chapter III, I describe my results and those of a former graduate student, Matt Snyder, regarding meiotic H3K9me2 expression in *pup-1/-2* double mutants and in several small RNA pathway mutants. We show that PUP-1 and PUP-2 activities, as well as the ALG-3/-4~CSR-1 small RNA pathway, are

redundantly required for correct H3K9me2 distribution and turnover in meiotic germ cells. In

Chapter IV, I discuss our current understanding regarding the possible functions of and the

relationship among PUP-1, PUP-2 and PUP-3.

Chapter II The balance of poly(U) polymerase activity ensures germline identity, survival, and development in *Caenorhabditis elegans*

2.1 INTRODUCTION

The germ line is a unique tissue responsible for gamete production and continuation of the species. Germ cell formation in the embryo and subsequent growth and survival of the germ line require patterns of gene expression distinct from somatic cells. One conundrum is that the germline is a highly specialized tissue producing unique cell types - sperm and oocytes - that, upon fusion at fertilization, produce a totipotent zygote. Gene expression studies in animals ranging from nematodes to mammals have identified repressive mechanisms acting at the transcriptional and post-transcriptional levels as essential for primordial germ cell formation and, subsequently, for germline viability and development [e.g., (Cinalli et al., 2008; Lai and King, 2013; Mu et al., 2014)]. In *Caenorhabditis elegans,* certain chromatin regulators and translational repressors limit somatic gene expression in the germ line and promote fertility (Ciosk et al., 2006; Gaydos et al., 2012; Mello et al., 1992; Strome and Lehmann, 2007; Updike et al., 2014). Interestingly, defects in some of these processes result in immediate sterility, whereas defects in others cause a gradual reduction in fertility over successive generations leading to eventual sterility (a "mortal" germline phenotype (Mrt)) (Smelick and Ahmed, 2005). Presumably the Mrt phenotype results from accumulated mis-regulation of gene expression essential for maintaining fertility.

RNA stability is regulated by numerous 5' and 3' modifications (Kwak and Wickens, 2007; Norbury, 2013; Scott and Norbury, 2013; Wickens and Kwak, 2008). The best-studied example is addition of a 3' poly(A) "tail," a modification well documented to increase mRNA stability. In addition, mRNAs can be 3' mono- or poly-uridylated, and these modifications generally correlate with reduced mRNA abundance (Lim et al., 2014). Interestingly, uridyl transferase activity may have distinct roles in different cellular contexts (Kim et al., 2015).

Recent studies have uncovered roles for uridylation in multiple aspects of RNA metabolism in diverse species. In Arabidopsis and mammalian cells, uridylation was first noticed at the 3' ends of microRNA (miRNA)-directed cleavage products (Shen and Goodman, 2004). A sequence of 1-9 uridine nucleotides is added at the 3' ends of cleaved mRNAs downstream of the corresponding miRNA cleavage site, suggesting one role of uridylation is to enhance decay of mRNA cleavage products. Uridylation has been detected on human replication-dependent histone mRNAs specifically at the end of S phase and when DNA synthesis is inhibited; uridylation presumably facilitates a rapid decrease in histone synthesis in response to the completion of DNA synthesis (Mullen and Marzluff, 2008). Terminal uridyl transferases, TUT1, TUT3, and TUT4 (Mullen and Marzluff, 2008; Schmidt et al., 2011; Su et al., 2013), have been identified as responsible for histone mRNA uridylation. The clearest insight into mRNA uridylation was acquired from using a uridylation-optimized deep sequencing method to compare the mRNA sequence signatures in mammalian TUT mutants (Lim et al., 2014). The results were consistent with poly(U) tails serving as a general molecular signal for mRNA decay.

Uridylation is implicated in miRNA biogenesis and stability in a variety of organisms, including human cell culture, zebrafish, and *C. elegans* (Kim et al., 2015; Thornton et al., 2014).

In *C. elegans*, 3' uridylation functions in regulating the stability of LIN28-blockaded *let-7* pre-miRNA (Lehrbach et al., 2009). The *let-7* ortholog in human is a candidate tumor suppressor and a regulator of stem cell differentiation, hence uridylation may be a factor in cancer biology and stem cell biology (Balzeau et al., 2017; Heo et al., 2012; Kim et al., 2015; Lehrbach et al., 2009). 3' uridylation may promote degradation of siRNA (Ibrahim et al., 2010; van Wolfswinkel et al., 2009). In contrast, 3' methylation prevents uridylation and correlates with increased steady state levels of small RNAs in many species (Kamminga et al., 2010; Ren et al., 2014). The widespread occurrence of 3' RNA uridylation in diverse species indicates its general importance as a regulatory mechanism.

Enzymes that add terminal uridine monophosphate groups are members of the DNA polymerase beta-like nucleotidyl transferase family (Norbury, 2013). The domain structure of these enzymes is conserved from yeast to mammals and includes an upstream nucleotidyl transferase domain and downstream PAP-associated domain. In *C. elegans*, these enzymes include: conventional poly(A) polymerases, GLD-2 and GLD-4; enzymes with demonstrated *in vitro* 3' uridylation activity, PUP-1 (aka CID-1, CDE-1), PUP-2, PUP-3 (Kwak & Wickens 2007), and USIP-1 (Rüegger et al., 2015) and several other proteins whose nucleotidyl transferase specificity is not known (Norbury, 2013). Initially, 3' uridyl transferases that add short oligo(U) tails were called terminal uridyl transferases (TUTases) and those that add longer poly(U) tails were called poly(U) polymerases (PUPs) (Wickens and Kwak, 2008). The terms are used interchangeably in the current literature (e.g., (Norbury, 2013)); here, we use the *C. elegans* designation, PUP.

Among *C. elegans* PUP enzymes, PUP-1 is reported to target a subclass of endogenous siRNAs that bind to CSR-1 Argonaute (van Wolfswinkel et al., 2009), and PUP-2 is reported to

target *let-7* miRNA (Lehrbach et al., 2009; Van Wynsberghe et al., 2011). Although PUP-3 has

validated uridyl transferase activity, targets are not known. By analogy with other systems, one

or more of these proteins may also target mRNAs. USIP-1 (<u>U</u> <u>S</u>ix snRNA-<u>I</u>nteracting <u>P</u>rotein –

1) has a distinct role in U6 snRNA accumulation (Rüegger et al., 2015). Our current

understanding of PUP function is based mainly on biochemical and structural data, and the

developmental functions of these proteins remain underappreciated. Given their roles in RNA

regulation and the global prevalence of uridylation in most eukaryotic species, a developmental

role for PUP activity seems likely. Here, we used genetic and molecular tools to investigate the

developmental function of PUP-1, PUP-2, and PUP-3. We report that *C. elegans* PUP-1 and

PUP-2 function redundantly to ensure that the germ line maintains its identity as distinct from

soma, produces functional gametes, and is sustained through successive generations under

conditions of temperature stress. PUP-3 also promotes germline development but appears to

work in opposition to PUP-1/PUP-2. PUP-3 abundance is limited by PUP-1/PUP-2 activity, and

the loss of PUP-3 activity rescues defects associated with PUP-1/PUP-2 loss of function. PUP-1

and PUP-2 have distinct expression patterns within the germ line and localize to distinct

subcellular compartments where they may carry out complementary functions. We propose that

germline survival, identity, and development require the correct balance of PUP activity.

2.2 RESULTS

2.2.1 PUP-1 and PUP-2 promote germline and embryonic development

To evaluate the impact of PUP activity on germline development and the possibility of redundant developmental functions among these three enzymes, we compared the germline phenotypes of three deletion alleles, *pup-1(tm1021)*, *pup-2(tm4344)*, and *pup-3(tm5089)*, to each other as well as to double and triple *pup* mutant combinations. Each allele causes a shift in the open reading frame and is predicted to be null for function (www.wormbase.org, Fig. 2.S1A). For simplicity, we refer to these alleles as *pup-1(0)*, *pup-2(0)*, and *pup-3(0)* for the remainder of the paper except where specified.

pup-1 and *pup-2* single mutants exhibit germline and embryonic lethal phenotypes that primarily result from an absence of maternal gene product and are more penetrant a culture temperature of 25°C than at 20°C (Table 2.1, Fig 2.1, Table 2.S1). Over 83% of *pup-1(0)* and *pup-2(0)* F1 hermaphrodites are viable and 100% of them are fertile, although these M+Z- animals (where M indicates maternal genotype and Z indicates embryonic genotype) have reduced brood sizes and exhibit low penetrance gamete defects (Table 2.1, Table 2.S2). In contrast, germline development of *pup-10)* and *pup-2(0)* F2 (M-Z-) hermaphrodites is significantly impaired: some individuals are sterile (Fig. 2.1), and fertile individuals produce fewer embryos than their M+Z- parents (Table 2.1). We observe two other phenotypes in the F2 population: some embryos are nonviable; and the frequency of XO male progeny is elevated (a Him phenotype) (Table 2.1). Embryonic viability depends strictly on maternal expression of *pup-1* and primarily on maternal expression of *pup-2*, although zygotic *pup-2* expression has a minor role (Table 2.S2). The Him phenotype of each gene is strictly maternal-effect. As a

consequence of the maternal-effect nature of these phenotypes, we maintain the mutations in a heterozygous state using a balancer chromosome, even at "permissive" temperature.

After completing our analysis, another deletion allele, *pup-1(gg519)*, was described, and its reported phenotype (Spracklin et al., 2017) was more severe than what we observed for *pup-1(tm1021)*. We obtained *pup-1(gg519)*, balanced the mutation, and evaluated the phenotype using the criteria described above (see Supplemental data). In our hands, *pup-1(tm1021)* and *pup-1(gg519)* had similar phenotypes (Table 2.1, Fig. 2.S2). We suspect we observe a milder phenotype because we maintain *pup-1(gg519)* in a heterozygous (balanced) state.

We further evaluated germline development by examining the germ cell morphology of *pup-1(0)* and *pup-2(0)* hermaphrodites (see Materials and methods) (Fig. 2.1A,C). Consistent with reduced brood sizes, some F1 (M+Z-) animals contained endomitotic oocytes where the oocyte endomitotically replicates its DNA (an Emo phenotype) (Fig. 2.1C). The Emo phenotype may reflect impaired sperm-egg interaction, egg activation, or ovulation (Geldziler et al., 2011), and it can be a direct or indirect result of either oocyte or sperm defects. We observed three general phenotypes among sterile F2 (M-Z-) adults (Fig. 2.1A-C). (i) Some sterile adults contained germ cells and sperm and/or oocytes. When both gametes types are present, at least one type is presumably fertilization-defective and, indeed, many of these animals had endomitotic oocytes. (ii) Some sterile adults contained germ cells, but no gametes. (iii) Some sterile adults contained no germ cells. Together, these results indicate that PUP-1 and PUP-2 activities promote germline survival and development, especially under conditions of temperature stress.

2.2.2 PUP-1 and PUP-2 have redundant developmental functions

To evaluate the *pup-1 pup-2* double mutant phenotype, we used a CRISPR-Cas9 genome editing approach to delete the adjacent *pup-1* and *pup-2* genes (see Materials and methods; Fig. 2.S1B). For brevity, we designate the double deletion as *pup-1/-2(0)*. We analyzed two independent deletions, *pup-1/-2(om129)* and *pup-1/-2(om130)*, and observed a similar phenotype with respect to brood size, embryonic viability, and production of male progeny (e.g., Table 2.1). We used *pup-1/-2(om129)* in subsequent studies reported here.

The *pup-1/-2(0)* double mutant has the same general pattern of defects observed in *pup-1* and *pup-2* single mutants, however the penetrance and severity of these defects are significantly worse in the *pup-1/-2(0)* double mutant, particularly at 25°C (Table 2.1, Fig. 2.1). The data indicate a synergistic interaction between *pup-1* and *pup-2* that has a catastrophic impact on fertility. Strikingly, in the F3 generation at 25°C, 97% of adult *pup-1/-2(0)* hermaphrodites lacked germ cells altogether compared with ~9% of F3 *pup-1(tm1021)* and ~7% of F3 *pup-2(0)* adult hermaphrodites (Table 2.1, Fig. 2.1A, B). The absence of germ cells might reflect either the failure of germ cell precursors to form in the embryo or to remain viable and proliferate during larval development. To distinguish between these alternatives, we raised synchronized *pup-1/-2(0)* F2 animals at 25°C and DAPI-stained their progeny at different developmental stages. 100% of late L3 larvae (~27 hours post-L1; n=36 gonad arms) examined contained germ cells whereas 60% of mid-late L4 larvae (~35 hours post-L1; n=50 gonad arms) contained no germ cells and 40% contained only a very few germ cells (Fig. 2.1B). We conclude that germ cells do indeed form in *pup-1/-2(0)* embryos, but then die during the latter portion of larval development. Therefore PUP-1 and PUP-2 function redundantly to ensure germline viability under conditions of temperature stress.

2.2.3 *pup-1/-2* sperm are fertilization defective

Given the highly penetrant gametogenesis defects observed in *pup-1/-2(0)* hermaphrodites, we were interested in evaluating the phenotype of mutant males. We tested sperm function by mating single *pup-1/-2(0)* M+Z- males, raised at 25°C, to *fog-1* (feminization of the germ line) females and counting cross-progeny number. Typically, XX *C. elegans* develop as hermaphrodites and XO *C. elegans* develop as males. FOG-1 is required in XX animals for production of sperm, and hence XX *fog-1* mutants produce only oocytes and are female (Barton and Kimble, 1990). 56% of *pup-1/-2(0)* M+Z- males produced no cross-progeny and 44% yielded on average fewer cross-progeny than wildtype males mated in parallel under the same conditions (Fig. 2.2A). We DAPI-stained the adults in the non-productive crosses and evaluated their gametes. We observed sperm in all of the *pup-1/-2(0)* males. We observed endomitotic oocytes in 93% of the *fog-1* females, a phenotype not observed in the unmated *fog-1* female controls under our assay conditions. Moreover, we observed sperm in 54% of these females, indicating that male sperm had transferred during mating (Fig. 2.2B). We interpret these results to mean that many sperm produced by *pup-1/-2(0)* M+Z- males are fertilization-defective.

We also assessed sperm production in DAPI-stained adult *pup-1/-2(0)* F2 (M-Z-) males raised at 25°C. Sperm condensation was variable, and sperm were not clustered in the proximal somatic gonad as is typical for wildtype, but instead were observed more distally within the gonad (Fig. 2.2C). The majority of F3 adult male germlines had an overall normal organization although a minority (25%) lacked germ cells altogether. Hence, the *pup-1/-2(0)* germ cell loss phenotype was less penetrant in males than in hermaphrodites. Unfortunately, the 100% sterility of F3 hermaphrodites precludes our analysis of male germ cell viability in a later generation. We conclude that the XO germ line can better tolerate loss of PUP activity than the XX germ line.

2.2.4 Germ cells express somatic genes in the absence of PUP-1/-2 activity

Many pup-1/-2(0) sterile hermaphrodites have a disorganized germ line with nuclei present in the cytoplasmic core (rachis) (e.g., Fig. 2.1C). This phenotype is reminiscent of P granule-depleted germ lines (Knutson et al., 2017; Updike et al., 2014). P granules are germline-specific ribonucleoprotein particles that assemble on the outer face of the nuclear envelope, typically spanning a nuclear pore, and associate with RNA molecules as they are exported from the nucleus (Wang and Seydoux, 2014). P granules are structurally similar to germline RNP particles described in other animal species. A striking outcome of P granule depletion is inappropriate expression of some somatic genes in the germ line, including the pan-neuronal genes, *unc-33* and *unc-119* (Knutson et al., 2017; Updike et al., 2014).

To test whether PUP-1/PUP-2 activity represses expression of somatic genes in the germ line, we evaluated expression of *unc-33p::gfp* and *unc-119::gfp* in the *pup-1/-2(0)* germ line. For these assays, we maintained the strains at 22°C and evaluated expression in the F2 generation to maximize the development of sterile animals that retained a germ line (see Materials and methods). UNC-33 is required for correct nervous system development in *C. elegans* and typically not expressed in the germ line (Fig. 2.3A) (Altun-Gultekin et al., 2001). *unc-33p::gfp* was expressed in 100% of sterile *pup-1/-2(0)* germ lines, with relatively abundant expression in 83% of individuals (Fig. 2.3B). Interestingly, we also observed weak *unc-33p::gfp* expression in 53% of fertile *pup-1/-2(0)* germ lines. Upregulation of *unc-33p::gfp* presumably occurs at the transcriptional level, therefore its expression is an indirect effect of losing PUP-1/-2 activity. In contrast to *unc-33*, we did not observe expression of either of two *unc-119::gfp* transgenes or another somatic reporter, *rab-3p::rfp* (see Materials and methods). We conclude

that loss of PUP-1/PUP-2 activity leads to expression of some soma-specific genes in the germ line, and we hypothesize that this inappropriate gene expression contributes to the developmental defects.

We further evaluated the impact of *pup-1/-2(0)* on germ cell fate identity by examining expression of two core P granule components, GLH (germline helicase) -1 and PGL (P granule component) -1. Expression of GLD-1 and PGL-1 in wildtype animals is strictly germline-specific and used as a diagnostic tool to evaluate germline versus somatic identity (Gruidl et al., 1996; Kawasaki et al., 1998). At 25°C, GLH-1::GFP and PGL-1::GFP foci were variable in size and relative intensity in the *pup-1/-2(0)* M+Z- germ line compared with controls, and large regions of M-Z- germlines lacked foci altogether (Fig. 2.3E). We interpret these results to indicate the absence of PUP-1/PUP-2 function leads to impaired P granule assembly, a phenotype consistent with inappropriate expression of *unc-33*.

In addition to abnormal germline GLH-1::GFP and PGL-1::GFP expression in *pup-1/-2(0)* mutants, we observed GLH-1::GFP expression in 41% of *pup-1/-2(0)* F1 animals in somatic cells in the tail (n=27, Fig. 2.S3A). We did not observe somatic expression of PGL-1::GFP in *pup-1/-2(0)* mutants. Somatic expression of P granule components has been observed in mutants with impaired activity of certain transcriptional regulators (Unhavaithaya et al., 2002; Wang et al., 2005) and in some cases only a subset of P granule proteins are expressed in somatic cells (Petrella et al., 2011). PUP-1/PUP-2 activity appears to limit GLH-1 expression in these somatic cells.

2.2.5 Loss of PUP-3 rescues developmental defects in *pup-1/-2* double mutant

pup-3(0) mutants raised at 25°C have germline defects. Brood sizes were considerably smaller than wildtype, e.g., 66 ± 11 in the F2 (M-Z-) generation (Table 2.1). More than 99% of *pup-3(0)* F2 (M-Z-) hermaphrodites were fertile in our assay (Table 2.1, Fig. 2.1), and P granule distribution appeared normal (Fig. 2.3F). However, DAPI-staining revealed germline developmental defects in some fertile individuals. ~19% of fertile individuals contained one healthy germ line and one disorganized germ line that lacked gametes (n=32 animals, ~9.5% of gonad arms). Another ~9.5% of gonad arms contained at least one endomitotic oocyte. We also evaluated *unc-33p::gfp* expression in the *pup-3(0)* germ line. 95% of gonad arms had barely detectable GFP throughout the cortical cytoplasm, and 5% gonad arms contained small domains (encompassing 2 - 4 nuclei) with moderate GFP signal (Fig. 2.3C) (n=38). Taken together, these data indicate that PUP-3 activity promotes germline development. The relatively low penetrance sterility makes sense given our previous gonad-specific RNA-seq data, which found *pup-3* transcripts at low abundance in the adult hermaphrodite germ line compared with *pup-1* and *pup-2* transcripts [Reads Per Kilobase of transcript per Million mapped reads (RPKM) values of 49.5 for *pup-1*, 437.8 for *pup-2*, and 7.1 for *pup-3*; (Guo et al., 2015)].

To investigate the relationship of PUP-3 activity to PUP-1 and PUP-2, we evaluated *pup-3(0); pup-2(0)* and *pup-3(0); pup-1(0)* double mutants and *pup-3(0); pup-1/-2(0)* triple mutants. We were surprised to find that *pup-3(0)* suppressed the germline mortality phenotype associated with *pup-1(0)*, *pup-2(0)*, and *pup-1/-2(0)* mutations, including in *pup-1/-2(0)* F3 animals at 25°C (Fig. 2.1A). Moreover, although *pup-3(0)* did not completely suppress sterility, the range of germline defects was less severe in the triple mutant (Fig. 2.1A). Strikingly, although ~25% of *pup-3(0); pup-1/-2(0)* F3 hermaphrodites produced at least a few embryos (Fig. 2.1A, Table 2.1),

these embryos were inviable. Taken together, these data indicate that the loss of PUP-3 activity

compensated for the combined loss of PUP-1/PUP-2 with respect to germline viability and

partially with respect to germline development.

We evaluated whether the loss of PUP-3 function might decrease inappropriate somatic

expression in the *pup-1/-2(0)* germ line. In *pup-3(0);pup-1/-2(0);unc-33p::gfp* hermaphrodites,

41% of germlines did not express detectable GFP in the cortex and 59% of germlines contained

low GFP abundance in the cortex (Fig. 2.3D). The latter was similar to the GFP level observed

in fertile *pup-1/-2* double mutants (Fig. 2.3B). These arms also contained GFP puncta in rachis,

as did another 7% of germlines (65% total) (Fig. 2.3D). Hence, the loss of PUP-3 function

reduces *unc-33p::gfp* expression in the *pup-1/-2(0)* germ line.

We also evaluated whether PUP-3 activity limits germline gene expression in the soma.

In *pup-3(0)* mutants, we observed expression of PGL-1::GFP (but not GLH-1::GFP) in a subset

of intestinal cells (Fig. 2.S3B). A similar PGL-1 distribution has been observed in certain

transcriptional regulatory mutants (Petrella et al., 2011). We conclude that PUP-3 activity plays a

minor role in preventing germline gene expression in the intestine.

2.2.6 PUP-2 localization is distinct from PUP-1

PUP-1 is reported as expressed in germline cytoplasm and associated with embryonic P granules

(van Wolfswinkel et al., 2009). To characterize the distribution of PUP-2 protein, including its

localization relative to PUP-1, we epitope-tagged *pup-1* and *pup-2* via CRISPR-Cas9 (Fig.

2.S1C). For PUP-2, we generated strains with a *3xflag* sequence inserted at either the N- or C-

terminus. Although *3xflag::pup-2* and *pup-2::3xflag* manifested similar expressions pattern via

indirect immunolabeling with anti-FLAG antibody, only 3xFLAG::PUP-2 was visible on protein

blots. We therefore used the *3xflag::pup-2* strain in subsequent studies. Within the same genetic

background, we tagged *pup-1* with 3xMYC (Fig. 2.S1C). The resulting *pup-1::3xmyc*

3xflag::pup-2 strain had an average clutch size of 252 $\pm$10, essentially the same as wildtype

animals assayed in parallel (253 $\pm$ 9). We concluded that the epitope tags did not appreciably

interfere with gene function.

       We co-labeled PUP-1::3xMYC and 3xFLAG::PUP-2 in order to visualize the relative

distribution of these two proteins within the germline. Both proteins were detected in male and

hermaphrodite germ lines. PUP-1::3xMYC was observed throughout the germ line where it

localized to perinuclear granules (Fig. 2.4A-C). In maturing oocytes, PUP-1::3xMYC foci were

observed throughout the cytoplasm (Fig. 2.4B). This PUP-1::3xMYC distribution is similar to

expression of GFP-tagged PUP-1 in a strain generated via bombardment by (Zhong et al., 2010)

(see Materials and methods) and is suggestive of P granules. 3xFLAG::PUP-2, in contrast, was

detected only in the proximal germ line where it was observed in scattered cytoplasmic foci (Fig.

2.4A,B, 2.S4, 2.S5). 3xFLAG::PUP-2 expression decreased sharply in late-stage oocytes at the -

1, -2, -3 positions (Fig. 2.4A, 2.S4, 2.S5). Our data indicate that PUP-1::3xMYC and

3xFLAG::PUP-2 expression domains overlap at diplotene - diakinesis stages of oogenesis and

mid-pachytene stage through the condensation phases of spermatogenesis. Both proteins are also

detected in developing spermatocytes in L4 stage hermaphrodites (data not shown).

       We evaluated PUP-1 and PUP-2 distribution at the subcellular level to determine if they

might localize to common foci within the meiotic germ line. In both male and hermaphrodite

germ lines, we observed only rare instances where PUP-1::3xMYC and 3xFLAG::PUP-2 foci

were in close proximity. These may be chance associations or may indicate a coordinated

function for PUP-1 and PUP-2 in these late-stage gametes.

We confirmed that PUP-1 foci are P granules by co-labeling for PUP-1::3xMYC and EKL-1 (enhancer of ksr-1 lethality), a P granule protein that is a component of the endogenous 22G RNA machinery. In the course of other studies, we had generated anti-EKL-1 antibody (see Materials and methods) and determined that EKL-1 co-localizes with the core P granule component, GLH-2 (Fig. 2.S6). Subsequent immunolabeling with anti-MYC and anti-EKL-1 revealed that PUP-1::3xMYC and EKL-1 co-localized at the nuclear periphery (Fig. 2.4C). We conclude that PUP-1 foci are P granules.

Our observation that PUP-1 and PUP-2 are developmentally redundant led us to investigate the possibility that their distribution might be interdependent. We treated *pup-1::3xmyc 3xflag::pup-2* animals with either *pup-1(RNAi)* or *pup-2(RNAi)* and evaluated expression of the non-targeted protein. PUP-1 and PUP-2 were each well depleted by the respective RNAi treatment (Fig. 2.S4). There was no obvious change in PUP-2 distribution in *pup-1(RNAi)* animals, i.e., PUP-2 was not observed in the distal germ line or in perinuclear foci. Similarly, there was no obvious change in PUP-1 distribution in *pup-2(RNAi)* animals (Fig. 2.S4). Therefore, the subcellular distributions of PUP-1 and PUP-2 appear to be independent.

Finally, we investigated two other aspects of PUP-2 expression in more detail. We hypothesized that PUP-2 might associate with processing (P) body-like granules previously described in the *C. elegans* hermaphrodite germ line and implicated in mRNA stability and translation (Parker and Sheth, 2007; Voronina et al., 2011). However, immunolabeling indicated that PUP-2 does not co-localize with CGH-1 (Conserved Germline Helicase - 1), a core component of *C. elegans* processing body-like granules (Fig. 2.S5A; see Supplemental text). We conclude that PUP-2 foci are distinct from processing body-like granules. We also hypothesized that OMA-1/-2 activity might be required for PUP-2 repression in -1, -2, and -3 oocytes. The

OMA-1/-2 translational regulators repress expression of numerous proteins in late-stage oocytes (Robertson & Lin 2015). However, *oma-1/-2(RNAi)* did not prevent the downregulation of PUP-2 in late-stage oocytes (Fig. 2.S5B; see Supplemental text). We conclude that OMA-1/-2 activity is not essential for the decrease in PUP-2 abundance in late-stage oocytes.

2.2.7 PUP-3 expression is elevated in the absence of PUP-1/-2 activity

Although *pup-3* mRNA has a low abundance in the wildtype gonad, its abundance increases substantially in P granule-depleted germ lines (Knutson et al., 2017; Updike et al., 2014). Because of the observed similarities between *pup-1/-2(0)* and P granule-depleted germ lines, we hypothesized that PUP-3 expression might be upregulated *pup-1/-2(0)* mutants. To test this idea, we epitope tagged the endogenous *pup-3* gene (see Materials and methods, Fig. 2.S1D). We readily detected epitope-tagged PUP-3 on protein blots, but not by immunolabeling, and we therefore evaluated PUP-3 abundance by protein blot.

Comparison of 3xHA::PUP-3 abundance in *pup-1/-2(+)* versus *pup-1/-2(0)* animals raised at 25°C revealed a significant increase in 3xHA::PUP-3 abundance, averaging ~1.6-fold, in *pup-1/-2(0)* F2 (M-Z-) adults relative to controls (Fig. 2.5). In strains raised at 20°C, we did not observe a significant increase in PUP-3 abundance in the absence of PUP-1 and PUP-2 (Fig. 2.S7). This temperature sensitive increase in PUP-3 abundance is consistent with the general pattern of more severe *pup-1/-2(0)* defects at elevated culture temperature.

Given our phenotypic suppression data, we hypothesized that 3xHA::PUP-3 abundance is elevated in the *pup-1/-2(0)* germ line at 25°C. To test this, we assayed 3xHA::PUP-3 in strains where germline size was greatly reduced due to a *glp-1(ts)* mutation. At 25°C, GLP-1 (germline proliferation defective – 1)/Notch signaling activity is severely reduced in *glp-1(bn18ts)* mutants;

all germline stem cells enter meiosis prematurely during larval development and adults typically contain only mature sperm (Kodoyianni et al., 1992). In our experiments, L1 larvae were upshifted to 25°C and harvested as adults in order to facilitate a direct comparison of all genotypes, including the *glp-1(bn18ts)* mutants that cannot be propagated at 25°C. PUP-3 abundance was not significantly reduced in *glp-1(bn18)* mutants compared with controls, suggesting PUP-3 expression is primarily somatic (Fig. 2.5B). Further, PUP-3 abundance was not significantly elevated in *glp-1(bn18) pup-1/-2(0)* mutants compared with *pup-1/-2(0)* mutants (Fig. 2.5B), indicating the elevated 3xHA::PUP-3 abundance in *pup-1/-2(0)* mutants is germline-dependent.

2.3 DISCUSSION

This study demonstrates the importance of poly(U) polymerase activity in *C. elegans* germline

development. Under conditions of temperature stress, PUP-1 and PUP-2 activities together

maintain germ cell identity and viability during larval development and ensuring production of

quality gametes and offspring viability. Despite their developmental redundancy, PUP-1 and

PUP-2 localize to distinct subcellular sites and may act at different points in the RNA processing

network and/or have complementary roles in regulating the abundance of target RNAs in the

germ line. Ultimately, their activities ensure expression of germline genes and limit expression

of somatic genes, thereby ensuring germline viability and gametogenesis. Target RNAs may

include both mRNAs and small RNAs. One (direct or indirect) outcome of PUP-1 and PUP-2

activity is to limit the expression of PUP-3, and overexpression of PUP-3 in turn contributes to

the loss of germline viability and identity (Fig. 2.7).

2.3.1 Germ cell identity and survival

A number of factors are known to ensure germ cell identity during larval development as well as

viability of the germline over successive generations, including certain histone modifying

enzymes, e.g., H3K4 demethylase, SPR-5(Katz et al., 2009; Käser-Pébernard et al., 2014), and

H3K4 methyltransferase, SET-2 (Robert et al., 2014; Xiao et al., 2011), and the heritable nuclear

RNAi (NRDE) pathway (Buckley et al., 2012; Sakaguchi et al., 2014). PUP-1 and PUP-2

provide examples of RNA regulators important for germ cell viability and identity. Previous

studies have linked RNA regulation to germ cell identity, although in these cases germline

defects are severe and the animals are sterile. Notably, germ cell identity is severely

compromised by the simultaneous loss of two broadly active translational regulators, MEX-3 and GLD-1 (Ciosk et al., 2006), and by depletion of P granules, a type of germline-specific RNP particle thought to function in regulation of RNA stability (Knutson et al., 2017; Updike et al., 2014). We hypothesize that the transgenerational germ cell loss we observe in *pup-1/-2(0)* mutants reflects a subtler misregulation of gene expression that compounds over successive generations until the germ line senesces.

2.3.2 Germline development relies on the correct balance of PUP activity

Although redundant for developmental function, evidence suggests that PUP-1 and PUP-2 are not strictly redundant with respect to their target RNAs. PUP-1 and PUP-2 have previously been implicated as modifying certain siRNAs and miRNAs, respectively (Billi et al., 2014). We observed PUP-1 and PUP-2 in distinct subcellular foci and hypothesize that their modification of siRNA and miRNA may occur at these distinct sites. Indeed, associate with P granules where they would be available as substrates for PUP-1(Billi et al., 2014). Alternative models consistent with our data are (1) PUP-1 and PUP-2 act in parallel to regulate distinct targets that have complementary roles in germline development, (2) PUP-1 and PUP-2 share some targets that are essential for germline development, or (3) a combination of the two. In any case, one consequence of PUP-1/PUP-2 activity is to limit accumulation of PUP-3, and overexpression of PUP-3 contributes to the loss of germline viability.

In addition to small RNAs, PUP-1 and/or PUP-2 may also modify mRNAs – as do their orthologs in other species - and that regulation could occur either pre- or post-translation. Most RNAs transcribed in germ cells are thought to associate with P granules upon nuclear export, where they would be available for modification by PUP-1. PUP-1 may uridylate somatic

mRNAs to limit/prevent their expression in the germ line. In contrast, PUP-2 apparently targets RNAs that have moved from the P granule to dispersed cytoplasmic foci. MiRNAs – and some siRNAs – are found in RNA processing bodies along with mRNAs whose translation is repressed (Parker and Sheth, 2007; Voronina et al., 2011). PUP-2 does not co-localize with the core component, CGH-1, and is presumably not located in RNA processing bodies. One possibility is that it may associate with and target RNAs as they are being shuttled to processing bodies. PUP-2 may limit the expression of RNAs that escape PUP-1 control at the P granule.

PUP-3 activity appears to be predominantly somatic, although its activity nonetheless contributes to fertility when PUP-1 and PUP-2 are present. In the absence of PUP-1/-2, PUP-3 abundance is elevated and it activity is detrimental to germline development. Together, these results are consistent with the hypothesis that germline development is highly sensitive to the balance of PUP activity. Comprehensive identification of PUP target RNAs in the future will resolve the relationship among these three enzymes with respect to germline gene expression.

2.4 MATERIALS AND METHODS

Nematode strains and culture

Strains were cultured using standard methods (Epstein & Shakes 1995). The *C. elegans* wildtype

Bristol variant (N2) and mutations used are as listed in Wormbase or described in the text.

Mutations used were: LG (linkage group) I: *fog-1(q253ts), pup-3(tm5089);* LGIII: *pup-1(tm1021), pup-1(gg519)*, *pup-2(tm4344), pup-1/-2(om129)* (this study), *pup-1/-2(om130)* (this

study). The following balancer was used: *qC1[dpy-19(e1259ts) glp-1(q339)]* (III). The

following transgene insertions were used: *wgIs428 [cid-1::TY1::EGFP::3xFLAG + unc-119(+)]*, *otIs117 [unc-33p::gfp]*, *edIs6 [unc-119::gfp]* containing the *unc-119* promoter and

encoding amino acids 1-101 of UNC-119 fused to GFP, *otIs45 [unc-119p::gfp]*, *otIs355 [rab-3::NLS::tagRFP]*, DUP64 *[glh-1::gfp]*, DUP75 *[pgl-1::gfp]*, *ltIs37 [his-58::mCherry]*.

Endogenous genes were epitope-tagged via CRISPR-Cas9 genome editing to produce *omIs7 [3xflag::pup-2]*, *omIs8 [pup-1::3xmyc]*, *omIs9 [3xHA::pup-3]*, and *omIs10 [3xflag::pup-3]*. See

Fig. 2.S1. Strain EL629 carries *pup-1::3xmyc* and *3xflag::pup-2*. Strain EL655 carries all

3xha::pup-3; pup-1::3xmyc 3xflag::pup-2. Strains carrying multiple mutations were confirmed

by PCR and/or sequencing, as appropriate.

CRISPR-Cas9 genome editing

Mutations were generated and epitope tags were added to endogenous genes via a CRISPR-Cas9

genome editing approach using a co-conversion strategy where a dominant co-inserted marker

gene mutation, *dpy-10(cn64),* was used to enrich for F1 individuals containing genome-editing

events (Arribere et al., 2014; Paix et al., 2014). In all injection mixtures, the Cas9 plasmid

[pDD162 (Dickinson et al., 2013)] was present at 50ng/ul, *dpy-10(cn64)* template DNA was present at 25ng/ul, gene of interest template DNA was present at 50ng/ul, and each sgRNA construct was present at 25ng/ul. Progeny of injected animals were screened via DNA amplification using the method described (Arribere et al., 2014). Candidate CRISPR-Cas9 genome editing events were confirmed by sequencing. To generate *pup-1 pup-2* double deletion alleles, we used a strategy designed to delete ~14.7 kb of genomic DNA beginning in *pup-1* exon 1 and ending in *pup-2* exon 6 (Fig. 2.S1A). We retained the 3' portion of *pup-2* because we did not want to disturb the nearby downstream gene, K10D2.8. We characterized two deletions, *pup-1/-2(om129)* and *pup-1/-2(om130)*, in detail and found that they have a similar phenotype (Table 2.1, Table 2.S2).

RNAi

RNAi was conducted using the feeding method as described (Timmons et al., 2001). For *pup-1* and *pup-2* RNAi experiments, gravid hermaphrodites were placed onto each bacterial "feeding" strain at 20°C for 1 hour and then removed. F1 progeny were allowed to develop at 25°C and analyzed at the appropriate stage. For *oma-1/-2* RNAi experiments, L1 hermaphrodites were placed onto plates seeded with a mixture of *oma-1* and *oma-2* "feeding" bacteria and allowed to develop at 25°C.

Immunocytochemistry

Immunolabeling experiments were performed as described (Guo et al., 2015; Maine et al., 2005; She et al., 2009) although with optimized fixation conditions. For single anti-FLAG, anti-MYC, and anti-HA labeling and co-labeling with anti-FLAG/anti-MYC and anti-MYC/anti-EKL-1, the

tissue was fixed in 3% PFA/PBS for 10 min and post-fixed in -20°C methanol for 10 min. For

single anti-CGH-1 labeling and anti-FLAG/anti-CGH-1 co-labeling, the tissue was fixed in 3%

PFA/PBS solution for 1 hr and post-fixed in -20°C methanol for 5 min. Antibodies were used at

the indicated dilution: mouse anti-FLAG (Sigma), 1:200; rabbit anti-MYC (ThermoFisher

Scientific), 1:200; rabbit anti-CGH-1 (gift from Dr. David Greenstein), 1:5000; rabbit anti-EKL-

1 (this study), 1:100; chicken anti-GLH-2 (gift from Dr. Karen Bennett), 1:100. Polyclonal

antiserum against the C-terminal portion of EKL-1 (amino acid residues 587-606,

DKDEAVRAAFSQKEPIEWPN) was generated in rabbits and affinity purified

(YenZym). Alexa Fluor 488-conjugated goat anti-mouse (1:200), Alexa Fluor 568-conjugated

donkey anti-rabbit (1:200), and Alexa Fluor 568-conjugated donkey anti-chicken (1:1000)

secondary antibodies were used.

DAPI staining and characterization of germlines

For DAPI staining intact animals, adults were fixed with -20°C methanol for 10 min, stained

with 0.2 µg/ml DAPI for 10 min, mounted in VECTASHIELD medium (Vector Laboratories),

and observed with a Zeiss Axioscope or Leica DM5500 microscope. Mitotic and meiotic nuclei

were identified based on nuclear morphology as described (Francis et al., 1995; Qiao et al., 1995;

Shakes et al., 2009; Smardon et al., 2000). For pan-neuronal reporters (i.e., *unc-33p::gfp* and

unc-119::gfp), dissected gonads were fixed in 3% paraformaldehyde/1XPBS for 5 min prior to

DAPI staining and visualization of the GFP signal. For *rab-3p::gfp* reporter, intact adults were

mounted on 2% agar pads with 10% sodium azide and visualized using fluorescence microscope.

Brood size analysis

Brood size was assayed using standard methods as described (Safdar et al., 2016). Individual L4 larvae were placed onto single plates; once they became gravid adults, they were transferred to fresh plates daily until they no longer produced embryos. Embryos were counted immediately after the adult was moved. Viable progeny were counted as L3-L4 larvae. Animals were evaluated for fertility in the first day of adulthood.

Protein blot analysis

Protein extracts were generated as follows. Synchronized animals were harvested at adulthood in M9 buffer, pelleted, resuspended in 2X Leammli buffer (BioRad) with 5% (v/v) 2-mercaptoethanol, and boiled for 10 min. Tissue debris was removed by centrifugation and supernatants were transferred to new tubes. Proteins were resolved by SDS-PAGE on a 10% separating gel and transferred to nitrocellulose membrane (BioRad). Membrane was incubated overnight at 4°C with either anti-HA (Roche) or anti-b-tubulin (DSHB) antibody diluted 1:500 into 5% (w/v) powdered milk/PBS solution, incubated 2h at room temperature with anti-mouse HRP-conjugated secondary antibody (Thermo Fisher) diluted 1:2000 in 5% milk solution, and visualized by Pierce SuperSignal West Femto (3xHA::PUP-3) or Pico (b-tubulin) detection substrate. Membranes were probed first for 3xHA::PUP-3 and then reprobed for b-tubulin. To reprobe, membranes were stripped in 1.5% (w/v) glycine, 0.1% (w/v) SDS, 1% (v/v) Tween-20, pH 2.2, buffer at 37°C with shaking for 10 min, washed 2X with PBS for 10 min, 1X with TBST for 5 min, and blocked in 5% milk/PBS solution.

Quantification analysis was performed using Image J. Background signal was subtracted from each 3xHA::PUP-3 signal, and the resulting value was normalized to the matching b-tubulin

signal from that protein sample. To address the variation of overall signal intensity due to

kinetics of the ECL enzymatic reaction across different biological replicates, we performed a

second normalization relative to the 25°C *3xha::pup-3* strain signal on the same membrane. The

normalized values for each genotype were averaged across replicates and the SEM was

calculated. To evaluate variation within the 3xHA::PUP-3 25°C control itself, we calculated the

average and SEM of the b-tubulin-normalized 3xHA::PUP-3 25°C signals.

2.5 SUPPLEMENTARY TEXT

Comparison of *pup-1(tm1021)* and *pup-1(gg519)*

After we had completed our analysis of *pup-1(tm1021)*, it was reported that another deletion allele, *pup-1(gg519)*, becomes 100% sterile in two generations at 25°C (Spracklin et al., 2017). This report led us to do a side-by-side comparison of the two mutants. We obtained homozygous *pup-1(gg519)* mutant strain from the Kennedy lab and generated a balanced *pup-1(gg519)/qC1gfp* strain. We then analyzed brood sizes and germline phenotypes of M+Z- and M-Z- offspring at 25°C following the same protocol we had used for *pup-1(tm1021)*. Although brood sizes are generally smaller than for *pup-1(tm1021)*, embryonic viability is the same and we were able to maintain the strain for 9-10 generations at 25°C. We also note that these animals did not exhibit the germ cell loss phenotype, but instead appeared to be sterile due to gametogenesis defects (Fig. 2.S2). *pup-3(0)* substantially suppressed the brood size defect and sterility (Fig. 2.S2), as was observed for *tm1021.* We also amplified and sequenced the *pup-2* gene present in the *gg519* strain in order to eliminate the possibility of a *pup-2* mutation that might contribute to the strain phenotype. We did not detect a mutation in *pup-2*. Based on our experience with other *pup* alleles, we suspect that maintaining *gg519* as a homozygote indefinitely at lower culture temperatures led to a gradual reduction in fertility that contributed to the rapid loss of fertility at 25°C as reported (Spracklin et al., 2017).

Embryonic development relies on both maternal and zygotic *pup-2* expression

We noted a difference between *pup-1(0)* and *pup-2(0)* with respect to embryonic lethality at 25°C. *pup-1(0)* embryonic lethality was strictly maternal-effect: viability of *pup-1* M+Z-

embryos produced by *pup-1/qC1* heterozygous mothers was not significantly different from *pup-1(+)* progeny of *pup-1(+)/qC1* controls. In contrast, *pup-2* embryonic lethality had a minor zygotic component: the viability of *pup-2* M+Z- embryos produced by *pup-2(0)/qC1* mothers was ~88% of wildtype (84% overall, Table 2.S2). Statistical analyses indicated that *pup-2(0)* M+Z- viability is significantly lower than wildtype. However, embryonic viability is not significantly different for either wildtype or *pup-2(0)* M+Z- compared with *pup-1/-2(0)* M+Z-. We conclude that expression of the embryonic *pup-2* gene has a minor role in embryonic development viability.

PUP-2 does not localize to processing bodies

C. elegans germ cells contain dispersed cytoplasmic ribonucleoprotein particles called P (processing) body-like granules that, like P bodies in other species, are implicated in regulating mRNA stability and translation (Draper et al., 1996; Huelgas-Morales et al., 2016; Jud et al., 2008; Noble et al., 2008; Schisa et al., 2001; Silva-García and Estela Navarro, 2013; Subramaniam and Seydoux, 1999; Voronina et al., 2011). To investigate whether PUP-2 associates with P body-like granules, we double-labeled PUP-2 and CGH-1 in dissected gonads from hermaphrodites raised at 20° and 25°C (see Materials and methods). At each temperature, 3xFLAG::PUP-2 and CGH-1 localized to distinct foci (Fig. 2.S5A, data not shown). Therefore, PUP-2 aggregates are distinct from P body-like granules. Consistent with this observation, we do not see a major reorganization of PUP-2 foci at elevated temperatures as is observed for P body-like granules.

PUP-2 downregulation in late-stage oocytes is not OMA-1/-2 - dependent

The sharp drop in PUP-2 signal in late-stage oocytes is similar to the pattern observed for LIN-41, a TRIM-NHL protein, whose expression is negatively regulated by the redundant OMA-1/-2 zinc finger proteins required for oocyte maturation (Detwiler et al., 2001; Spike et al., 2014). OMA-1/-2 control translation in oocytes in a 3'UTR-dependent manner, and *pup-2* mRNA was identified as a candidate target of OMA-1/-2-mediated translational repression (Spike et al. 2014b). We investigated whether expression of 3xFLAG::PUP-2 protein increases in late-stage oocytes when OMA-1/-2 are knocked down by RNAi. In our hands, *oma-1(RNAi); oma-2(RNAi)* treatment triggered the phenotype described in (Detwiler et al., 2001), including accumulation of late-stage oocytes in the oviduct and absence of embryos in the uterus (Fig. 2.S5B). The 3xFLAG::PUP-2 level decreased in these late-stage oocytes in a manner similar to what we observed in controls (Fig. 2.S5B). We conclude that OMA activity is not essential for the decrease in PUP-2 abundance in late-stage oocytes.

2.6 TABLES

Table 2.1. *pup* **mutations impair germline development and embryogenesis**

Genotype	Maternal Gen	Avg clutch size $\pm$ SEM	As % of Wt	Progeny Gen	% Progeny	
					Viable	Male
WT	F1	144±11		F2	100	0.1
	F2	140±15		F3	100	0.1
	F3	132±12		F4	100	0.1
pup-1(tm1021)	F1	73 ±11	51	F2	89	1.0
	F2	65 ±15	46	F3	89	1.0
	F3	67 ±7	51	F4	86	1.0
pup-2(tm4344)	F1	78±10	54	F2	78	1.0
	F2	44±9	31	F3	75	0.9
	F3	48±7	36	F4	77	1.0
pup-1/-2(om129)	F1	48±4*$	33	F2	82	1.0
	F2	9±2*$	6	F3	44	4.0
	F3	0*$	0	F4	n.a.	n.a.
pup-1/-2(om130)	F1	35±3*$	24	F2	56	1.0
	F2	6±2*$	4	F3	28	3.0

	F3	$0^{*\$}$	0	F4	n.a.	n.a.
pup-3(tm5089)	F1	96±11	67	F2	99	0.1
	F2	66±11	47	F3	98	0.1
	F3	63±11	48	F4	97	0.1
pup-3(tm5089); pup-1(tm1021)	F1	73±7	51	F2	93	0.1
	F2	$57±7^{*\#}$	41	F3	93	0.2
	F3	37±6	28	F4	92	0.2
pup-3(tm5089); pup-2(tm4344)	F1	$122±7^{\$}$	85	F2	98	0.1
	F2	55±6	39	F3	90	0.2
	F3	44±10	33	F4	88	0.2
pup-3(tm5089); pup-1/-2(om129)	F1	$24±6^{\#\&}$	17	F2	79	4.0
	F2	$11±3^{\#}$	8	F3	62	1.4
	F3	$1±0.5^{\#}$	1	F4	0	0

Experiments were performed at 25°C. Gen, generation. Clutch size is the total number of viable

and inviable progeny produced by the individuals of the generation listed as Maternal Gen.

The % viable offspring and males in each clutch is listed to the right under % Progeny. F1

represents the first generation produced by heterozygous mothers, designated M+Z- in the text.

F2 and subsequent generations are M-Z-. To summarize: *pup/qC1* → F1 *pup* M+Z- → F2 *pup*

M-Z- → F3 *pup* M-Z- → etc. *pup-1/qC1* brood size data are listed in Table S1. N=10-57

complete clutches were counted for each genotype and generation. A one-way ANOVA plus

Dunnett's multiple comparison post-ANOVA test indicates that the average clutch size for each

mutant is significantly different from wildtype of the same generation ($P<0.01$). * indicates

$P<0.05$ compared to *pup-1* mutant of the same generation. $ indicates $P<0.05$ compared to *pup-2* mutant of the same generation. # indicates $P<0.05$ compared to *pup-3* mutant of the same

generation. & indicates $P<0.05$ compared to *pup-1/-2(om129)* mutant of the same generation.

Progeny viability and % male offspring were calculated as follows: $viability = \frac{\sum viableprogeny}{\sum clutchsize}\%$; $male\% = \frac{\sum viablemales}{\sum viableprogeny}\%$.

Table 2.S1. Viability and fertility of *pup* mutants at 20°C

Genotype	Maternal Gen	Avg. clutch size ± SEM	% Progeny viable	% Progeny sterile
WT	F1	260±9	99	2
	F2	268±10$^{\wedge}$	97	12
	F3	257±4$^{\wedge}$	80	17
pup-1(tm1021)	F1	214±19	99	2
	F2	188±23$^{\wedge}$	97	12
	F3	177±21$^{\wedge}$	80	17
pup-2(tm4344)	F1	260±12	83	1
	F2	212±8$^{\wedge}$	89	3
	F3	211±10$^{\wedge}$	85	3
pup-1/-2(om129)	F1	108±8$^{\wedge*\$}$	80	46
	F2	55±7$^{\wedge*\$}$	55	51
	F3	43±12$^{\wedge*\$}$	58	55

80

Experiments were performed at 20°C. N=10-57 complete clutches were counted per genotype. ^ indicates $P<0.05$ compared to WT of the same generation. * indicates $P<0.05$ compared to *pup-1* mutant of the same generation. $ indicates $P<0.05$ compared to *pup-2* mutant of the same generation.

Table 2.S2. Viability and fertility of *pup* M+Z- individuals

Genotype	Avg. clutch size ± SEM	% Progeny viable	% Sterile non-green progeny
pup(+)/qC1g	95±7	95	0
pup-1(tm1021)/qC1g	99±10	98	0
pup-2(tm4344)/qC1g	121±8	84[^]	0
pup-1/-2(om129)/qC1g	109±14	87	0

Experiments were performed at 25°C. Clutch size includes the total number of viable and inviable progeny of three offspring genotypes: *pup/pup*, *pup/qC1g*, and *qC1g/qC1g*. Non-green progeny are *pup/pup* M+Z- offspring of the *pup/qC1* mother. N=12-24 complete clutches were counted per genotype. A one-way ANOVA plus Dunnett's multiple comparison post-ANVOA test indicates that the average clutch size for each mutant has no significant difference from *pup(+)/qC1*. ^ indicates P<0.05 calculated by Z-test compared to *pup(+)/qC1* (*P*<0.05).

2.7 FIGURES

Figure 2.1. PUP activity is critical for germline development. (A) Histograms indicate the % fertile and sterile adults produced in the F1 (M+Z-), F2 (M-Z-), and F3 (M-Z-) generation at 25°C. Adult sterile hermaphrodites were classified as containing (i) germ cells, including sperm and/or oocytes, (ii) germ cells, but no gametes, or (iii) no germ cells.

(B) Representative images of DAPI-stained F3 *pup-1/-2(0)* hermaphrodites raised at 25°C. Top panel, L3 (~27 hr post-L1) gonad containing germ cells is outlined with a dotted line. Middle panel, L4 larva (~35 hr post-L1) lacks germ cells. Bottom panel, adult lacks germ cells. (C) Examples of defects observed in F2 *pup-1/-2(0)* hermaphrodites at 25°C. (i) Arrowheads indicate endomitotic oocyte nuclei in the uterus, adjacent to the vulva. (ii) Nuclei abnormally positioned in the rachis. (iii) Disorganized germ cells. *, distal tip; gonad arm is outlined with a dotted line. Scale bar = 16µm.

A

B

L3 gonad

Late L4 larva

vulva

Adult

vulva

C

(i)

vulva

(ii)

(iii)
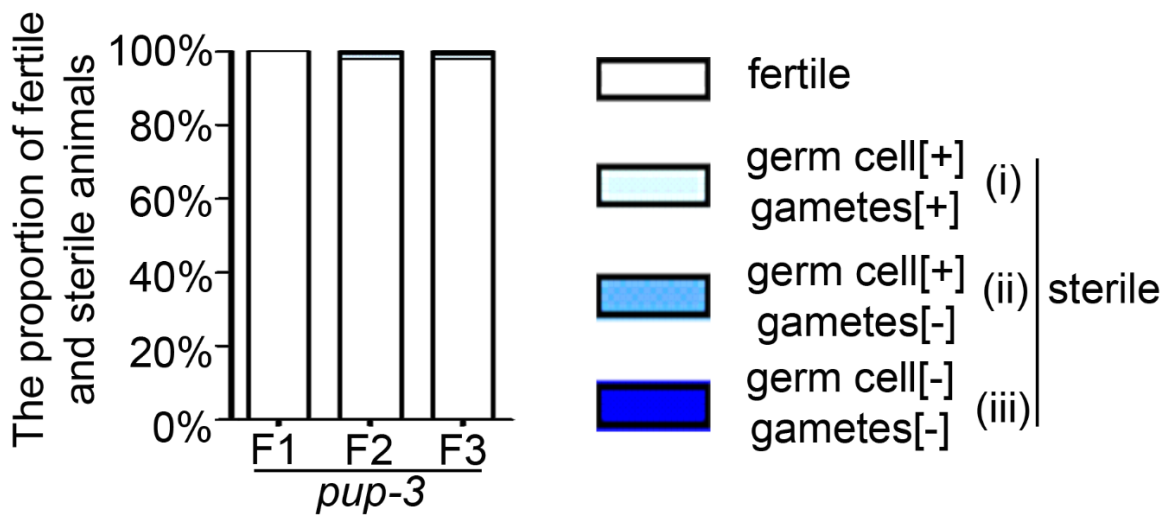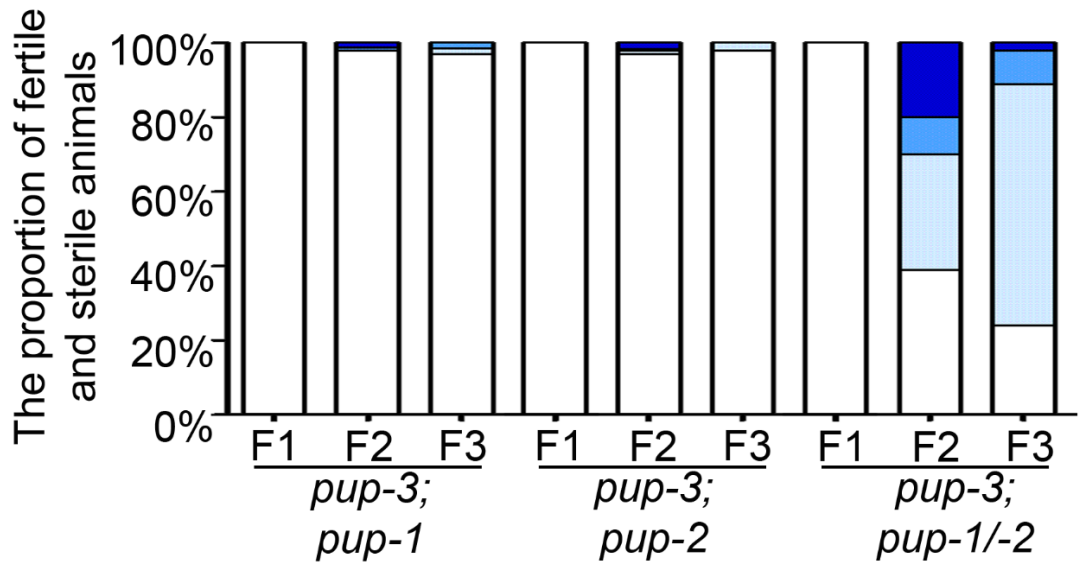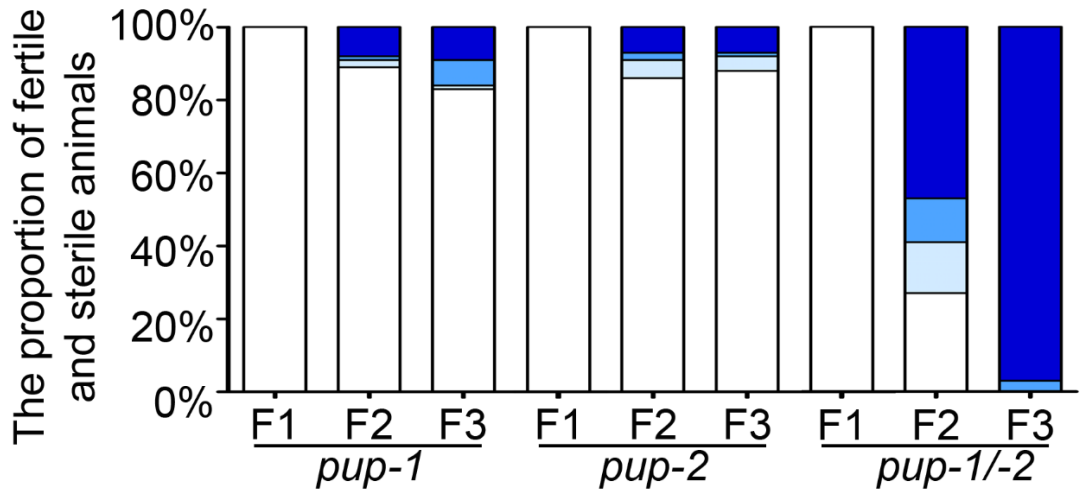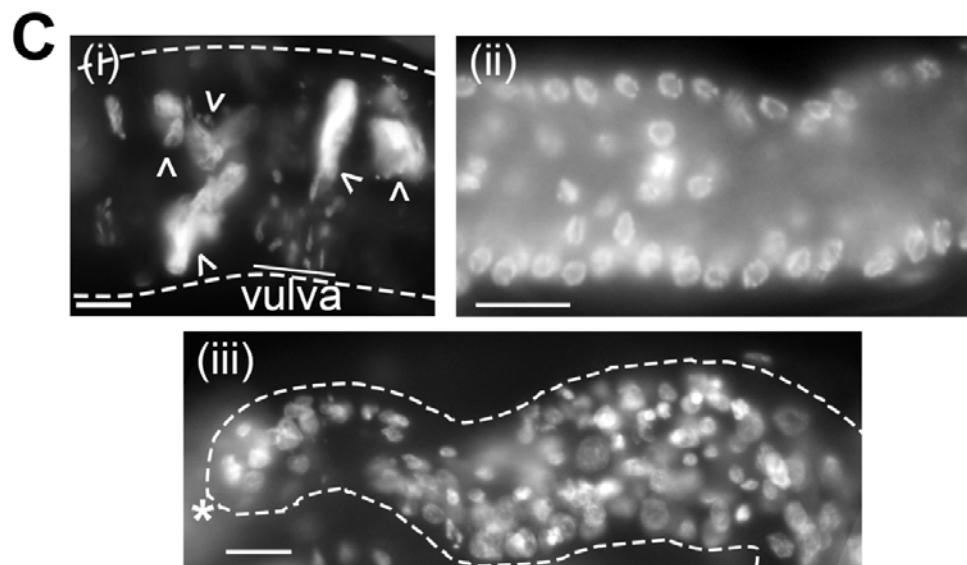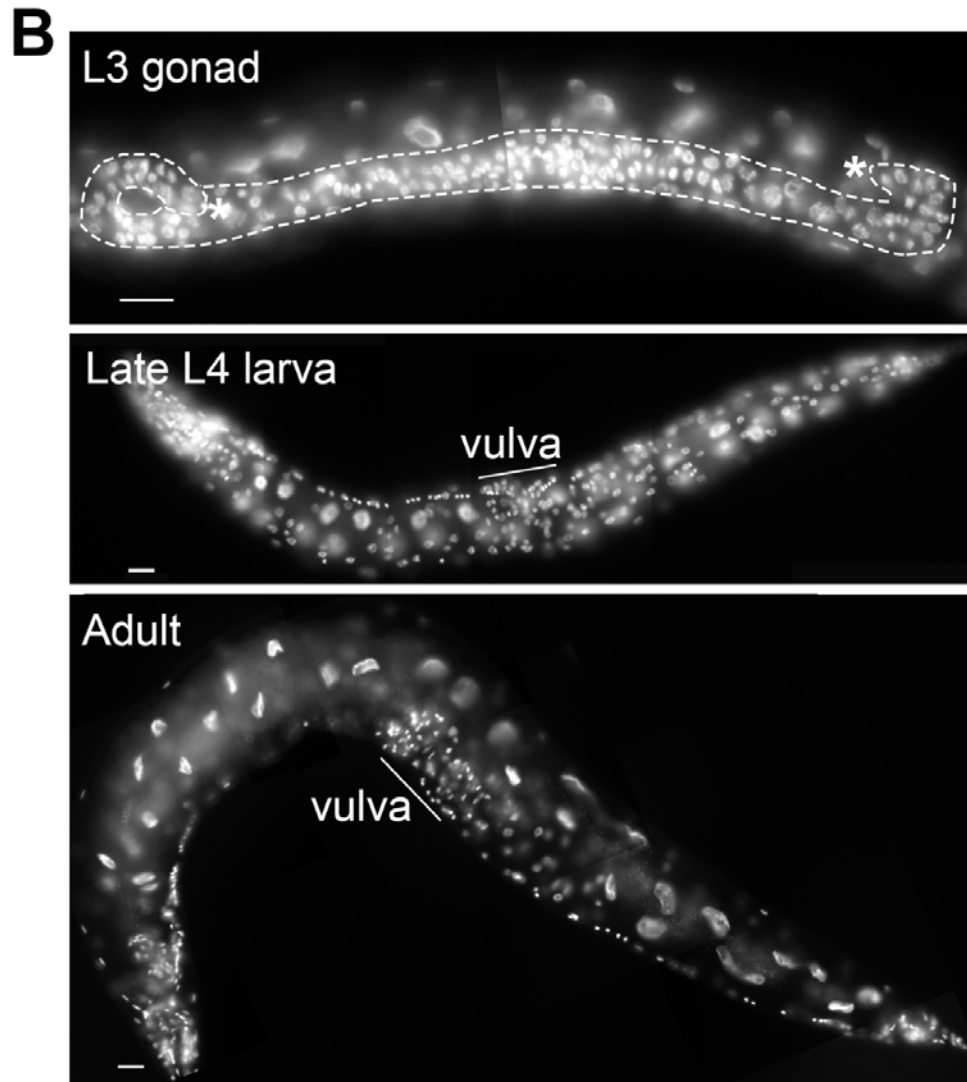
Figure 2.2. *pup-1/-2(0)* **males exhibit fertility defects at 25°C.** (A) Box-and-whiskers plots of viable offspring produced by *fog-1* females mated with wild-type or *pup-1/-2(0)* males, as indicated (n = 18 experimental and 7 control crosses). Box represents the middle 50% of values; line represents the 50th percentile (median) value; bars indicate the full range of values. (B) A representative image of DAPI-stained oocytes in a *fog-1* female after mating to a *pup-1/-2(0)* male. Arrowheads indicate endomitotic oocyte nuclei; arrows indicate sperm transferred in the mating. (C) Representative DAPI-stained germlines of wildtype control male and *pup-1/-2(0)* male used in the mating assay. Gonads are outlined with a dotted line. Insets, sperm nuclei. Note the *pup-1/-2(0)* male sperm are variable in size, presumably reflecting different degrees of chromatin compaction.
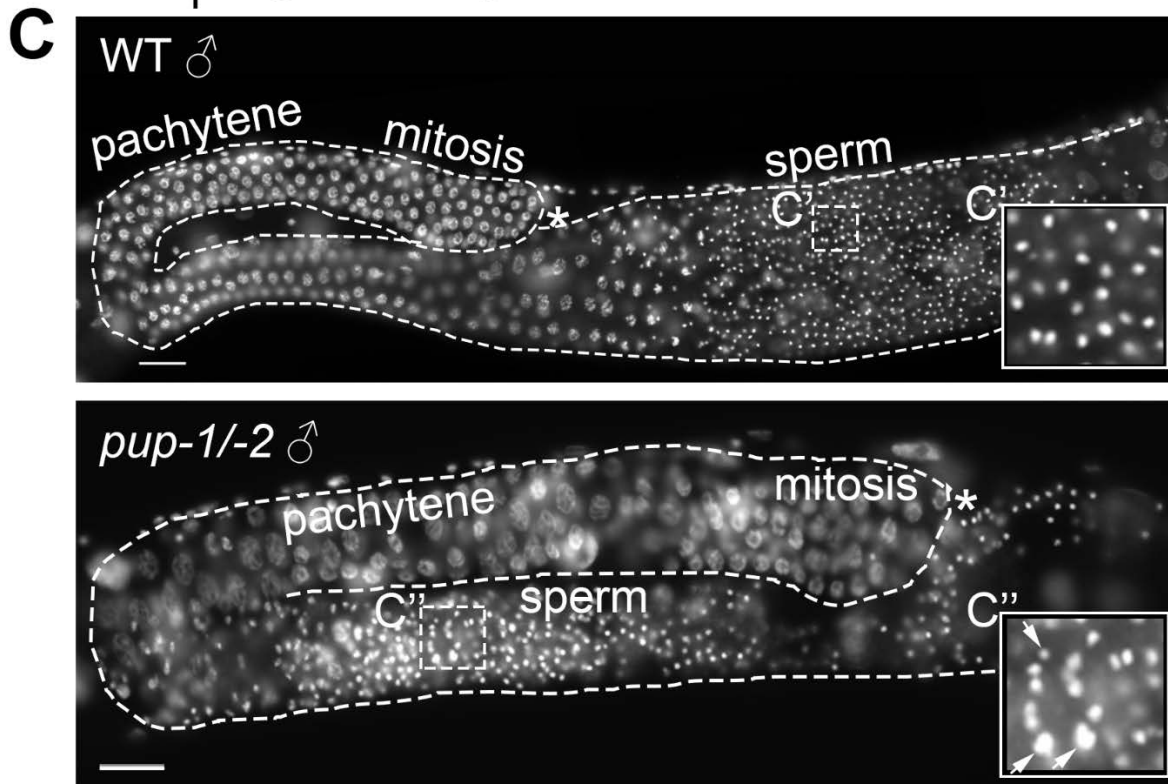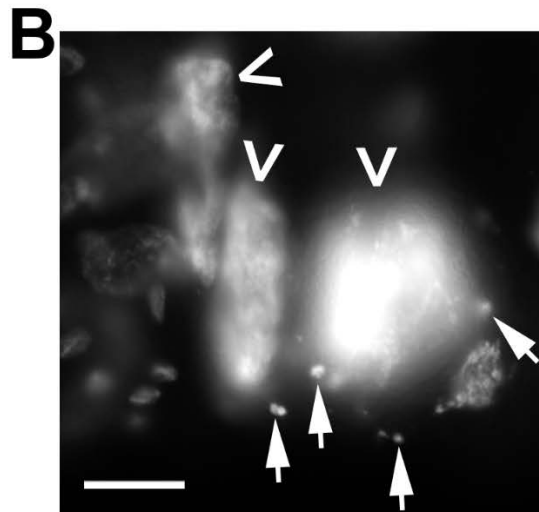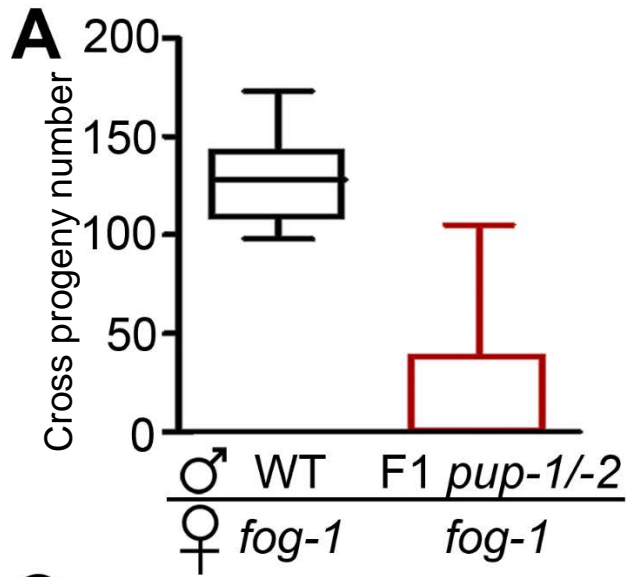
Figure 2.3. Compromised gene expression in the *pup-1/-2(0)* mutant germ line. (A-D) Expression of the pan-neuronal *unc-33p::gfp* transgene was evaluated in animals raised at 22°C (see text). (A) *unc33p::gfp* expression was not detected in otherwise wildtype germ cells. (B) *unc33p::gfp* expression was detected in 53% of fertile and 100% of sterile *pup-1/-2* F2 (M-Z-) germ lines. GFP abundance was relatively high in 83% of sterile germ lines and limited to cortical cytoplasm. (C) Uniform low *unc-33p::gfp* expression was observed in 95% of *pup-3(0)* germlines. Localized regions of stronger expression were observed in 5% of *pup-3(0)* germ lines. (D) *unc-33p::gfp* expression was substantially reduced in *pup-3;pup-1/-2* F2 (M-Z-) germ lines compared with (B). GFP was detected at a low level in cortical cytoplasm in 59% of germ lines; in addition, GFP puncta were observed in the cytoplasmic core (rachis) of the germ line in 65% of gonad arms. (E-F) Expression of P granule proteins, PGL-1::GFP and GLH-1::GFP, was evaluated in animals raised at 25°C. (E) PGL-1::GFP and GLH-1::GFP expression was reduced and less uniform in *pup-1/-2(0)* M+Z- and M-Z- germ cells relative to controls. Circles indicate nuclei where PGL-1 or GLH-1 expression is very low/absent. M-Z- germlines contain large patches with little/no detectable GLH-1 or PGL-1 expression. (F) PGL-1::GFP and GLH-1::GFP expression generally appear normal in *pup-3(0)*, consistent with the >99% fertility of this strain.

A WT

unc-33p::GFP — 100%

B *pup-1/-2*

F2 fertile — 47%, 53%

F2 sterile — 83%, 17%

C *pup-3* — 95%, 5%

D *pup-3;pup-1/-2* — 41%, 59%, 65% rachis

E WT

GLH-1::GFP

PGL-1::GFP

pup-1/-2

GLH-1::GFP M+Z-

GLH-1::GFP M-Z-

PGL-1::GFP M+Z-

PGL-1::GFP M-Z-

F *pup-3*

GLH-1::GFP

PGL-1::GFP
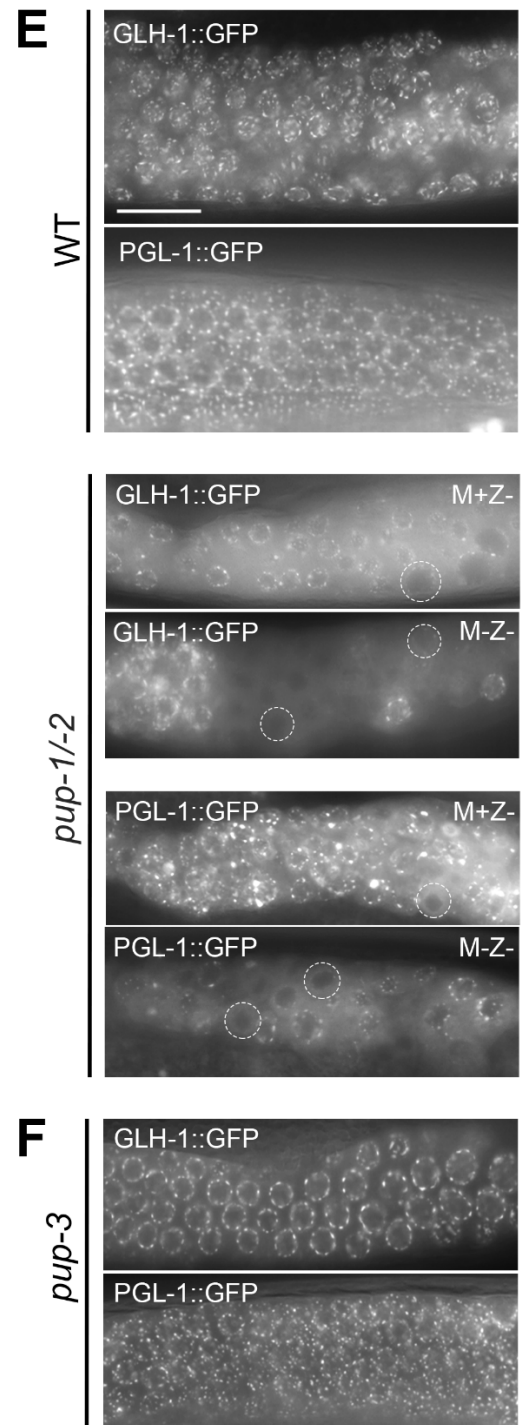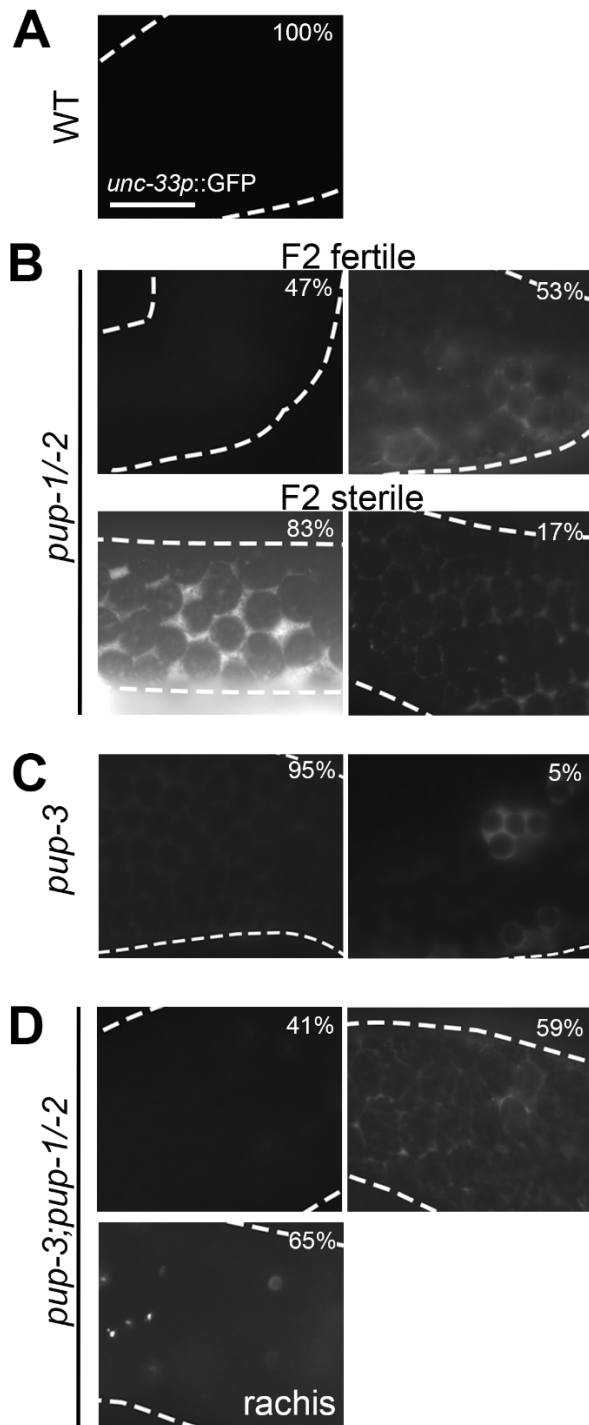
Figure 2.4. PUP-1 and PUP-2 have distinct expression patterns. (A) Image shows a dissected adult hermaphrodite gonad labeled with anti-MYC and anti-FLAG to visualize the relative distribution of PUP-1::3xMYC and 3xFLAG::PUP-2 in the germ line. The gonad is outlined with a dotted line. PUP-1::3xMYC is observed throughout the gonad, and 3xFLAG::PUP-2 is detected primarily in diplotene-diakinesis stages. (B) Higher magnification view of PUP-1::3xMYC and 3xFLAG::PUP-2 distribution in pachytene and diakinesis regions of the hermaphrodite germ line and pachytene and condensation zones of the male germ line. PUP-1 puncta are perinuclear; PUP-2 puncta are more evenly distributed throughout the cytoplasm. Little no overlap is observed. (C) Co-localization of PUP-1::3xMYC and EKL-1 on P granules. See Figure S3. Scale bar = 16μm.

A

B

	PUP-1::3xMYC	3xFLAG::PUP-2	merge
pachytene XX			
diakinesis XX			
pachytene XO			
condensation zone XO			

C
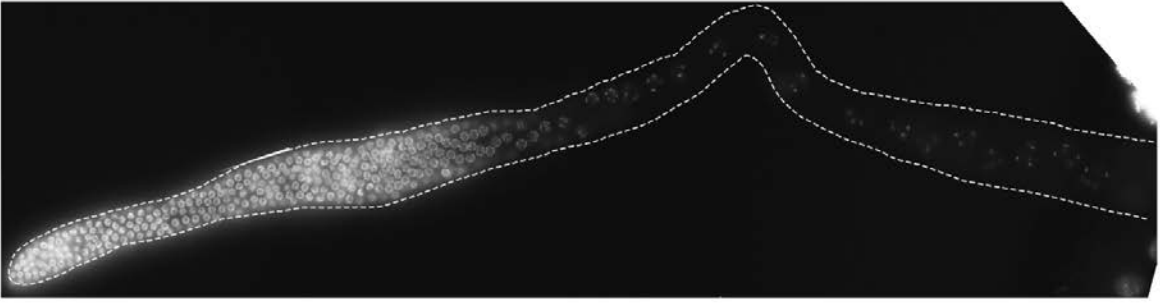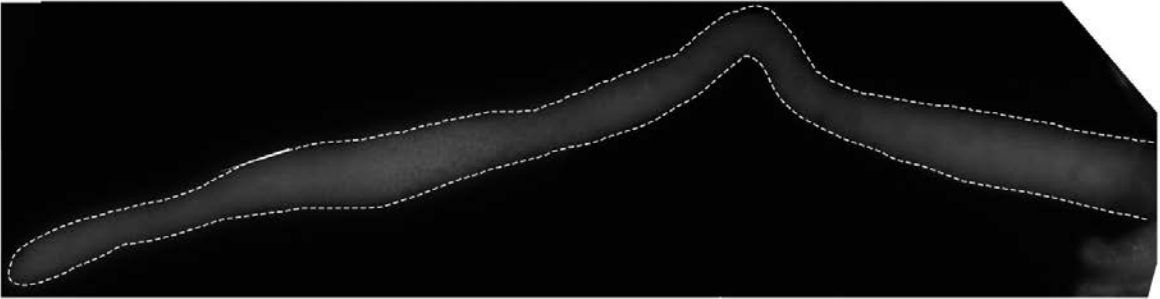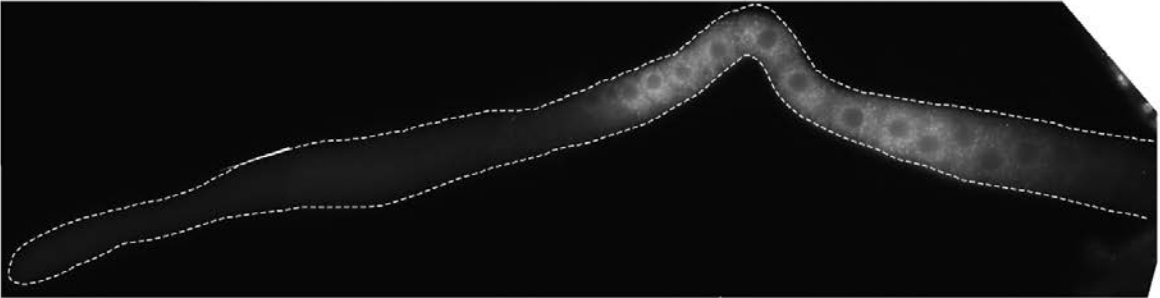
	PUP-1::3xMYC	EKL-1	merge
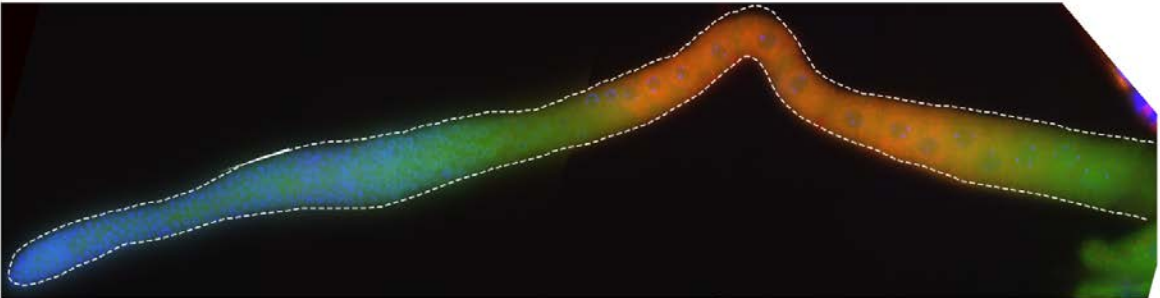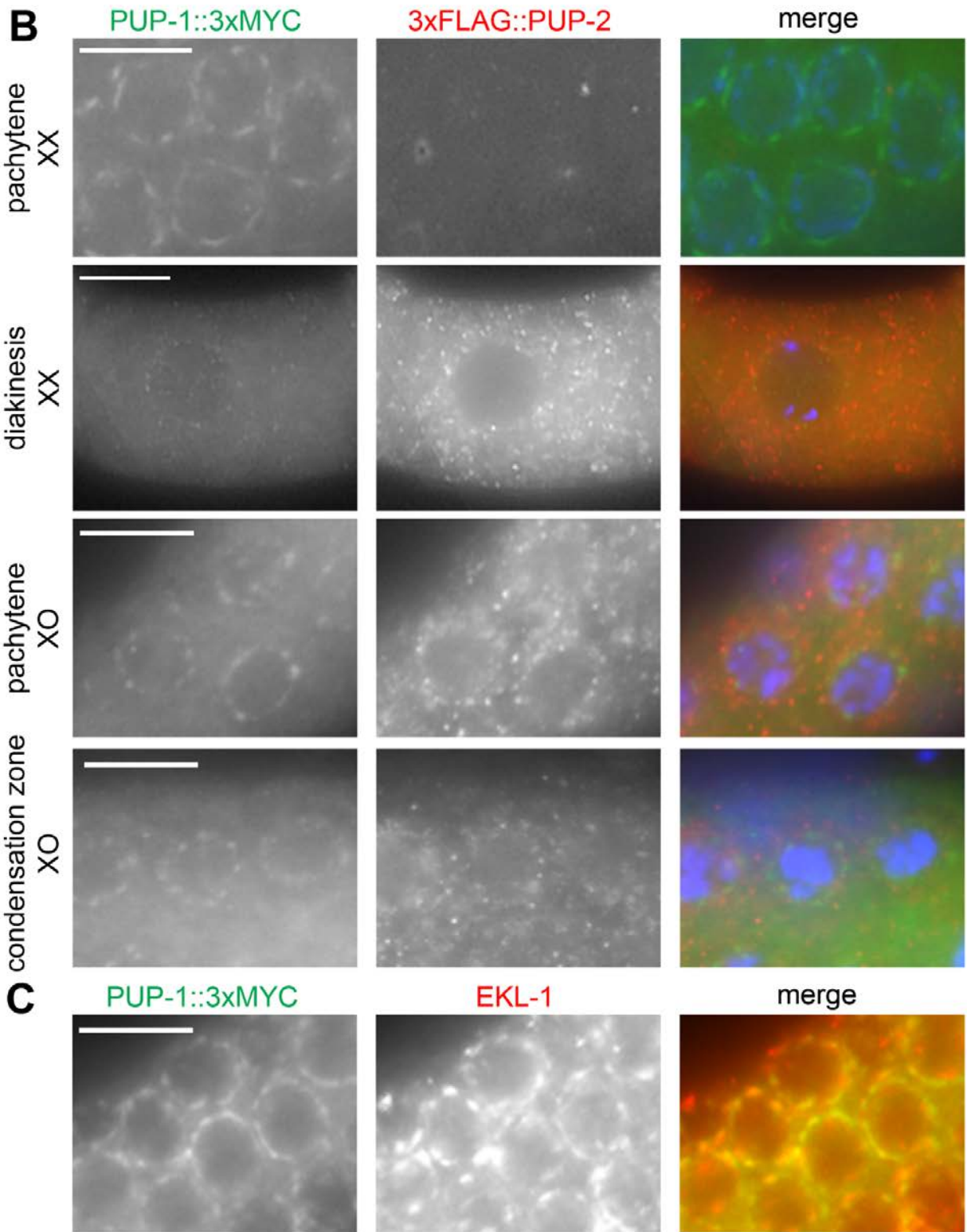
Figure 2.5. 3xHA::PUP-3 is upregulated in *pup-1/-2(0)* mutants. (A) Representative protein

blot generated with protein extracts from adult hermaphrodites of the designated genotypes

raised at 25°C. Blot was immunoprobed with anti-HA to visualize 3xHA::PUP-3 and re-

incubated with anti-b-tubulin as a loading control. Numbers indicate signal intensity minus

background signal as measured by Image J software. (B) Quantification of the 3xHA::PUP-3

abundance in each strain. The 3xHA::PUP-3 signal in each genotype has been normalized to the

3xha::pup-3; glp-1(+) pup-1/2(+) control. See Materials and methods. Error bars indicate $\pm$

SEM. * indicates $P < 0.05$ calculated by one-way ANOVA and Tukey post hoc test. N = 4

biological replicates.

A

~60 kDa > 3xHA::PUP-3

50 kDa > β-tubulin

B

Relative 3xHA::PUP-3 expression (fold over *3xha::pup-3* 25°C)

3xha::pup-3	-/-	+/+	+/+	+/+	+/+
pup-1/-2	+/+	+/+	-/-	+/+	-/-
glp-1	+/+	-/-	-/-	+/+	+/+

95
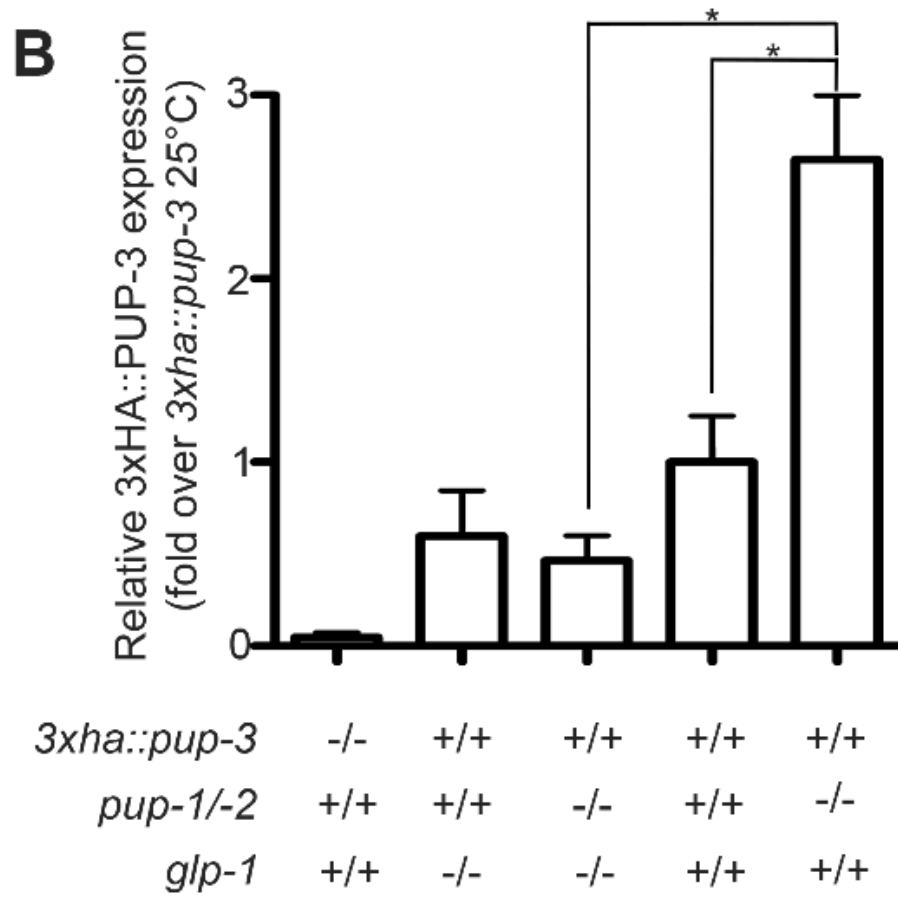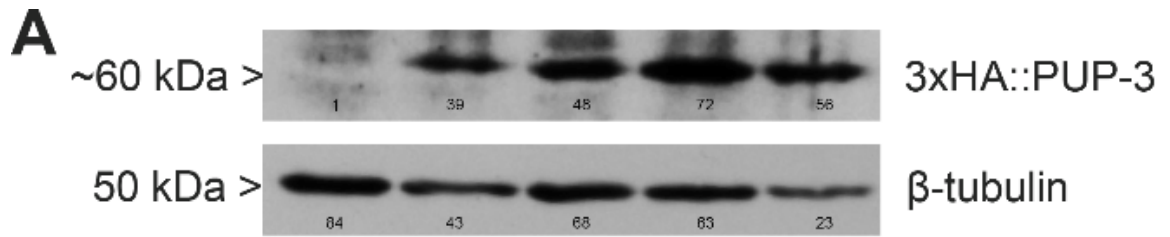
Figure 2.6. Model for regulation of germline gene expression by PUP proteins. (A)
Wildtype germline development requires a balance of PUP-1, -2, and -3 activities, and net PUP
activity promotes the correct abundance of RNA targets to allow germline development. (B) In
pup-1/-2(0) mutants, PUP-3 abundance is increased. The normal pattern of germline gene
expression is compromised due to loss of PUP-1 and PUP-2 and overexpression of PUP-3.
Under conditions of temperature stress, the net effect severely impairs germline development and
leads to the loss of germline viability within three generations.

germline
identity, viability, development

net target
regulation

PUP-1

PUP-2

PUP-3

loss of identity, viability

net target
regulation

PUP-1

PUP-2

PUP-3
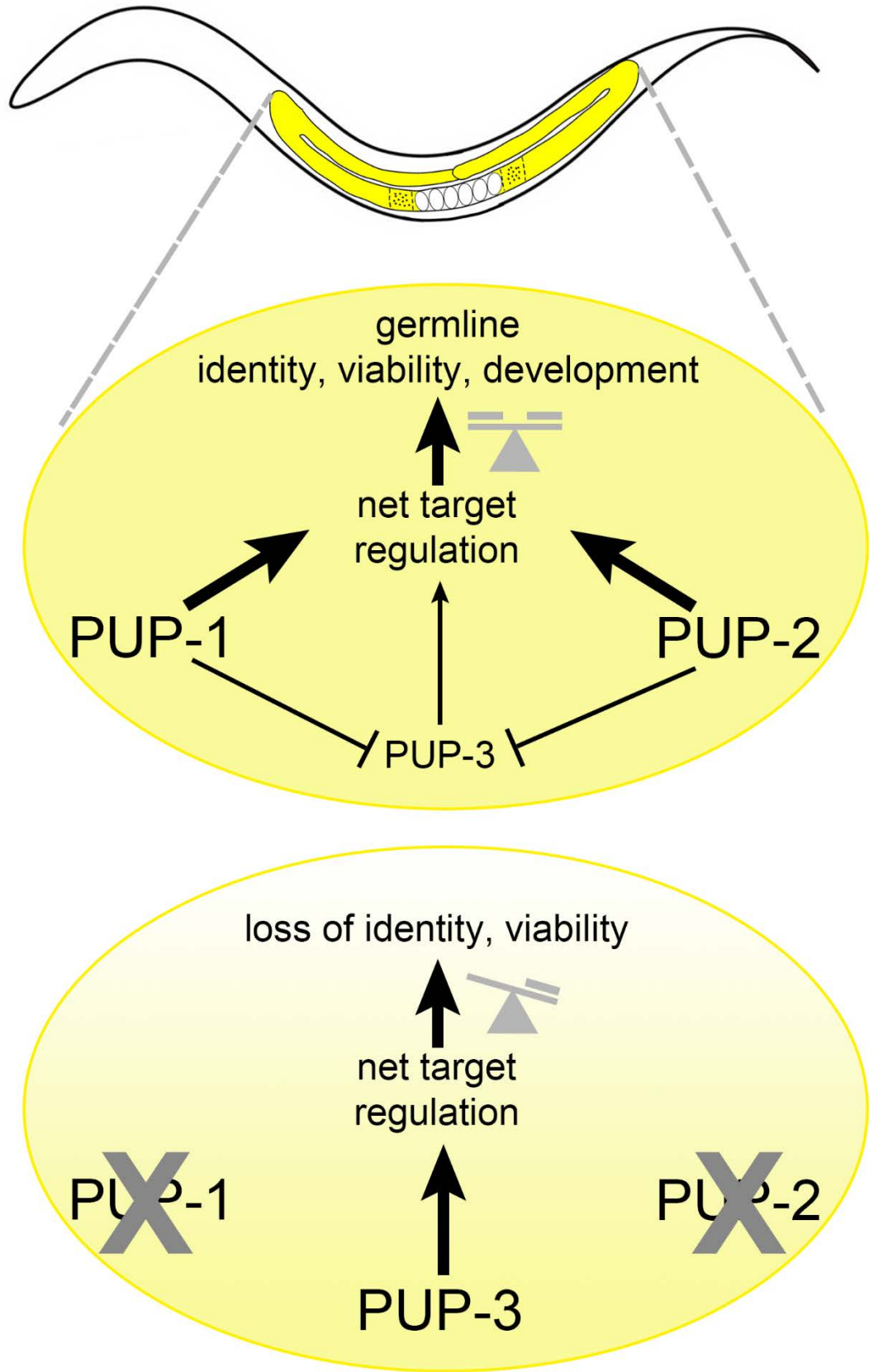
Figure 2.S1. Schematic illustration of the CRISPR-Cas9 strategies used to generate mutations and epitope-tagged strains. Boxes and lines represent exons and introns, respectively. Scissors mark predicted Cas9 cleavage sites. (A) Diagram of *pup-1 – pup-2* region before and after deletion. (B) Diagram of the *pup-1 – pup-2* region after addition of epitope tags. We generated strains with only *pup-1* (*omIs8*) or *pup-2* (*omIs7*) containing an epitope tag as well as doubly-tagged strains (EL629). (C) Diagram of *3xha*-tagged *pup-3* gene (*omIs9*). A strain was also generated containing *3xflag* at the N-terminus rather than *3xha* (*omIs10*).
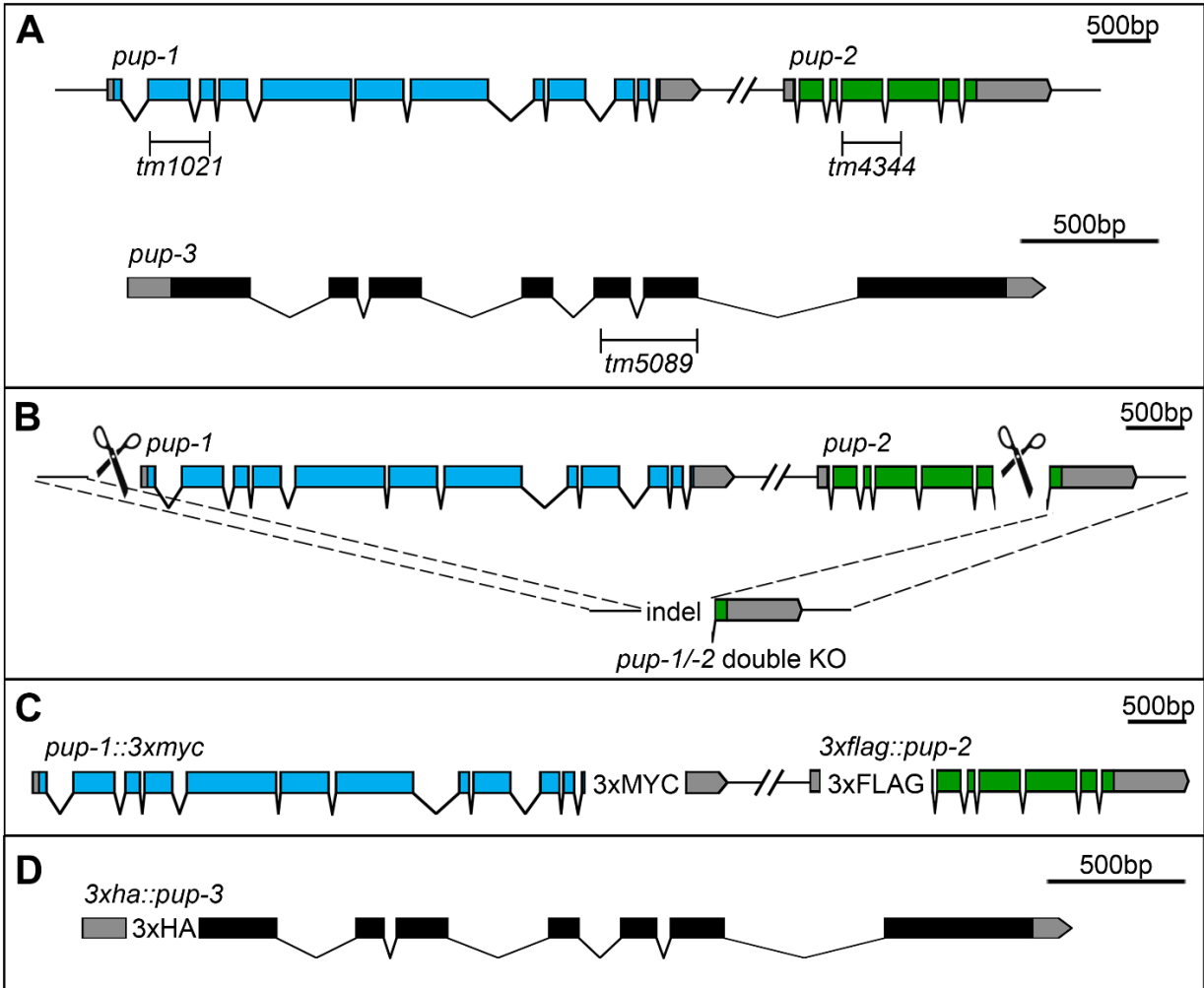
Figure 2.S2. *pup-1(tm1021)* **and** *pup-1(gg519)* **mutants have similar phenotypes.** Histograms display % fertile and % sterile F1 (M+Z+), F2 (M-Z-), and F3 (M-Z-) adults raised at 25°C. Table provides brood size data and % viable progeny produced by these animals raised at 25°C. Note that *pup-3(0)* partially suppresses the *pup-1(gg519)* phenotype. Statistical significance calculated by Student t-test. * indicates P < 0.05 compared to *pup-1(tm1021)* of the same generation. # indicates P < 0.05 compared to *pup-3(tm5089)* of the same generation. % indicates P < 0.05 compared to *pup-3(tm5089); pup-1(tm1021)* of the of the same generation. See Table 1 and Supplemental text.

The proportion of fertile and sterile animals

100%
80%
60%
40%
20%
0%

F1 F2 F3
pup-1(gg519)

F1 F2 F3
pup-3(tm5089);
pup-1(gg519)

☐ fertile

germ cell[+] gametes[+] (i)
germ cell[+] gametes[-] (ii) } sterile
germ cell[-] gametes[-] (iii)
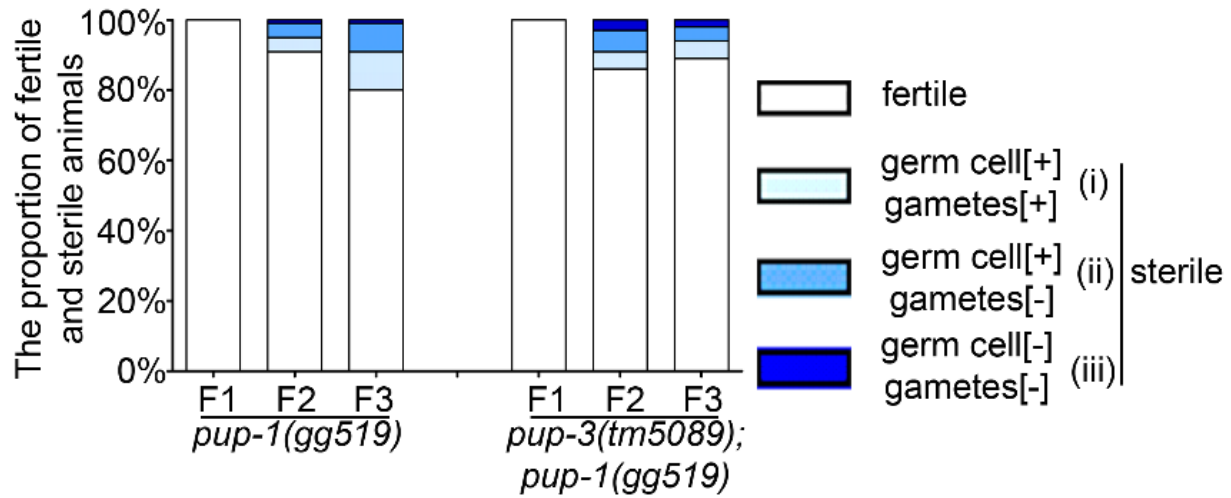
Genotype	Maternal Gen	Avg clutch size±SEM	% Progeny viable
pup-1(gg519)	F1	61 ± 13	90
	F2	32 ± 8*	91
	F3	23 ± 5*	83
pup-3(tm5089); pup-1(gg519)	F1	147 ± 10[#%]	96
	F2	57 ± 6	90
	F3	37 ± 8	90

Figure 2.S3. Somatic expression of P granule proteins in *pup-1/-2(0)* and *pup-3(0)* mutants.

(A) Expression of GLH-1::GFP in somatic cells in the *pup-1/-2(0)* tail. The strain contains

mCherry::his-58 to help visualize nuclei. The control genotype is *pup-1/-2(0)/qC1*. (B)

Expression of PGL-1::GFP in *pup-3(0)* intestinal cells. Scale bar = 16□m.
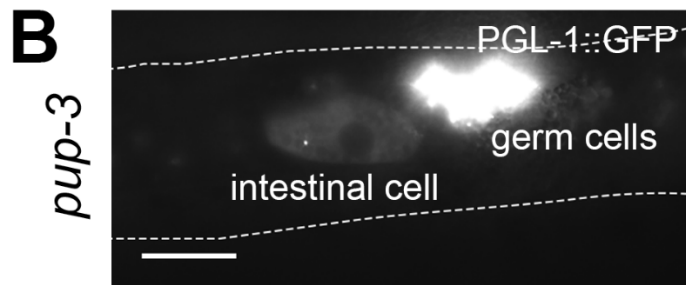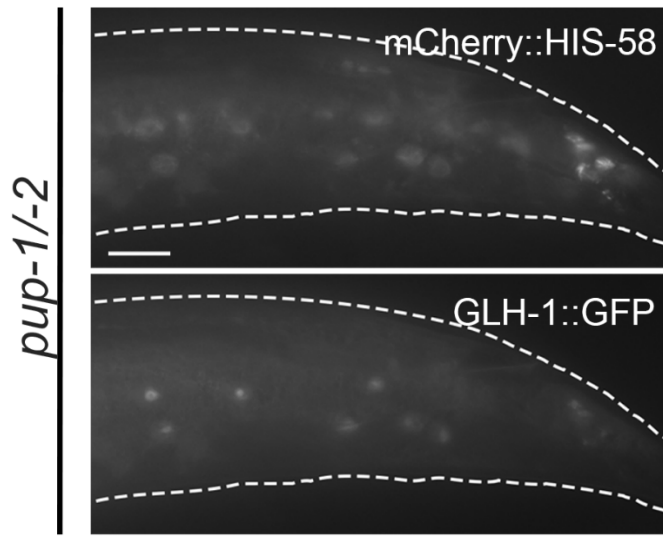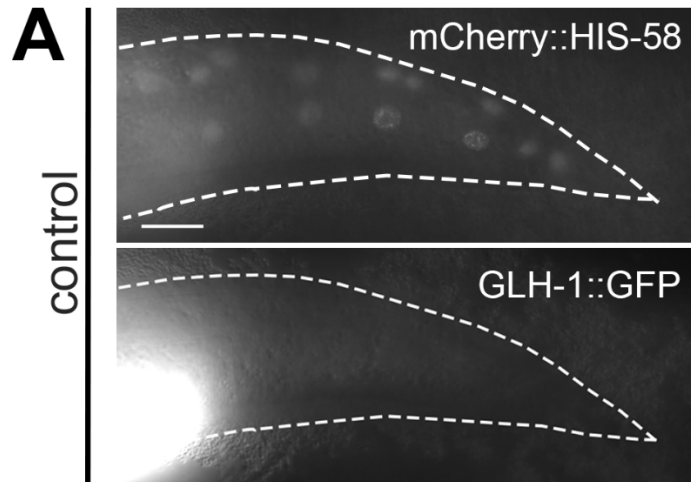
Figure 2.S4. Expression of PUP-1 and PUP-2 are independent of each other. The *pup-1::3xmyc 3xflag::pup-2* stain was subjected to *pup-1(RNAi)* or *pup-2(RNAi)*, as indicated. Images show dissected gonad arms that were immunolabeled to visualize PUP-1::3XMYC or 3XFLAG::PUP-2. Top panel shows PUP-1 and PUP-2 expression in *pup-1(RNAi)* pachytene region and maturing oocytes. Treatment successfully knocked down PUP-1 as shown, but did not alter the distribution of PUP-2. Bottom panel shows examples of PUP-2 and PUP-1 expression in *pup-2(RNAi)* maturing oocytes and pachytene region. Treatment largely reduced PUP-2 expression, as shown, but did not alter the distribution of PUP-1.

PUP-1::3xMYC 3xFLAG::PUP-2 3xFLAG::PUP-2

+ *pup-1 (RNAi)*

pachytene pachytene oocytes

3xFLAG::PUP-2 PUP-1::3xMYC PUP-1::3xMYC

+ *pup-2 (RNAi)*

oocytes pachytene oocytes
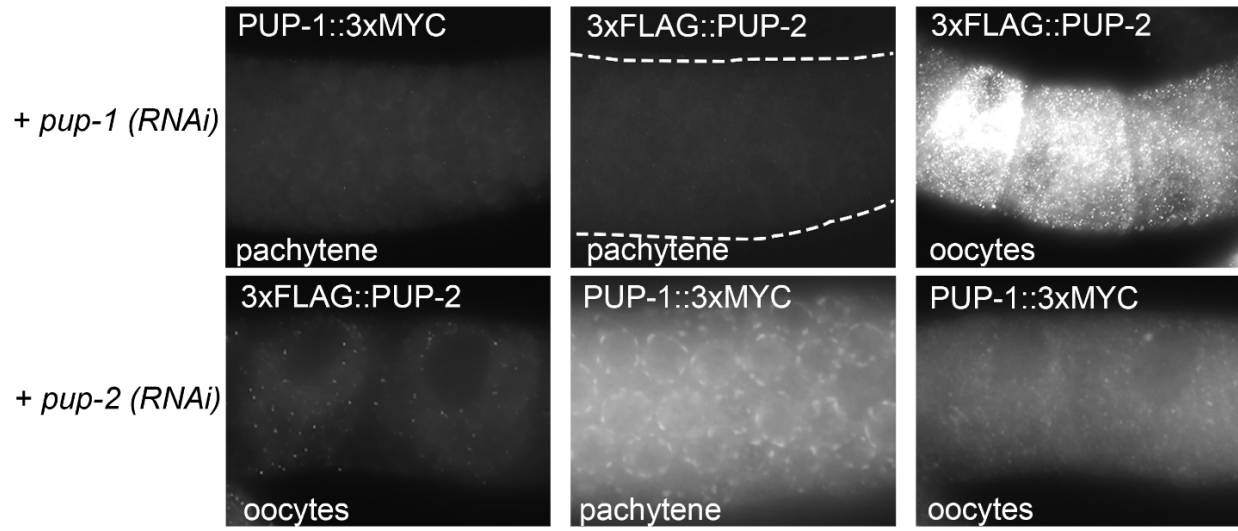
Figure 2.S5. A. Relative location of 3xFLAG::PUP-2 and CGH-1 foci. Images show dissected germline tissue immunolabeled with anti-FLAG and anti-CGH-1 antibody. Arrows indicate examples of PUP-2 foci that do not contain CGH-1. Arrowheads indicate rare co-labeling of both proteins.

B. Downregulation of PUP-2 abundance in -1, -2, and -3 oocytes is independent of OMA-1 and OMA-2 activity. *3xflag::pup-2* L1 hermaphrodites were treated with *oma-1/oma-2* dsRNA until adulthood, and their gonads were dissected and immunolabeled with anti-FLAG antibody. 3xFLAG::PUP-2 abundance drops in late-stage oocytes in control and *oma-1/-2(RNAi)* germlines. Bars indicate oocytes at equivalent stages in control and *oma-1/-2(RNAi)* gonads. Note that *oma-1/-2(RNAi)* causes accumulation of late-stage oocytes in the oviduct. Scale bar = 16 μm.

A

3XFLAG::PUP-2   CGH-1   merge

B

oma-1(+);oma-2(+)   DNA   3XFLAG::PUP-2   merge
-1 -2 -3

oma-1(RNAi);oma-2(RNAi)   DNA   3XFLAG::PUP-2   merge
-1 -2 -3 -4 -5 -6 -7 -8 -9
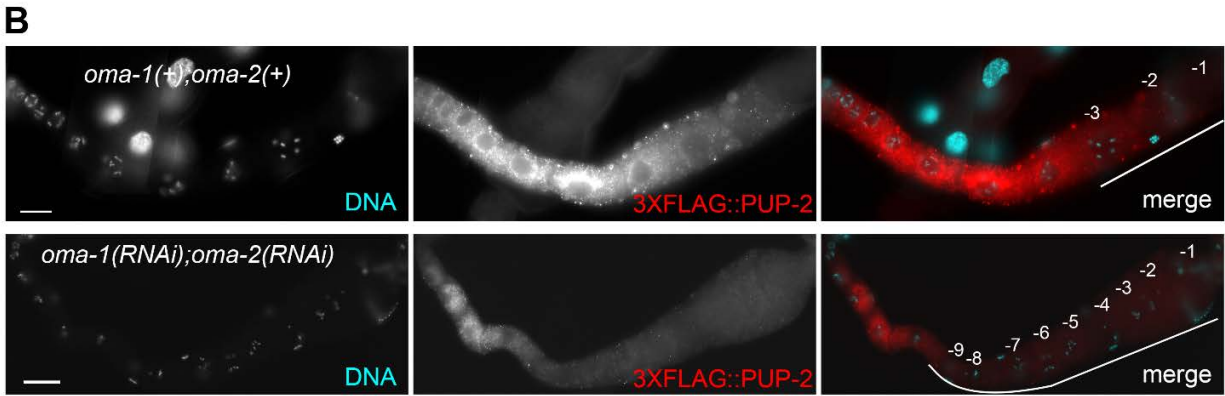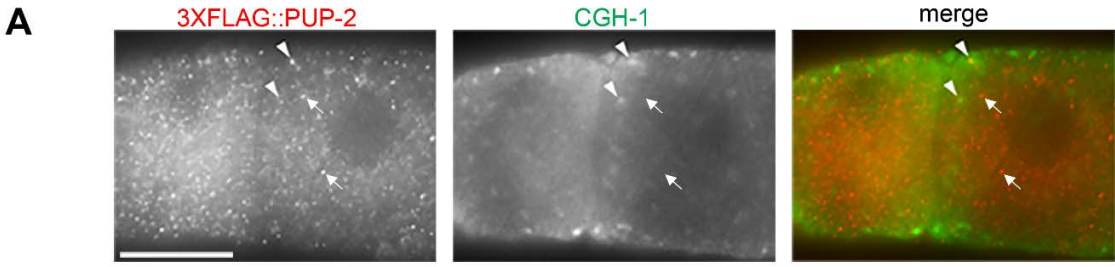
Figure 2.S6. EKL-1 localizes to germline P granules. Dissected (A) *ekl-1(+)* and (B) *ekl-1(om83)* gonads were immunolabeled with anti-EKL-1. Note perinuclear EKL-1 foci in *ekl-1(+)* and their absence in the *ekl-1(om83)* null mutant. (C) Confocal image of *ekl-1(+)* gonad co-labeled with anti-EKL-1 and anti-GLH-2. DNA is visualized with DAPI (red). Arrows indicate examples of GLH-2 (blue) co-localizing with EKL-1 (green). Scale bar = 16µm.

A

ekl-1(+)

DNA

EKL-1

B

ekl-1(null)

DNA

EKL-1

C

GLH-2
EKL-1
GLH-2+EKL-1
DNA
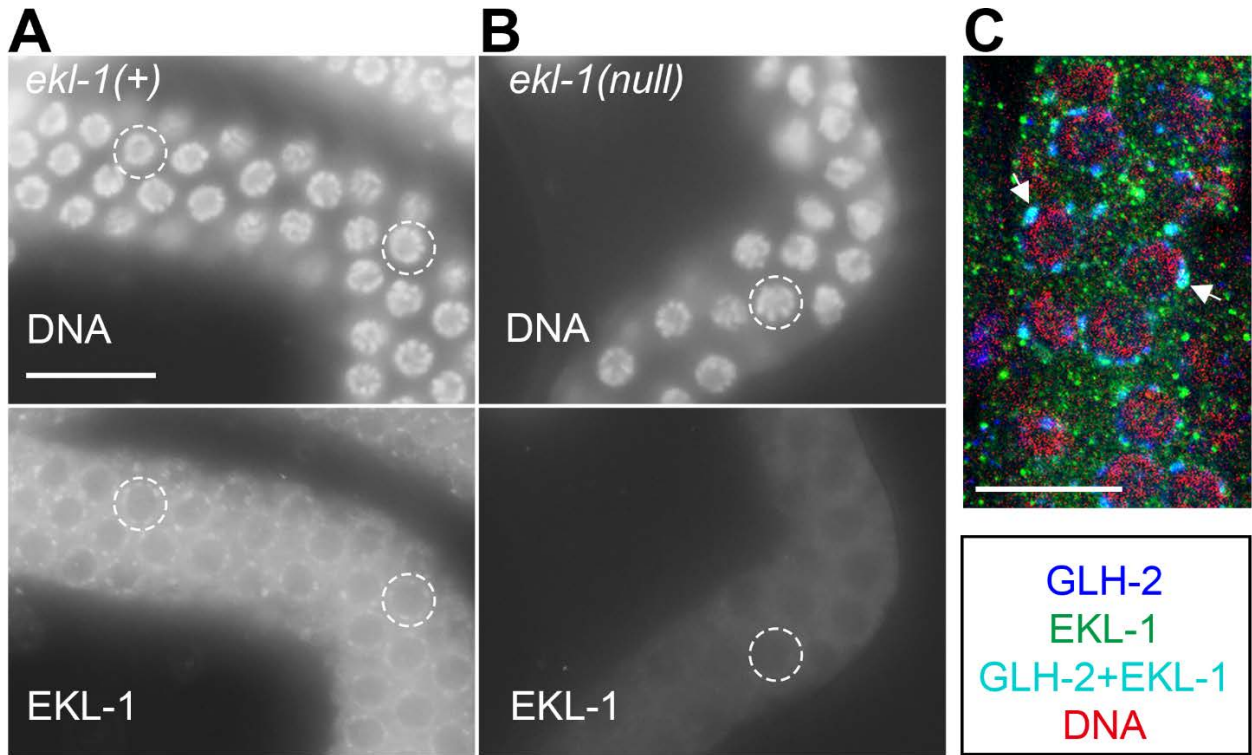
Figure 2.S7. 3xHA::PUP-3 abundance at 20°C. Histogram indicates the abundance of

3xHA::PUP-3 in each strain compared with control 3xHA::PUP-3 abundance at 25°C (see Fig.

5). At 20°C, 3xHA::PUP-3 abundance is not significantly altered in the absence of PUP-1 and

PUP-2.

3xha::pup-3	-/-	+/+	+/+	+/+	+/+
pup-1/-2	+/+	+/+	-/-	+/+	-/-
glp-1	+/+	-/-	-/-	+/+	+/+
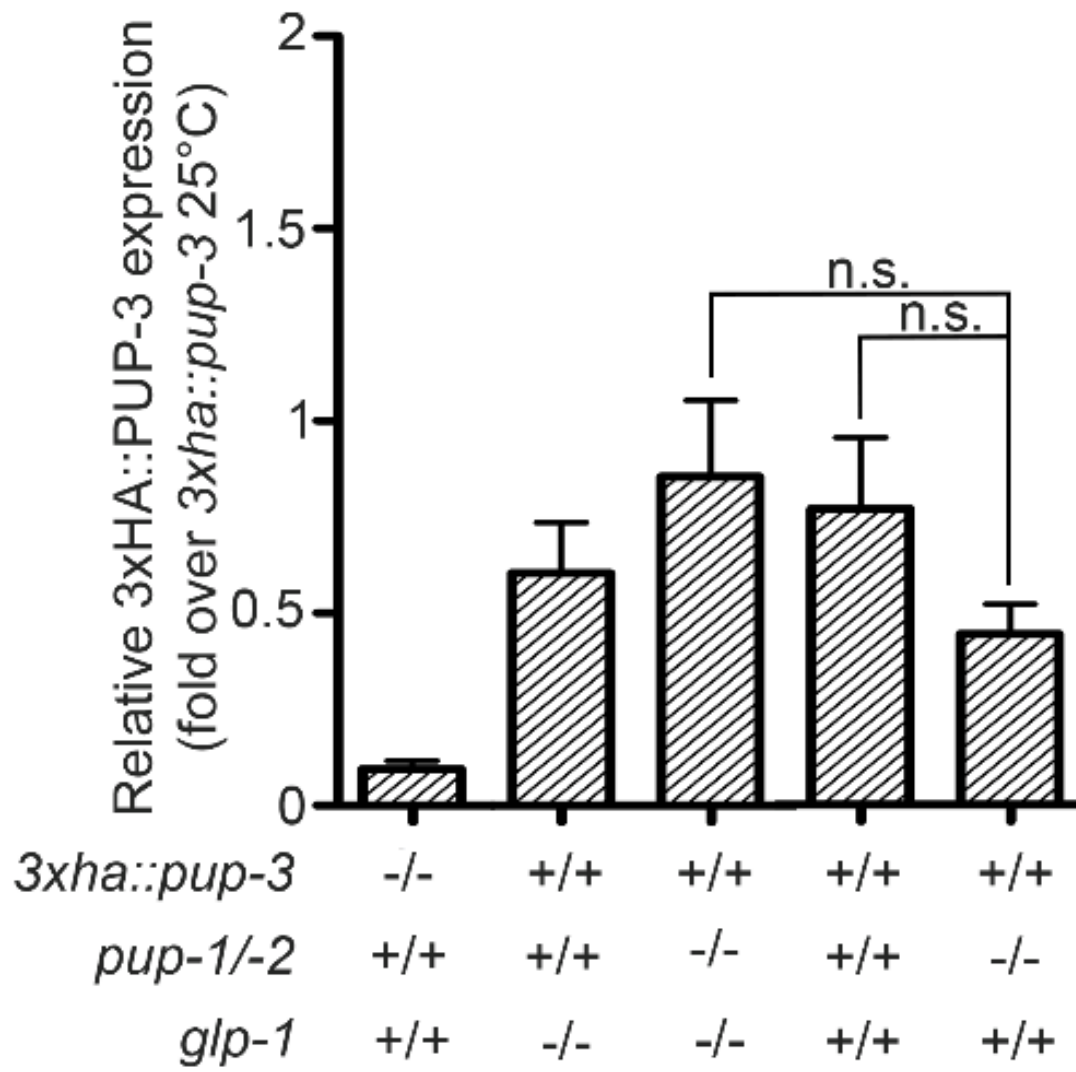
Chapter III   Meiotic H3K9me2 distribution is altered in *pup-1/-2* double mutants

3.1 INTRODUCTION

PUP-1/CDE-1 has been implicated in modifying siRNAs, specifically those produced by EGO-1 RdRP and associating with CSR-1 Argonaute (van Wolfswinkel et al., 2009).   We previously showed that meiotic H3K9me2 distribution depends on activity of the siRNA network (Maine et al., 2005; She et al., 2009). Components of the CSR-1/Argonaute pathway promote this targeted H3K9me2 enrichment on unsynapsed chromosomes (Maine et al., 2005; She et al., 2009) whereas RRF-3, a component of the ALG-3/-4 Argonaute pathway, promote H3K9me2 turnover after diplotene (Maine et al., 2005). CSR-1 and ALG-3/-4 act in a common mechanism to promote spermatogenesis (Conine et al., 2013). Because of these findings, we decided to evaluate the histone H3 lysine 9 dimethylation (H3K9me2) labeling pattern in *pup-1/-2* versus *pup-1* and *pup-2* mutants.

This study was initiated by a former graduate student, Matt Snyder. He analyzed H3K9me2 distribution in *alg-3/-4* and *eri* mutants. In addition, he did the ground work of evaluating H3K9me2 distribution in *pup-1(0), pup-2(0)* and *pup-1(RNAi) pup-2(0)* germ lines, which provides constructive preliminary data for me to generate the *pup-1/-2(0)* double knockout mutation and investigate its phenotype.

3.2 RESULTS AND DISCUSSION

H3K9me2 is detected predominantly on nonsynapsed chromatin, e.g., the male X, in leptotene-diplotene stages of meiotic prophase I, and the level then decreases in diakinesis oocytes and primary spermatocytes in males and L4 hermaphrodites (Bean et al., 2004; Kelly et al., 2002; Maine et al., 2005) (see *him-8* control in Fig. 3.1A, B). The *him-8* mutation prevents pairing and subsequent synapsis of X chromosomes in hermaphrodites. We generated *pup* strains carrying *him-8(e1490)* in order to evaluate nonsynapsed chromosomes in both male and hermaphrodite meiotic nuclei. For comparison, we labeled H3K9me2 in *csr-1 him-8* mutants as well as several ALG-3/-4 pathway mutants. We observed ectopic H3K9me2 in *csr-1* mutants, as previously reported (She et al., 2009). Mutations in ALG-3/-4 pathway components, *alg-3/-4, eri-1* and *eri-5*, caused persistent H3K9me2 labeling in primary spermatocytes in XO male germ lines (Fig. 3.1) similar to what was observed in *rrf-3* males (Maine et al., 2005).

H3K9me2 labeling in *pup-1* and *pup-2* single mutants appeared normal (Fig. 3.2), yet we observed an intriguing H3K9me2 distribution in *pup-1/-2(om129); him-8* mutants (Fig. 3.1). In *pup-1/-2(om129); him-8* males and hermaphrodites, H3K9me2 appeared elevated on autosomes in pachytene nuclei compared with controls (Fig. 3.1). In males, H3K9me2 signal was detected throughout the condensation phase of spermatogenesis, in contrast to controls (Fig. 3.1). This labeling pattern resembles a combination of the ectopic H3K9me2 observed in *csr-1* mutants and persistent H3K9me2 detected in ALG-3/-4 pathway mutants (Fig. 3.1). We conclude that PUP-1 and PUP-2 activities together promote the normal distribution of H3K9me2 in meiotic nuclei and its timely turnover during XO spermatogenesis. We hypothesize that PUP-1 and PUP-2 activity may promote the correct activity of CSR-1 and ALG-3/-4 pathways with

respect to meiotic H3K9me2 regulation. Intriguingly, we observed an increased level of

H3K9me2 accumulation on autosomes in *eri-5* mutants, similar to *csr-1* and *pup-1/-2* mutants

(Fig. 3.1).

3.3 MATERIALS AND METHODS

Immunocytochemistry and DAPI staining

H3K9me2 labeling was performed as described (Maine *et al.* 2005; She *et al.* 2009; Guo *et al.*

2015). Tissue was fixed in 3% PFA/PBS solution for 5 min. Primary antibody was used at the

indicated dilution: mouse anti-H3K9me2 (Abcam 1220), 1:200. Secondary antibody was used at

the indicated dilution: Alexa Fluor 488-conjugated goat anti-mouse (1:200). Slides were

observed with a Zeiss Axioscope or Leica DM5500 microscope.
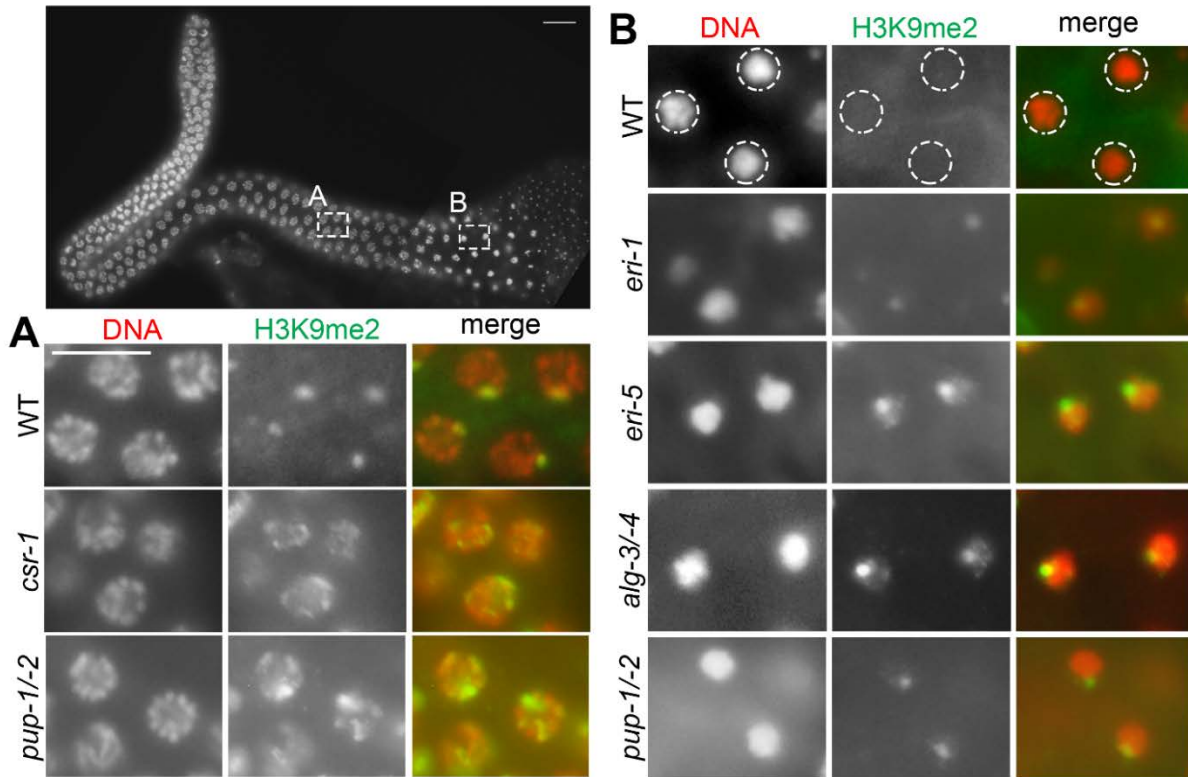
Figure 3.1. Meiotic H3K9me2 distribution appears abnormal in males mutant for *pup-1/-2* or components of the ALG-3/-4 or CSR-1 pathways. Region (A) shows pachytene nuclei co-labeled with DAPI and anti-H3K9me2 antibody. In wild-type, H3K9me2 is highly enriched on the X chromosome in each pachytene nucleus. In contrast, ectopic H3K9me2 is observed across the genome in *csr-1* and *pup-1/-2* mutants. Region (B) shows nuclei undergoing spermatogenesis (circled). In wild-type, H3K9me2 is not observed in these nuclei. In contrast, H3K9me2 turnover is delayed in *eri-1, eri-5, alg-3/-4* and *pup-1/-2* male germ cells during spermatogenesis. *him-8* mutant was used as the wild-type control; all mutant strains carry *him-8* in the background in order to facilitate production of males. Scale bar = 16μm.
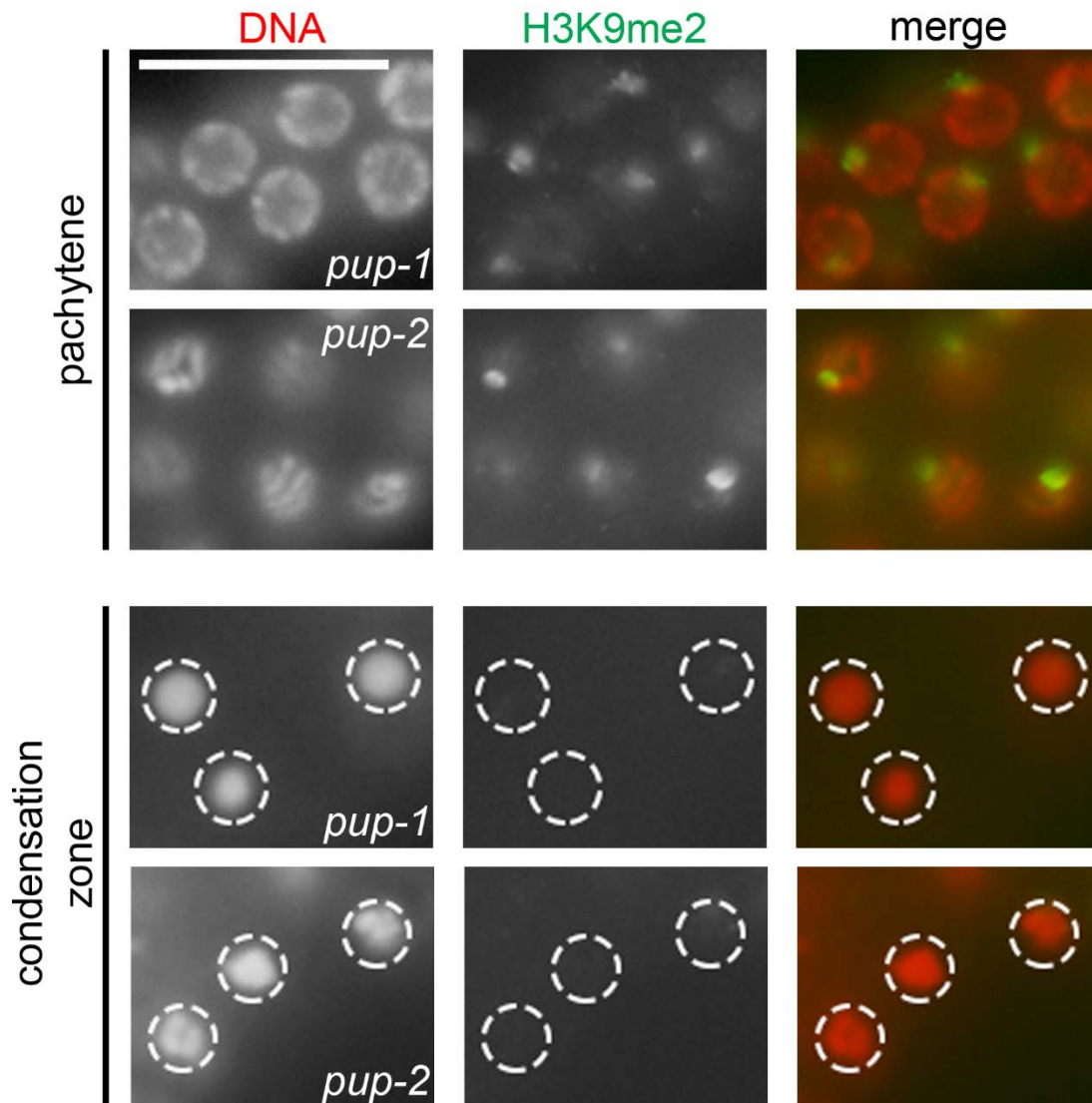
Figure 3.2. Meiotic H3K9me2 distribution appears normal in male mutants for *pup-1* and *pup-2*. Top panel shows pachytene nuclei co-labeled with DAPI and anti-H3K9me2 antibody. Bottom panel shows nuclei undergoing spermatogenesis (circled). All mutant strains carry *him-8* in the background in order to facilitate production of males. Scale bar = 16μm.

Chapter IV Discussion

In this Chapter, I discuss aspects that were not covered in detail in Chapters II and III, such as some thoughts on the potential targets of PUP-1, PUP-2 and PUP-3 based on our phenotypic, expression, and H3K9me2 data, and the putative localization of endogenous PUP-3 in *C. elegans*. I also discuss the H3K9me2 phenotypes described in Chapter III and previous findings regarding small RNA pathway components regulating H3K9me2. Finally, I propose a model to explain how PUP-1, PUP-2 and PUP-3 may regulate germline identity, viability, development, and H3K9me2 pattern.

4.1 Possible targets of PUP-1, PUP-2 and PUP-3 action

One class of PUP-1, PUP-2 and PUP-3 target could be small RNAs. PUP-1 is known to target CSR-1-bound 22G siRNAs. *pup-1(0)* exhibited an increase of siRNA population while an appreciable decrease of miRNA population (van Wolfswinkel et al., 2009). It has been characterized that PUP-1-mediated uridylation regulates CSR-1 22G siRNA for decay; however, little is known about its role in miRNA regulation. Studies of the human PUP-1 orthologs have revealed a dual role of PUP-mediated uridylation on miRNAs: addition of processive Us for target degradation or addition of distributive Us for target regulation. Accordingly, it is likely that PUP-1 targets miRNA as well, perhaps to promote its biogenesis. PUP-2 is known to target LIN28-bound pre-*let-7* for degradation. Based on our results, PUP-2 is likely to have siRNA targets, more than just miRNA targets. 26G siRNAs may be the candidate targets of PUP-2. In support of this idea, the expression pattern of PUP-2 in oogenesis coincides with the expression of 26G siRNAs (Han et al., 2009; Billi et al 2012). In addition, the H3K9me2 phenotype is

noticed to be more penetrant in later generations (M-Z-) than early generations (M+Z-), indicating a possible transmission of siRNAs across generations. PUP-3 has validated *in vitro* uridylation activity whereas no target has been identified. In order to identify the potential small RNA targets of PUP-1, PUP-2 and PUP-3, we currently are performing small RNA sequencing in the wild type and *pup-1/-2(0)* mutant and will continue with each single *pup* mutants. By doing so, it may help us to identify redundant and/or complementary small RNA targets of PUP-1 and PUP-2, as well as the targets of PUP-3. Mapping the small RNA targets to the *C. elegans* genome will provide us with insight of small RNA target genes whose expression abundance or Argonaute association can impact germline identity, viability and development.

In addition to small RNAs, PUP-1, PUP-2 and PUP-3 may also target mRNAs as their orthologs do. Uridylation-mediated mRNA decay is well studied in human and mouse. PUP-1 localizes on P granules in the vicinity of nuclear pore. Most mRNAs transcribed from the nucleus must pass through a P granule on their way to the cytoplasm. Therefore, PUP-1 may immediately uridylate unnecessary or aberrant transcripts for decay on P granules. In contrast, PUP-2 localizes in the cytoplasm, which could degrade the transcripts that escape the P granule regulation. In addition, considering the enrichment of PUP-2 in oogenesis and depletion in matured oocytes, it is possible that PUP-2 may regulate maternal transcripts for clearance. Although the expression pattern is not available, PUP-3 may also target mRNAs. To identify the potential mRNA targets of PUP-1, PUP-2 and PUP-3, we are preparing mRNA samples via uridylation optimized TAIL-seq protocol for mRNA sequencing analysis. By doing so, we would be able to understand how the specificity of small RNA-mediated mechanism is modulated to ensure the proper regulation of target RNAs. To specifically confirm the targets of

PUP-1, PUP-2 and PUP-3, we can further validate the PUP-bound RNAs via RNA-immunoprecipitation method.

4.2 PUP-3 expression

We failed to detect endogenous PUP-3 expression via indirect immunofluorescence with a transgenic strain carrying an in-frame amino terminal 3xHA epitope tag. However, several lines of evidence suggest its potential role in both germ cells and somatic cells. First, *pup-3(0)* mutants possess multiple germline defects, such as reduced brood size, suggesting PUP-3 has an essential role in the germ line. Second, through protein blot assay, 3xHA::PUP-3 was detected in *pup-1/-2(+)* whole adults. Third, reduction of the germ line leads to a decrease, although not statistically significant, in 3xHA::PUP-3 expression level; see Figure 5, comparison between *pup-1/-2(+) glp-1(+)* vs. *pup-1/-2(+) glp-1(-)*. This result suggests that PUP-3 is expressed in the germ line, but at a very low level compared to somatic cells. Fourth, consistent with the protein blot results, RNA sequencing results revealed that *pup-3* mRNA is present at a fairly low level in dissected adult germ lines (Guo et al., 2015). In summary, these data indicate that PUP-3 has a major somatic function and a relatively minor germline function. Explanations for our failure to detect PUP-3 via immunofluorescence method could be: 1) germline PUP-3 abundance is below detection level; or 2) the protein folding structure of PUP-3 prevents antibody binding. To try to solve the second problem, we can add an epitope tag at the carboxyl terminus or in the middle of the PUP-3 protein.

pup-1(0) and *pup-2(0)* exhibited a low penetrance protruding vulva phenotype, whereas *pup-3(0)* did not exhibit noticeable somatic defects. To investigate the somatic function of PUP-3 in depth, we can examine multiple aspects in more detail, for example, to monitor whether

pup-3(0) has a somatic developmental delay. Additionally, PUP orthologs in other species are found to regulate miRNA. miRNAs in *C. elegans* are majorly present in somatic tissues, mis-expression of which commonly cause defects of somatic cell division and misregulation of somatic cell fate. For example, overexpression of miR-84 results in skipping of the L2 proliferative seam cell division (Resnick et al., 2010); and overexpression of miR-61 leads to the descendants of 1° vulval precursor cells (VPCs) expressing a 2° fate marker (Yoo and Greenwald, 2005). Therefore, perhaps we can utilize reporter genes to examine whether loss of PUP-3 activity has an impact on somatic cell division or somatic cell fate. However, we cannot rule out the possibility that PUP-1 and PUP-2 may function in somatic tissues to some extent, and their activity may be redundant to PUP-3 in somatic tissues.

4.3 H3K9me2 distribution and small RNA pathways

Two H3K9me2 phenotypes have been observed in the study. Animals lacking PUP-1/-2 or CSR-1 activity exhibited ectopic labeling of H3K9me2 on synapsed chromosomes in pachytene germ cells. In wildtype males, the X chromosome acquires a relative high level of H3K9me2 in leptotene-diplotene germ cells that is proposed to be important for X chromosome condensation and to help limit transcription of X-linked genes. H3K9me2 signals are low on autosomes but with a slight increase of H3K9me2 on autosomal ends (Bean et al., 2004; Guo et al., 2015; Kelly et al., 2002; Maine et al., 2005). Such a low level of repressive marks on autosomes is consistent with the expression of germline genes on autosomes to promote germ cell progression. Therefore, ectopic dispersal of H3K9me2 onto autosomes in pachytene cells implies inappropriate chromatin structural change and/or transcriptional repression during meiotic progression. It is likely that insufficient expression of germline genes and/or the

repression of genes that are antagonistic to somatic gene expression on autosomes may contribute to the germline developmental abnormality we observed in *pup-1/-2(0)*, such as somatic gene expression in germ cells and cell death around late L3 stage when germ cells progress to the pachytene stage. Notably, *csr-1* mutant and *pup-1/-2* mutant both retain H3K9me2 on the male X chromosome. The detection of H3K9me2 on both X chromosome and autosomes in these mutants may indicate that some H3K9me2 marks that normally target the X chromosome are now ectopically depositing onto autosomes. An alternative hypothesis is that H3K9me2 on the X chromosome stays the same in these mutants and wildtype, whereas additional H3K9me2 deposits onto autosomes. To test the hypotheses, a method of micro chromatin immunoprecipitation assay plus sequencing (microChIP-seq) could be considered (Dahl and Collas, 2008, 2009). MicroChIP is suitable in this study because it requires as few as 100 cells to analyze the protein-genome association.

The previous studies from our lab have shown that several other members of the siRNA pathway regulate proper meiotic H3K9me2 deposition: loss of 22G siRNA master RdRp, EGO-1, causes significant loss of H3K9me2 in pachytene germ cells; loss of 26G/22G siRNA master regulator, DRH-3, or loss of 22G siRNA Tudor domain protein, EKL-1, causes ectopic autosomal H3K9me2 accumulation with loss of X-associated H3K9me2; and loss of CSR-1 activity causes elevated H3K9me2 on autosomes (summarized as a table below) (Maine et al., 2005; She et al., 2009). Accordingly, it appears that loss of CSR-1-associated 22G siRNAs generally correlates with increased H3K9me2 on autosomes. Since the CSR-1 pathway is associates with active transcription and defines euchromatin (Claycomb et al., 2009), a compelling explanation is that perturbation of the CSR-1 pathway debilitates protection of euchromatin and thereby results in occupancy of repressive marks such as H3K9me2 on

autosomes. In contrast, the WAGO pathway may correlate with the repressed state on chromosomes such as the X chromosomes, as we observed reduced H3K9me2 levels in mutants with reduced abundance of WAGO-associated 22G siRNAs (i.e., *ego-1, drh-3, ekl-1*) (Maine et al., 2005; She et al., 2009). In support of this idea, Guo et al 2015 revealed that H3K9me2 levels have a strong correlation with candidate targets of WAGO-1 (Guo et al., 2015). In addition, evidence suggests that the same siRNA may load onto different Argonautes. van Wolfswinkel et al., 2009 suggested that siRNAs may load onto atypical Argonaute when siRNAs accumulate to inappropriately high levels (van Wolfswinkel et al., 2009). The *pup-1/-2(0)* germ line has elevated H3K9me2 on autosomes, which resembles the *csr-1(0)* germ line, indicating a potential loss of euchromatin regions. This may result from over-accumulation of 22G siRNAs, which inappropriately load onto WAGOs due to the absence of CSR-1, and leads to increased H3K9me2 and a repressed chromatin state. Another explanation could be that PUP-1 and PUP-2 activity regulates both 26G and 22G siRNAs. Excessive amount of 26G siRNAs in the *pup-1/-2(0)* germ line yield an overwhelming abundance of 22G siRNAs that load onto WAGOs. Alternatively, PUP-1 and PUP-2 activity may be required for siRNAs to load onto CSR-1 Argonaute. It is likely that PUP-1 and PUP-2 may not necessarily associate with target degradation in *C. elegans,* as learnt from the studies of their human orthologs (Heo et al, 2012; Thornton et al 2014). PUP-1 and PUP-2 may act as "writers" to mark certain siRNAs that can be recognized by "reader" CSR-1. In the *pup-1/-2(0)* mutant, target siRNAs lacking U-tails cannot be recognized by CSR-1. The function of CSR-1 in promoting transcription and protecting euchromatin relies on RNAs (Cecere et al 2014). Therefore, disrupted CSR-1-siRNA association in the *pup-1/-2(0)* mutant causes spreading of repressed chromatin state.

We also observed delayed turnover of H3K9me2 in *pup-1/-2*, *eri-1*, *eri-5* and *alg-3/-4*

mutant males. In addition, *rrf-3* had been characterized in an early study to manifest a similar

H3K9me2 phenotype (Maine et al., 2005). RRF-3, ERI-1 and ERI-5 are components of the ERI

complex required for the production of both ERGO-1-associated and ALG-3/-4-associated 26G

siRNAs. However, loss of any *rrf-3, eri-1* or *eri-5* only exhibits sperm-origin sterility (Duchaine

et al., 2006). This developmental phenotype is consistent with our spermato-H3K9me2

phenotype in those mutants. In addition, small RNA sequencing analyses have shown that loss

of *eri-1, eri-5* and *rrf-3* all result in compromised 26G siRNA and WAGO-associated 22G

siRNA abundance. Loss of *alg-3/-4* causes reduction of sperm-specific 26G siRNAs and overall

2-fold reduction in 22G siRNAs (the 22G siRNAs are not classified in Conine et al 2010) (see

table below) (Conine et al., 2010; Conine et al., 2013). These data suggest a possibility that

H3K9me2 presence in spermatocytes correlates with the 26G siRNA pathways, reflecting a

chromatin state change via misregulated siRNA level. In spermatogenic germ lines, ALG-3/-4 is

the dominant 26G siRNA pathway, rather than ERGO-1 pathway (Conine et al., 2010; Conine et

al., 2013). A vast majority of ALG-3/-4 26G-dependent 22G siRNAs associate with CSR-1

(Conine et al., 2010; Conine et al., 2013). Therefore, mutants with reduced 26G siRNAs possess

fewer 22G siRNAs loading onto CSR-1. Downregulation of the CSR-1 22G pathway leads to

invasion of repressive H3K9me2 marks to euchromatin regions. In addition, the 26G siRNA

machinery is not detected until germ cells undergo spermatogenesis or oogenesis (Han et al.,

2009). Therefore, the expression pattern of 26G siRNAs may explain why *eri-1, eri-5, rrf-3* and

alg-3/-4 mutants do not exhibit ectopic H3K9me2 in pachytene stage or earlier stages but have

abnormal H3K9me2 presence in spermatocytes. In contrast, *pup-1/-2(0)* exhibited H3K9me2

abnormality in both pachytene and spermatocytes, indicating a mis-regulation of both 22G and 26G pathways.

To test whether the abnormal H3K9me2 present in spermatocytes discussed above links with loss of euchromatin regions and decreased transcription level, we can next stain the germ lines with antibodies recognizing euchromatin marks such as H3K4me2 and elongating polymerase II. H3K4me2 is known to be expressed in normal developing sperm, conserved in multiple organisms (Conine et al., 2013). The H3K4me2 expression is consistent with active transcription via RNA Pol II. Therefore, if the hypothesis is correct, those mutants with spermato-H3K9me2 phenotypes may have reduced H3K4me2 detection and reduced elongating Pol II occupancy in spermatocytes.

As a side thought, it also might be interesting to examine whether loss of *eri-1, eri-5, rrf-3* or *alg-3/-4* causes accumulation of ectopic pachytene H3K9me2 in later generations. Since the production of CSR-1-associated 22G siRNAs is dependent on ALG-3/-4 pathway, loss of essential components of ALG-3/-4 pathway is expected to impact the downstream CSR-1 pathway and yield a pachytene H3K9me2 phenotype as observed in *csr-1(0)*. However, we did not observe a pachytene H3K9me2 phenotype in any of those mutants. A possible explanation could be that impaired production of ALG-3/-4 26Gs in the parental generation is not sufficient to reduce the amount of dependent 22G siRNAs in the germ line of the offspring to the extent that will show a phenotype. In this sense, later generations of those mutants when continuous depletion of 26G siRNAs from generation to generation may phenocopy *csr-1(0)* due to limited level of 22G siRNAs that bind to CSR-1. Considering some of those mutants have temperature sensitive sterility (Duchaine et al., 2006), we may have to raise the animals at room temperature or maybe utilize RNAi feeding strategy to knockdown the genes.

124

Alternatively, the persistence of H3K9me2 signal in spermatocytes could result from an inefficient removal of H3K9me2 via demethylase. H3K9 demethylases have been shown to be closely associated with reproduction. In *S. pombe,* H3K9me1/2 demethylase LSD1/KDM1 is important for sporulation (Lan et al., 2007). In mouse, H3K9me2 demethylase JHDM2A/ KDM3A expression starts in late pachytene and peaks in round spermatids, coincident with the reduction of H3K9me2 in the same stages. Loss of JHDM2A/KDM3A results in male sterility with condensation defects during spermatogenesis (Okada et al., 2007). Although no *C. elegans* H3K9me2 demethylase has been yet reported in germ lines or to correlate with germline defects, indirect evidence from H3K4 demethylase suggests a potential connection between endogenous small RNA pathways and demethylases (Greer et al., 2015). Therefore, it is possible that small RNAs in the germ line may guide demethylases for targeting. In this sense, WAGO-10 and WAGO-1-associated pathways are good candidates for guiding demethylase activity because the expression of WAGO-1 protein and *wago-10* transcript coincides with the expression of H3K9me2 demethylase characterized in mouse (Conine et al., 2013; Reinke et al., 2004). Consistently, all the mutants with spermato-H3K9me2 have decreased level of WAGO 22G siRNAs. If it is true that the spermato-H3K9me2 persistence is related to deficient small RNA-mediated targeting, mutation of *wago-1* or *wago-10* should phenocopy the spermato-H3K9me2 phenotypes. *wago-1 (0)* does not exhibit noticeable H3K9me2 phenotype (She et al., 2009), which is not surprising because WAGO-1 is a cytoplasmic Argonaute and does not enter nucleus. Therefore, WAGO-10 appears to be a better candidate to regulate H3K9me2. Although *wago-10* has not been studied up to the present, it may be interesting to examine the H3K9me2 in the *wago-10(0).*

Taken together, based on the results, I propose that CSR-1-associated 22G siRNA pathway protects autosomal regions from H3K9me2 spreading in pachytene cells while WAGO-associated 22G siRNA pathway links with H3K9me2 deposition on the repressed chromosomes such as the X chromosome. In addition, 26G siRNA pathways function at the spermatogenesis and may indirectly regulate the recruitment of H3K9me2 demethylase via spermatogenesis-enriched WAGO pathway. In *pup-1/-2(0),* both 26G and 22G siRNAs seem to be mis-regulated which results in inappropriate accumulation of siRNAs. The inappropriate abundance of siRNAs could cause imbalance or overflow between siRNA pathways, which consequently leads to ectopic H3K9me2 deposition and repression of chromosomes.

Pachytene H3K9me2 phenotypes	Mutated gene	siRNA abundance
A ↓, X ↓	*ego-1*	26G →, WAGO 22G ↓
A ↑, X ↓	*drh-3*	26G ↓, WAGO 22G ↓, CSR-1 22G ↓
A ↑, X ↓	*ekl-1*	WAGO 22G ↓, CSR-1 22G ↓
A ↑, X normal	*csr-1*	ALG-¾ 26G ↓, CSR-1 22G →
Spermato-H3K9me2 phenotypes		
Delayed turnover	*eri-1*	26G ↓, WAGO 22G ↓
Delayed turnover	*eri-5*	26G ↓, WAGO 22G ↓
Delayed turnover	*rrf-3*	26G ↓, WAGO 22G ↓
Delayed turnover	*alg-3/-4*	ERGO 26G →, ALG-¾ 26G ↓, some 22G ↓

4.4 A working model

As stated in the discussion of Chapter 2, PUP-1 and PUP-2 function together to ensure the germline identity, viability and development under temperature stress whereas PUP-3 functions oppositely. These developmental defects observed in the *pup-1/-2* mutant may correlate with an imbalance among small RNA species loading onto different Argonautes and/or mRNA transcripts. The fairly improved phenotypes observed in the *pup-3; pup-1/-2* mutant may associate with a re-balance of small RNAs and/or mRNAs. H3K9me2 phenotypes observed in the mutant could be a cause or a consequence of such mis-regulation in RNA abundance. In consistent with the idea of RNA balance, our preliminary result shows that in the *pup-3; pup-1/-2* mutant where the RNA level tends to be re-balanced, H3K9me2 in pachytene cells is superficially wildtype with low autosomal H3K9me2 and high enrichment on the X chromosome in males, although the overall expression is relatively low.

Appendix

We wondered whether *pup-1/-2(0)* has a paternal effect on development. To test this, we crossed *unc13ccIs; pup-1/-2(0)* hermaphrodites (M+Z- *pup-1/-2(0)* generation) with *pup-1/-2(0)/qC1gfp* males at 25 °C, and we evaluated sterility present in the self- and cross-progeny. The purpose of introducing *unc13ccIs* is to distinguish cross-progeny from the self-progeny of *pup-1/-2(0)* hermaphrodites. The cross yielded three genotypes of progeny (see table below): 1) *unc13ccIs; pup-1/-2(0)* self-progeny, which are M-P-Z- (no <u>m</u>aternal contribution, <u>p</u>aternal contribution or <u>z</u>ygotic contribution); 2) *unc13ccIs/+; pup-1/-2(0)* cross-progeny, which are M-P+Z-; and 3) *unc13ccIs/+; pup-1/-2(0)/+* cross-progeny, which are M-P+Z+. We observed that 66% of the self progeny were sterile; this number is consistent with our previous data from brood assays. We observed 71% sterility in the *unc13ccIs/+; pup-1/-2(0)* (M-P+Z-) population. If *pup-1/-2(0)* had a paternal effect, we would expect to see some rescue by the P+ allele, and therefore less than 66% sterility in the *unc13ccIs/+; pup-1/-2(0)* animals. Therefore, we conclude that *pup-1/-2(0)* does not have a paternal-rescue effect on development. In addition, we observed 42% sterility in the *unc13ccIs/+; pup-1/-2(0)/+* (M-P+Z+) population, which shows that introduction of a wild type allele to progeny of M+Z- *pup-1/-2(0)* mother failed to rescue the animals to a wild type phenotype but slightly reduced the sterility (compared to 66% sterility in the *unc13ccIs; pup-1/-2(0)*). This observation suggests the possibility that the *pup-1* and *pup-2* genes may be expressed in the embryo, but their expression levels are not sufficient to compensate for the absence of maternal contribution.

Table A1 *pup-1/-2(0)* **mutation has no paternal-rescue effect on development**

Progeny	Self	Cross	Cross
Genotype	*unc13ccIs;pup-1/-2(0)*	*unc13ccIs/+; pup-1/-2(0)*	*unc13ccIs/+; pup-1/-2(0)/+*
M/P/Z	M-P-Z-	M-P+Z-	M-P+Z+
% Sterility	66%	71%	42%

Experiments were performed at 25°C. The number of viable progeny and sterile progeny of the three indicated genotypes were counted from N=9 complete crosses. A Chi-square test indicates that the sterility of *unc13ccIs/+; pup-1/-2(0)/+* is significantly different from that of *unc13ccIs;pup-1/-2(0)* (P<0.01).

Reference

Alberts B, J.A., Lewis J, et al. (2002). The RNA World and the Origins of Life, 4th edition edn (Molecular Biology of the Cell: New York: Garland Science).

ALLFREY, V.G., FAULKNER, R., and MIRSKY, A.E. (1964). ACETYLATION AND METHYLATION OF HISTONES AND THEIR POSSIBLE ROLE IN THE REGULATION OF RNA SYNTHESIS. Proc Natl Acad Sci U S A *51*, 786-794.

Altun-Gultekin, Z., Andachi, Y., Tsalik, E.L., Pilgrim, D., Kohara, Y., and Hobert, O. (2001). A regulatory cascade of three homeobox genes, ceh-10, ttx-3 and ceh-23, controls cell fate specification of a defined interneuron class in C. elegans. Development *128*, 1951-1969.

Aravind, L., and Koonin, E.V. (1999). Novel predicted RNA-binding domains associated with the translation machinery. J Mol Evol *48*, 291-302.

Arribere, J.A., Bell, R.T., Fu, B.X., Artiles, K.L., Hartman, P.S., and Fire, A.Z. (2014). Efficient marker-free recovery of custom genetic modifications with CRISPR/Cas9 in Caenorhabditis elegans. Genetics *198*, 837-846.

Ashe, A., Sapetschnig, A., Weick, E.M., Mitchell, J., Bagijn, M.P., Cording, A.C., Doebley, A.L., Goldstein, L.D., Lehrbach, N.J., Le Pen, J.*, et al.* (2012). piRNAs can trigger a multigenerational epigenetic memory in the germline of C. elegans. Cell *150*, 88-99.

Bagijn, M.P., Goldstein, L.D., Sapetschnig, A., Weick, E.M., Bouasker, S., Lehrbach, N.J., Simard, M.J., and Miska, E.A. (2012). Function, targets, and evolution of Caenorhabditis elegans piRNAs. Science *337*, 574-578.

Balzeau, J., Menezes, M.R., Cao, S., and Hagan, J.P. (2017). The LIN28/let-7 Pathway in Cancer. Front Genet *8*, 31.

Bartel, D.P. (2009). MicroRNAs: target recognition and regulatory functions. Cell *136*, 215-233.

Barton, M.K., and Kimble, J. (1990). fog-1, a regulatory gene required for specification of spermatogenesis in the germ line of Caenorhabditis elegans. Genetics *125*, 29-39.

Bean, C.J., Schaner, C.E., and Kelly, W.G. (2004). Meiotic pairing and imprinted X chromatin assembly in Caenorhabditis elegans. Nat Genet *36*, 100-105.

Bender, L.B., Cao, R., Zhang, Y., and Strome, S. (2004). The MES-2/MES-3/MES-6 complex and regulation of histone H3 methylation in C. elegans. Curr Biol *14*, 1639-1643.

Bharadwaj, P.S., and Hall, S.E. (2017). Endogenous RNAi Pathways Are Required in Neurons for Dauer Formation in. Genetics *205*, 1503-1516.

Billi, A.C., Alessi, A.F., Khivansara, V., Han, T., Freeberg, M., Mitani, S., and Kim, J.K. (2012). The Caenorhabditis elegans HEN1 ortholog, HENN-1, methylates and stabilizes select subclasses of germline small RNAs. PLoS Genet *8*, e1002617.

Billi, A.C., Fischer, S.E., and Kim, J.K. (2014). Endogenous RNAi pathways in C. elegans. WormBook, 1-49.

Buckley, B.A., Burkhart, K.B., Gu, S.G., Spracklin, G., Kershner, A., Fritz, H., Kimble, J., Fire, A., and Kennedy, S. (2012). A nuclear Argonaute promotes multigenerational epigenetic inheritance and germline immortality. Nature *489*, 447-451.

Carrington, J.C., and Ambros, V. (2003). Role of microRNAs in plant and animal development. Science *301*, 336-338.

Cecere, G., Hoersch, S., O'Keeffe, S., Sachidanandam, R., and Grishok, A. (2014). Global effects of the CSR-1 RNA interference pathway on the transcriptional landscape. Nat Struct Mol Biol *21*, 358-365.

Cecere, G., Zheng, G.X., Mansisidor, A.R., Klymko, K.E., and Grishok, A. (2012). Promoters recognized by forkhead proteins exist for individual 21U-RNAs. Mol Cell *47*, 734-745.

Cech, T.R., and Steitz, J.A. (2014). The noncoding RNA revolution-trashing old rules to forge new ones. Cell *157*, 77-94.

Chang, H., Lim, J., Ha, M., and Kim, V.N. (2014). TAIL-seq: genome-wide determination of poly(A) tail length and 3' end modifications. Mol Cell *53*, 1044-1052.

Cinalli, R.M., Rangan, P., and Lehmann, R. (2008). Germ cells are forever. Cell *132*, 559-562.

Ciosk, R., DePalma, M., and Priess, J.R. (2006). Translational regulators maintain totipotency in the Caenorhabditis elegans germline. Science *311*, 851-853.

Claycomb, J.M., Batista, P.J., Pang, K.M., Gu, W., Vasale, J.J., van Wolfswinkel, J.C., Chaves, D.A., Shirayama, M., Mitani, S., Ketting, R.F.*, et al.* (2009). The Argonaute CSR-1 and its 22G-RNA co-factors target germline genes and are required for holocentric chromosome segregation. Cell *139*, 123-134.

Conine, C.C., Batista, P.J., Gu, W., Claycomb, J.M., Chaves, D.A., Shirayama, M., and Mello, C.C. (2010). Argonautes ALG-3 and ALG-4 are required for spermatogenesis-specific 26G-RNAs and thermotolerant sperm in Caenorhabditis elegans. Proc Natl Acad Sci U S A *107*, 3588-3593.

Conine, C.C., Moresco, J.J., Gu, W., Shirayama, M., Conte, D., Yates, J.R., and Mello, C.C. (2013). Argonautes promote male fertility and provide a paternal memory of germline gene expression in C. elegans. Cell *155*, 1532-1544.

Dahl, J.A., and Collas, P. (2008). A rapid micro chromatin immunoprecipitation assay (microChIP). Nat Protoc *3*, 1032-1045.

Dahl, J.A., and Collas, P. (2009). MicroChIP: chromatin immunoprecipitation for small cell numbers. Methods Mol Biol *567*, 59-74.

de Albuquerque, B.F., Luteijn, M.J., Cordeiro Rodrigues, R.J., van Bergeijk, P., Waaijers, S., Kaaij, L.J., Klein, H., Boxem, M., and Ketting, R.F. (2014). PID-1 is a novel factor that operates during 21U-RNA biogenesis in Caenorhabditis elegans. Genes Dev *28*, 683-688.

de Albuquerque, B.F., Placentino, M., and Ketting, R.F. (2015). Maternal piRNAs Are Essential for Germline Development following De Novo Establishment of Endo-siRNAs in Caenorhabditis elegans. Dev Cell *34*, 448-456.

Detwiler, M.R., Reuben, M., Li, X., Rogers, E., and Lin, R. (2001). Two zinc finger proteins, OMA-1 and OMA-2, are redundantly required for oocyte maturation in C. elegans. Dev Cell *1*, 187-199.

Devanapally, S., Ravikumar, S., and Jose, A.M. (2015). Double-stranded RNA made in C. elegans neurons can enter the germline and cause transgenerational gene silencing. Proc Natl Acad Sci U S A *112*, 2133-2138.

Dickinson, D.J., Ward, J.D., Reiner, D.J., and Goldstein, B. (2013). Engineering the Caenorhabditis elegans genome using Cas9-triggered homologous recombination. Nat Methods *10*, 1028-1034.

Draper, B.W., Mello, C.C., Bowerman, B., Hardin, J., and Priess, J.R. (1996). MEX-3 is a KH domain protein that regulates blastomere identity in early C. elegans embryos. Cell *87*, 205-216.

Duchaine, T.F., Wohlschlegel, J.A., Kennedy, S., Bei, Y., Conte, D., Jr., Pang, K., Brownell, D.R., Harding, S., Mitani, S., Ruvkun, G.*, et al.* (2006). Functional proteomics reveals the biochemical niche of C. elegans DCR-1 in multiple small-RNA-mediated pathways. Cell *124*, 343-354.

Faehnle, C.R., Walleshauser, J., and Joshua-Tor, L. (2014). Mechanism of Dis3l2 substrate recognition in the Lin28-let-7 pathway. Nature *514*, 252-256.

Fagegaltier, D., Falciatori, I., Czech, B., Castel, S., Perrimon, N., Simcox, A., and Hannon, G.J. (2016). Oncogenic transformation of Drosophila somatic cells induces a functional piRNA pathway. Genes Dev *30*, 1623-1635.

Fischer, S.E., Butler, M.D., Pan, Q., and Ruvkun, G. (2008). Trans-splicing in C. elegans generates the negative RNAi regulator ERI-6/7. Nature *455*, 491-496.

Fischer, S.E., Montgomery, T.A., Zhang, C., Fahlgren, N., Breen, P.C., Hwang, A., Sullivan, C.M., Carrington, J.C., and Ruvkun, G. (2011). The ERI-6/7 helicase acts at the first stage of an siRNA amplification pathway that targets recent gene duplications. PLoS Genet *7*, e1002369.

Fong, Y., Bender, L., Wang, W., and Strome, S. (2002). Regulation of the different chromatin states of autosomes and X chromosomes in the germ line of C. elegans. Science *296*, 2235-2238.

Francis, R., Maine, E., and Schedl, T. (1995). Analysis of the multiple roles of gld-1 in germline development: interactions with the sex determination cascade and the glp-1 signaling pathway. Genetics *139*, 607-630.

Furuhashi, H., Takasaki, T., Rechtsteiner, A., Li, T., Kimura, H., Checchi, P.M., Strome, S., and Kelly, W.G. (2010). Trans-generational epigenetic regulation of C. elegans primordial germ cells. Epigenetics Chromatin *3*, 15.

Gaydos, L.J., Rechtsteiner, A., Egelhofer, T.A., Carroll, C.R., and Strome, S. (2012). Antagonism between MES-4 and Polycomb repressive complex 2 promotes appropriate gene expression in C. elegans germ cells. Cell Rep *2*, 1169-1177.

Gaydos, L.J., Wang, W., and Strome, S. (2014). Gene repression. H3K27me and PRC2 transmit a memory of repression across generations and during development. Science *345*, 1515-1518.

Geldziler, B.D., Marcello, M.R., Shakes, D.C., and Singson, A. (2011). The genetics and cell biology of fertilization. Methods Cell Biol *106*, 343-375.

Gent, J.I., Lamm, A.T., Pavelec, D.M., Maniar, J.M., Parameswaran, P., Tao, L., Kennedy, S., and Fire, A.Z. (2010). Distinct phases of siRNA synthesis in an endogenous RNAi pathway in C. elegans soma. Mol Cell *37*, 679-689.

Gent, J.I., Schvarzstein, M., Villeneuve, A.M., Gu, S.G., Jantsch, V., Fire, A.Z., and Baudrimont, A. (2009). A Caenorhabditis elegans RNA-directed RNA polymerase in sperm development and endogenous RNA interference. Genetics *183*, 1297-1314.

Goh, W.S., Seah, J.W., Harrison, E.J., Chen, C., Hammell, C.M., and Hannon, G.J. (2014). A genome-wide RNAi screen identifies factors required for distinct stages of C. elegans piRNA biogenesis. Genes Dev *28*, 797-807.

Greer, Eric L., Blanco, Mario A., Gu, L., Sendinc, E., Liu, J., Aristizábal-Corrales, D., Hsu, C.-H., Aravind, L., He, C., and Shi, Y. (2015). DNA Methylation on N6-Adenine in C. elegans. Cell *161*, 868-878.

Gruidl, M.E., Smith, P.A., Kuznicki, K.A., McCrone, J.S., Kirchner, J., Roussell, D.L., Strome, S., and Bennett, K.L. (1996). Multiple potential germ-line helicases are components of the germ-line-specific P granules of Caenorhabditis elegans. Proc Natl Acad Sci U S A *93*, 13837-13842.

Gu, S.G., Pak, J., Guang, S., Maniar, J.M., Kennedy, S., and Fire, A. (2012a). Amplification of siRNA in Caenorhabditis elegans generates a transgenerational sequence-targeted histone H3 lysine 9 methylation footprint. Nat Genet *44*, 157-164.

Gu, W., Lee, H.C., Chaves, D., Youngman, E.M., Pazour, G.J., Conte, D., and Mello, C.C. (2012b). CapSeq and CIP-TAP identify Pol II start sites and reveal capped small RNAs as C. elegans piRNA precursors. Cell *151*, 1488-1500.

Gu, W., Shirayama, M., Conte, D., Vasale, J., Batista, P.J., Claycomb, J.M., Moresco, J.J., Youngman, E., Keys, J., Stoltz, M.J.*, et al.* (2009). Distinct Argonaute-mediated 22G-RNA pathways direct genome surveillance in the C. elegans germline. Molecular cell *36*, 231-244.

Guang, S., Bochner, A.F., Burkhart, K.B., Burton, N., Pavelec, D.M., and Kennedy, S. (2010). Small regulatory RNAs inhibit RNA polymerase II during the elongation phase of transcription. Nature *465*, 1097-1101.

Guedes, S., and Priess, J.R. (1997). The C. elegans MEX-1 protein is present in germline blastomeres and is a P granule component. Development *124*, 731-739.

Guo, Y., Yang, B., Li, Y., Xu, X., and Maine, E.M. (2015). Enrichment of H3K9me2 on Unsynapsed Chromatin in Caenorhabditis elegans Does Not Target de Novo Sites. G3 (Bethesda) *5*, 1865-1878.

Ha, M., and Kim, V.N. (2014). Regulation of microRNA biogenesis. Nat Rev Mol Cell Biol *15*, 509-524.

Han, T., Manoharan, A.P., Harkins, T.T., Bouffard, P., Fitzpatrick, C., Chu, D.S., Thierry-Mieg, D., Thierry-Mieg, J., and Kim, J.K. (2009). 26G endo-siRNAs regulate spermatogenic and zygotic gene expression in Caenorhabditis elegans. Proc Natl Acad Sci U S A *106*, 18674-18679.

Heo, I., Ha, M., Lim, J., Yoon, M.J., Park, J.E., Kwon, S.C., Chang, H., and Kim, V.N. (2012). Mono-uridylation of pre-microRNA as a key step in the biogenesis of group II let-7 microRNAs. Cell *151*, 521-532.

Hillers, K.J., Jantsch, V., Martinez-Perez, E., and Yanowitz, J.L. (2015). Meiosis. WormBook, 1-54.

Hirsh, D., Oppenheim, D., and Klass, M. (1976). Development of the reproductive system of Caenorhabditis elegans. Dev Biol *49*, 200-219.

Hodgkin, J., Horvitz, H.R., and Brenner, S. (1979). Nondisjunction Mutants of the Nematode CAENORHABDITIS ELEGANS. Genetics *91*, 67-94.

Hubbard, E.J.A., and Greenstein, D. (2005). Introduction to the germ line (Wormbook, ed: The C. *elegans* Research Community).

Huelgas-Morales, G., Silva-García, C.G., Salinas, L.S., Greenstein, D., and Navarro, R.E. (2016). The Stress Granule RNA-Binding Protein TIAR-1 Protects Female Germ Cells from Heat Shock in Caenorhabditis elegans. G3 (Bethesda) *6*, 1031-1047.

Ibrahim, F., Rymarquis, L.A., Kim, E.J., Becker, J., Balassa, E., Green, P.J., and Cerutti, H. (2010). Uridylation of mature miRNAs and siRNAs by the MUT68 nucleotidyltransferase promotes their degradation in Chlamydomonas. Proc Natl Acad Sci U S A *107*, 3906-3911.

Jud, M.C., Czerwinski, M.J., Wood, M.P., Young, R.A., Gallo, C.M., Bickel, J.S., Petty, E.L., Mason, J.M., Little, B.A., Padilla, P.A*., et al.* (2008). Large P body-like RNPs form in C. elegans oocytes in response to arrested ovulation, heat shock, osmotic stress, and anoxia and are regulated by the major sperm protein pathway. Dev Biol *318*, 38-51.

Kamminga, L.M., Luteijn, M.J., den Broeder, M.J., Redl, S., Kaaij, L.J., Roovers, E.F., Ladurner, P., Berezikov, E., and Ketting, R.F. (2010). Hen1 is required for oocyte development and piRNA stability in zebrafish. EMBO J *29*, 3688-3700.

Kamminga, L.M., van Wolfswinkel, J.C., Luteijn, M.J., Kaaij, L.J., Bagijn, M.P., Sapetschnig, A., Miska, E.A., Berezikov, E., and Ketting, R.F. (2012). Differential impact of the HEN1 homolog HENN-1 on 21U and 26G RNAs in the germline of Caenorhabditis elegans. PLoS Genet *8*, e1002702.

Katz, D.J., Edwards, T.M., Reinke, V., and Kelly, W.G. (2009). A C. elegans LSD1 demethylase contributes to germline immortality by reprogramming epigenetic memory. Cell *137*, 308-320.

Kawasaki, I., Amiri, A., Fan, Y., Meyer, N., Dunkelbarger, S., Motohashi, T., Karashima, T., Bossinger, O., and Strome, S. (2004). The PGL family proteins associate with germ granules and function redundantly in Caenorhabditis elegans germline development. Genetics *167*, 645-661.

Kawasaki, I., Shim, Y.H., Kirchner, J., Kaminker, J., Wood, W.B., and Strome, S. (1998). PGL-1, a predicted RNA-binding component of germ granules, is essential for fertility in C. elegans. Cell *94*, 635-645.

Kelly, W.G., Schaner, C.E., Dernburg, A.F., Lee, M.H., Kim, S.K., Villeneuve, A.M., and Reinke, V. (2002). X-chromosome silencing in the germline of C. elegans. Development *129*, 479-492.

Kim, B., Ha, M., Loeff, L., Chang, H., Simanshu, D.K., Li, S., Fareh, M., Patel, D.J., Joo, C., and Kim, V.N. (2015). TUT7 controls the fate of precursor microRNAs by using three different uridylation mechanisms. EMBO J *34*, 1801-1815.

Kim, V.N., Han, J., and Siomi, M.C. (2009). Biogenesis of small RNAs in animals. Nat Rev Mol Cell Biol *10*, 126-139.

Knutson, A.K., Egelhofer, T., Rechtsteiner, A., and Strome, S. (2017). Germ Granules Prevent Accumulation of Somatic Transcripts in the Adult. Genetics *206*, 163-178.

Kodoyianni, V., Maine, E.M., and Kimble, J. (1992). Molecular basis of loss-of-function mutations in the glp-1 gene of Caenorhabditis elegans. Mol Biol Cell *3*, 1199-1213.

Kozlowski, E., Wasserman, G.A., Morgan, M., O'Carroll, D., Ramirez, N.P., Gummuluru, S., Rah, J.Y., Gower, A.C., Ieong, M., Quinton, L.J.*, et al.* (2017). The RNA uridyltransferase Zcchc6 is expressed in macrophages and impacts innate immune responses. PLoS One *12*, e0179797.

Kuznicki, K.A., Smith, P.A., Leung-Chiu, W.M., Estevez, A.O., Scott, H.C., and Bennett, K.L. (2000). Combinatorial RNA interference indicates GLH-4 can compensate for GLH-1; these two P granule components are critical for fertility in C. elegans. Development *127*, 2907-2916.

Kwak, J.E., and Wickens, M. (2007). A family of poly(U) polymerases. RNA *13*, 860-867.

Käser-Pébernard, S., Müller, F., and Wicky, C. (2014). LET-418/Mi2 and SPR-5/LSD1 cooperatively prevent somatic reprogramming of C. elegans germline stem cells. Stem Cell Reports *2*, 547-559.

Lai, F., and King, M.L. (2013). Repressive translational control in germ cells. Mol Reprod Dev *80*, 665-676.

Lan, F., Zaratiegui, M., Villén, J., Vaughn, M.W., Verdel, A., Huarte, M., Shi, Y., Gygi, S.P., Moazed, D., and Martienssen, R.A. (2007). S. pombe LSD1 homologs regulate heterochromatin propagation and euchromatic gene transcription. Mol Cell *26*, 89-101.

Lawrence, M., Daujat, S., and Schneider, R. (2016). Lateral Thinking: How Histone Modifications Regulate Gene Expression. Trends Genet *32*, 42-56.

Lee, H.C., Gu, W., Shirayama, M., Youngman, E., Conte, D., and Mello, C.C. (2012). C. elegans piRNAs mediate the genome-wide surveillance of germline transcripts. Cell *150*, 78-87.

Lehrbach, N.J., Armisen, J., Lightfoot, H.L., Murfitt, K.J., Bugaut, A., Balasubramanian, S., and Miska, E.A. (2009). LIN-28 and the poly(U) polymerase PUP-2 regulate let-7 microRNA processing in Caenorhabditis elegans. Nat Struct Mol Biol *16*, 1016-1020.

Lim, J., Ha, M., Chang, H., Kwon, S.C., Simanshu, D.K., Patel, D.J., and Kim, V.N. (2014). Uridylation by TUT4 and TUT7 marks mRNA for degradation. Cell *159*, 1365-1376.

Luciano, D.J., Mirsky, H., Vendetti, N.J., and Maas, S. (2004). RNA editing of a miRNA precursor. RNA *10*, 1174-1177.

Lui, D.Y., and Colaiácovo, M.P. (2013). Meiotic development in Caenorhabditis elegans. Adv Exp Med Biol *757*, 133-170.

Maine, E.M., Hauth, J., Ratliff, T., Vought, V.E., She, X., and Kelly, W.G. (2005). EGO-1, a putative RNA-dependent RNA polymerase, is required for heterochromatin assembly on unpaired dna during C. elegans meiosis. Curr Biol *15*, 1972-1978.

Mangone, M., Manoharan, A.P., Thierry-Mieg, D., Thierry-Mieg, J., Han, T., Mackowiak, S.D., Mis, E., Zegar, C., Gutwein, M.R., Khivansara, V.*, et al.* (2010). The landscape of C. elegans 3'UTRs. Science *329*, 432-435.

Martin, G., and Keller, W. (2007). RNA-specific ribonucleotidyl transferases. RNA *13*, 1834-1849.

McKee, B.D., and Handel, M.A. (1993). Sex chromosomes, recombination, and chromatin conformation. Chromosoma *102*, 71-80.

Mello, C.C., Draper, B.W., Krause, M., Weintraub, H., and Priess, J.R. (1992). The pie-1 and mex-1 genes and maternal control of blastomere identity in early C. elegans embryos. Cell *70*, 163-176.

Mello, C.C., Schubert, C., Draper, B., Zhang, W., Lobel, R., and Priess, J.R. (1996). The PIE-1 protein and germline specification in C. elegans embryos. Nature *382*, 710-712.

Morgan, H.D., Santos, F., Green, K., Dean, W., and Reik, W. (2005). Epigenetic reprogramming in mammals. Hum Mol Genet *14 Spec No 1*, R47-58.

Morgan, M., Much, C., DiGiacomo, M., Azzi, C., Ivanova, I., Vitsios, D.M., Pistolic, J., Collier, P., Moreira, P.N., Benes, V.*, et al.* (2017). mRNA 3' uridylation and poly(A) tail length sculpt the mammalian maternal transcriptome. Nature *548*, 347-351.

Morozov, I.Y., Jones, M.G., Razak, A.A., Rigden, D.J., and Caddick, M.X. (2010). CUCU modification of mRNA promotes decapping and transcript degradation in Aspergillus nidulans. Mol Cell Biol *30*, 460-469.

Mu, W., Starmer, J., Fedoriw, A.M., Yee, D., and Magnuson, T. (2014). Repression of the soma-specific transcriptome by Polycomb-repressive complex 2 promotes male germ cell development. Genes Dev *28*, 2056-2069.

Mullen, T.E., and Marzluff, W.F. (2008). Degradation of histone mRNA requires oligouridylation followed by decapping and simultaneous degradation of the mRNA both 5' to 3' and 3' to 5'. Genes Dev *22*, 50-65.

Munoz-Tello, P., Rajappa, L., Coquille, S., and Thore, S. (2015). Polyuridylation in Eukaryotes: A 3'-End Modification Regulating RNA Life. Biomed Res Int *2015*, 968127.

Newman, M.A., Thomson, J.M., and Hammond, S.M. (2008). Lin-28 interaction with the Let-7 precursor loop mediates regulated microRNA processing. RNA *14*, 1539-1549.

Noble, S.L., Allen, B.L., Goh, L.K., Nordick, K., and Evans, T.C. (2008). Maternal mRNAs are regulated by diverse P body-related mRNP granules during early Caenorhabditis elegans development. J Cell Biol *182*, 559-572.

Norbury, C.J. (2013). Cytoplasmic RNA: a case of the tail wagging the dog. Nat Rev Mol Cell Biol *14*, 643-653.

Okada, Y., Scott, G., Ray, M.K., Mishina, Y., and Zhang, Y. (2007). Histone demethylase JHDM2A is critical for Tnp1 and Prm1 transcription and spermatogenesis. Nature *450*, 119-123.

Paix, A., Wang, Y., Smith, H.E., Lee, C.Y., Calidas, D., Lu, T., Smith, J., Schmidt, H., Krause, M.W., and Seydoux, G. (2014). Scalable and versatile genome editing using linear DNAs with microhomology to Cas9 Sites in Caenorhabditis elegans. Genetics *198*, 1347-1356.

Pandey, N.B., and Marzluff, W.F. (1987). The stem-loop structure at the 3' end of histone mRNA is necessary and sufficient for regulation of histone mRNA stability. Mol Cell Biol *7*, 4557-4559.

Parker, R., and Sheth, U. (2007). P bodies and the control of mRNA translation and degradation. Mol Cell *25*, 635-646.

Patel, T., Tursun, B., Rahe, D.P., and Hobert, O. (2012). Removal of Polycomb repressive complex 2 makes C. elegans germ cells susceptible to direct conversion into specific somatic cell types. Cell Rep *2*, 1178-1186.

Pavelec, D.M., Lachowiec, J., Duchaine, T.F., Smith, H.E., and Kennedy, S. (2009). Requirement for the ERI/DICER complex in endogenous RNA interference and sperm development in Caenorhabditis elegans. Genetics *183*, 1283-1295.

Pazdernik, N., and Schedl, T. (2013). Introduction to germ cell development in Caenorhabditis elegans. Adv Exp Med Biol *757*, 1-16.

Petrella, L.N., Wang, W., Spike, C.A., Rechtsteiner, A., Reinke, V., and Strome, S. (2011). synMuv B proteins antagonize germline fate in the intestine and ensure C. elegans survival. Development *138*, 1069-1079.

Phillips, C.M., Brown, K.C., Montgomery, B.E., Ruvkun, G., and Montgomery, T.A. (2015). piRNAs and piRNA-Dependent siRNAs Protect Conserved and Essential C. elegans Genes from Misrouting into the RNAi Pathway. Dev Cell *34*, 457-465.

Qiao, L., Lissemore, J.L., Shu, P., Smardon, A., Gelber, M.B., and Maine, E.M. (1995). Enhancers of glp-1, a gene required for cell-signaling in Caenorhabditis elegans, define a set of genes required for germline development. Genetics *141*, 551-569.

Rechtsteiner, A., Ercan, S., Takasaki, T., Phippen, T.M., Egelhofer, T.A., Wang, W., Kimura, H., Lieb, J.D., and Strome, S. (2010). The histone H3K36 methyltransferase MES-4 acts

epigenetically to transmit the memory of germline gene expression to progeny. PLoS Genet *6*, e1001091.

Reinke, V., Gil, I.S., Ward, S., and Kazmer, K. (2004). Genome-wide germline-enriched and sex-biased expression profiles in Caenorhabditis elegans. Development *131*, 311-323.

Reinke, V., Smith, H.E., Nance, J., Wang, J., Van Doren, C., Begley, R., Jones, S.J., Davis, E.B., Scherer, S., Ward, S.*, et al.* (2000). A global profile of germline gene expression in C. elegans. Mol Cell *6*, 605-616.

Ren, G., Xie, M., Zhang, S., Vinovskis, C., Chen, X., and Yu, B. (2014). Methylation protects microRNAs from an AGO1-associated activity that uridylates 5' RNA fragments generated by AGO1 cleavage. Proc Natl Acad Sci U S A *111*, 6365-6370.

Resnick, T.D., McCulloch, K.A., and Rougvie, A.E. (2010). miRNAs give worms the time of their lives: small RNAs and temporal control in Caenorhabditis elegans. Dev Dyn *239*, 1477-1489.

Rissland, O.S., Mikulasova, A., and Norbury, C.J. (2007). Efficient RNA polyuridylation by noncanonical poly(A) polymerases. Mol Cell Biol *27*, 3612-3624.

Rissland, O.S., and Norbury, C.J. (2009). Decapping is preceded by 3' uridylation in a novel pathway of bulk mRNA turnover. Nat Struct Mol Biol *16*, 616-623.

Robert, V.J., Mercier, M.G., Bedet, C., Janczarski, S., Merlet, J., Garvis, S., Ciosk, R., and Palladino, F. (2014). The SET-2/SET1 histone H3K4 methyltransferase maintains pluripotency in the Caenorhabditis elegans germline. Cell Rep *9*, 443-450.

Ruby, J.G., Jan, C., Player, C., Axtell, M.J., Lee, W., Nusbaum, C., Ge, H., and Bartel, D.P. (2006). Large-scale sequencing reveals 21U-RNAs and additional microRNAs and endogenous siRNAs in C. elegans. Cell *127*, 1193-1207.

Rüegger, S., Miki, T.S., Hess, D., and Großhans, H. (2015). The ribonucleotidyl transferase USIP-1 acts with SART3 to promote U6 snRNA recycling. Nucleic Acids Res *43*, 3344-3357.

Safdar, K., Gu, A., Xu, X., Au, V., Taylor, J., Flibotte, S., Moerman, D.G., and Maine, E.M. (2016). UBR-5, a Conserved HECT-Type E3 Ubiquitin Ligase, Negatively Regulates Notch-Type Signaling in Caenorhabditis elegans. G3 (Bethesda) *6*, 2125-2134.

Sakaguchi, A., Sarkies, P., Simon, M., Doebley, A.L., Goldstein, L.D., Hedges, A., Ikegami, K., Alvares, S.M., Yang, L., LaRocque, J.R.*, et al.* (2014). Caenorhabditis elegans RSD-2 and RSD-6 promote germ cell immortality by maintaining small interfering RNA populations. Proc Natl Acad Sci U S A *111*, E4323-4331.

Sano, M., Wang, S.C., Shirai, M., Scaglia, F., Xie, M., Sakai, S., Tanaka, T., Kulkarni, P.A., Barger, P.M., Youker, K.A.*, et al.* (2004). Activation of cardiac Cdk9 represses PGC-1 and confers a predisposition to heart failure. EMBO J *23*, 3559-3569.

Schaner, C.E., Deshpande, G., Schedl, P.D., and Kelly, W.G. (2003). A conserved chromatin architecture marks and maintains the restricted germ cell lineage in worms and flies. Dev Cell *5*, 747-757.

Schaner, C.E., and Kelly, W.G. (2006). Germline chromatin. WormBook, 1-14.

Schapira, M., Tyers, M., Torrent, M., and Arrowsmith, C.H. (2017). WD40 repeat domain proteins: a novel target class? Nat Rev Drug Discov *16*, 773-786.

Schisa, J.A., Pitt, J.N., and Priess, J.R. (2001). Analysis of RNA associated with P granules in germ cells of C. elegans adults. Development *128*, 1287-1298.

Schmidt, M.J., West, S., and Norbury, C.J. (2011). The human cytoplasmic RNA terminal U-transferase ZCCHC11 targets histone mRNAs for degradation. RNA *17*, 39-44.

Scott, D.D., and Norbury, C.J. (2013). RNA decay via 3' uridylation. Biochim Biophys Acta *1829*, 654-665.

Seth, M., Shirayama, M., Gu, W., Ishidate, T., Conte, D., and Mello, C.C. (2013). The C. elegans CSR-1 argonaute pathway counteracts epigenetic silencing to promote germline gene expression. Dev Cell *27*, 656-663.

Shakes, D.C., Wu, J.C., Sadler, P.L., Laprade, K., Moore, L.L., Noritake, A., and Chu, D.S. (2009). Spermatogenesis-specific features of the meiotic program in Caenorhabditis elegans. PLoS Genet *5*, e1000611.

She, X., Xu, X., Fedotov, A., Kelly, W.G., and Maine, E.M. (2009). Regulation of heterochromatin assembly on unpaired chromosomes during *Caenorhabditis elegans* meiosis by components of a small RNA-mediated pathway. PLoS Genet *5*, e1000624.

Shen, B., and Goodman, H.M. (2004). Uridine addition after microRNA-directed cleavage. Science *306*, 997.

Shirayama, M., Seth, M., Lee, H.C., Gu, W., Ishidate, T., Conte, D., and Mello, C.C. (2012). piRNAs initiate an epigenetic memory of nonself RNA in the C. elegans germline. Cell *150*, 65-77.

Silva-García, C.G., and Estela Navarro, R. (2013). The C. elegans TIA-1/TIAR homolog TIAR-1 is required to induce germ cell apoptosis. Genesis *51*, 690-707.

Siomi, M.C., Sato, K., Pezic, D., and Aravin, A.A. (2011). PIWI-interacting small RNAs: the vanguard of genome defence. Nat Rev Mol Cell Biol *12*, 246-258.

Slezak-Prochazka, I., Durmus, S., Kroesen, B.J., and van den Berg, A. (2010). MicroRNAs, macrocontrol: regulation of miRNA processing. RNA *16*, 1087-1095.

Smardon, A., Spoerke, J.M., Stacey, S.C., Klein, M.E., Mackin, N., and Maine, E.M. (2000). EGO-1 is related to RNA-directed RNA polymerase and functions in germ-line development and RNA interference in C. elegans. Curr Biol *10*, 169-178.

Smelick, C., and Ahmed, S. (2005). Achieving immortality in the C. elegans germline. Ageing Res Rev *4*, 67-82.

Spike, C.A., Coetzee, D., Nishi, Y., Guven-Ozkan, T., Oldenbroek, M., Yamamoto, I., Lin, R., and Greenstein, D. (2014). Translational control of the oogenic program by components of OMA ribonucleoprotein particles in Caenorhabditis elegans. Genetics *198*, 1513-1533.

Spracklin, G., Fields, B., Wan, G., Becker, D., Wallig, A., Shukla, A., and Kennedy, S. (2017). The RNAi Inheritance Machinery of. Genetics *206*, 1403-1416.

Strome, S. (2005). Specification of the germ line (Wormbook, ed: The *C. elegans* Research Community).

Strome, S., Kelly, W.G., Ercan, S., and Lieb, J.D. (2014). Regulation of the X chromosomes in Caenorhabditis elegans. Cold Spring Harb Perspect Biol *6*.

Strome, S., and Lehmann, R. (2007). Germ versus soma decisions: lessons from flies and worms. Science *316*, 392-393.

Strome, S., and Updike, D. (2015). Specifying and protecting germ cell fate. Nat Rev Mol Cell Biol *16*, 406-416.

Su, W., Slepenkov, S.V., Slevin, M.K., Lyons, S.M., Ziemniak, M., Kowalska, J., Darzynkiewicz, E., Jemielity, J., Marzluff, W.F., and Rhoads, R.E. (2013). mRNAs containing the histone 3' stem-loop are degraded primarily by decapping mediated by oligouridylation of the 3' end. RNA *19*, 1-16.

Subramaniam, K., and Seydoux, G. (1999). nos-1 and nos-2, two genes related to Drosophila nanos, regulate primordial germ cell development and survival in Caenorhabditis elegans. Development *126*, 4861-4871.

Thornton, J.E., Chang, H.M., Piskounova, E., and Gregory, R.I. (2012). Lin28-mediated control of let-7 microRNA expression by alternative TUTases Zcchc11 (TUT4) and Zcchc6 (TUT7). RNA *18*, 1875-1885.

Thornton, J.E., Du, P., Jing, L., Sjekloca, L., Lin, S., Grossi, E., Sliz, P., Zon, L.I., and Gregory, R.I. (2014). Selective microRNA uridylation by Zcchc6 (TUT7) and Zcchc11 (TUT4). Nucleic Acids Res *42*, 11777-11791.

Tian, B., and Manley, J.L. (2013). Alternative cleavage and polyadenylation: the long and short of it. Trends Biochem Sci *38*, 312-320.

Timmons, L., Court, D.L., and Fire, A. (2001). Ingestion of bacterially expressed dsRNAs can produce specific and potent genetic interference in Caenorhabditis elegans. Gene *263*, 103-112.

Tursun, B., Patel, T., Kratsios, P., and Hobert, O. (2011). Direct conversion of C. elegans germ cells into specific neuron types. Science *331*, 304-308.

Unhavaithaya, Y., Shin, T.H., Miliaras, N., Lee, J., Oyama, T., and Mello, C.C. (2002). MEP-1 and a homolog of the NURD complex component Mi-2 act together to maintain germline-soma distinctions in C. elegans. Cell *111*, 991-1002.

Updike, D., and Strome, S. (2010). P Granule Assembly and Function in Caenorhabditis elegans Germ Cells. Journal of andrology *31*, 53-60.

Updike, D.L., Knutson, A.K., Egelhofer, T.A., Campbell, A.C., and Strome, S. (2014). Germ-granule components prevent somatic development in the C. elegans germline. Curr Biol *24*, 970-975.

van Wolfswinkel, J.C., Claycomb, J.M., Batista, P.J., Mello, C.C., Berezikov, E., and Ketting, R.F. (2009). CDE-1 affects chromosome segregation through uridylation of CSR-1-bound siRNAs. Cell *139*, 135-148.

Van Wynsberghe, P.M., Kai, Z.S., Massirer, K.B., Burton, V.H., Yeo, G.W., and Pasquinelli, A.E. (2011). LIN-28 co-transcriptionally binds primary let-7 to regulate miRNA maturation in Caenorhabditis elegans. Nat Struct Mol Biol *18*, 302-308.

Van Wynsberghe, P.M., and Maine, E.M. (2013). Epigenetic control of germline development. Adv Exp Med Biol *757*, 373-403.

Vasale, J.J., Gu, W., Thivierge, C., Batista, P.J., Claycomb, J.M., Youngman, E.M., Duchaine, T.F., Mello, C.C., and Conte, D. (2010). Sequential rounds of RNA-dependent RNA transcription drive endogenous small-RNA biogenesis in the ERGO-1/Argonaute pathway. Proc Natl Acad Sci U S A *107*, 3582-3587.

Vella, M.C., Choi, E.Y., Lin, S.Y., Reinert, K., and Slack, F.J. (2004). The C. elegans microRNA let-7 binds to imperfect let-7 complementary sites from the lin-41 3'UTR. Genes Dev *18*, 132-137.

Voronina, E., Seydoux, G., Sassone-Corsi, P., and Nagamori, I. (2011). RNA granules in germ cells. Cold Spring Harb Perspect Biol *3*.

Wang, D., Kennedy, S., Conte, D., Kim, J.K., Gabel, H.W., Kamath, R.S., Mello, C.C., and Ruvkun, G. (2005). Somatic misexpression of germline P granules and enhanced RNA interference in retinoblastoma pathway mutants. Nature *436*, 593-597.

Wang, J.T., and Seydoux, G. (2014). P granules. Curr Biol *24*, R637-R638.

Wang, L., Nam, Y., Lee, A.K., Yu, C., Roth, K., Chen, C., Ransey, E.M., and Sliz, P. (2017). LIN28 Zinc Knuckle Domain Is Required and Sufficient to Induce let-7 Oligouridylation. Cell Rep *18*, 2664-2675.

Wang, S., Fisher, K., and Poulin, G.B. (2011). Lineage specific trimethylation of H3 on lysine 4 during C. elegans early embryogenesis. Dev Biol *355*, 227-238.

Wang, S.W., Norbury, C., Harris, A.L., and Toda, T. (1999). Caffeine can override the S-M checkpoint in fission yeast. J Cell Sci *112 (Pt 6)*, 927-937.

Wang, S.W., Toda, T., MacCallum, R., Harris, A.L., and Norbury, C. (2000). Cid1, a fission yeast protein required for S-M checkpoint control when DNA polymerase delta or epsilon is inactivated. Mol Cell Biol *20*, 3234-3244.

Wedeles, C.J., Wu, M.Z., and Claycomb, J.M. (2013). Protection of germline gene expression by the C. elegans Argonaute CSR-1. Dev Cell *27*, 664-671.

Weick, E.M., and Miska, E.A. (2014). piRNAs: from biogenesis to function. Development *141*, 3458-3471.

Weick, E.M., Sarkies, P., Silva, N., Chen, R.A., Moss, S.M., Cording, A.C., Ahringer, J., Martinez-Perez, E., and Miska, E.A. (2014). PRDE-1 is a nuclear factor essential for the biogenesis of Ruby motif-dependent piRNAs in C. elegans. Genes Dev *28*, 783-796.

Wickens, M., and Kwak, J.E. (2008). Molecular biology. A tail tale for U. Science *319*, 1344-1345.

Xiao, Y., Bedet, C., Robert, V.J., Simonet, T., Dunkelbarger, S., Rakotomalala, C., Soete, G., Korswagen, H.C., Strome, S., and Palladino, F. (2011). Caenorhabditis elegans chromatin-associated proteins SET-2 and ASH-2 are differentially required for histone H3 Lys 4 methylation in embryos and adult germ cells. Proc Natl Acad Sci U S A *108*, 8305-8310.

Xu, F., Feng, X., Chen, X., Weng, C., Yan, Q., Xu, T., Hong, M., and Guang, S. (2018). A Cytoplasmic Argonaute Protein Promotes the Inheritance of RNAi. Cell Rep *23*, 2482-2494.

Xu, K., Lin, J., Zandi, R., Roth, J.A., and Ji, L. (2016). MicroRNA-mediated target mRNA cleavage and 3'-uridylation in human cells. Sci Rep *6*, 30242.

Xu, L., Paulsen, J., Yoo, Y., Goodwin, E.B., and Strome, S. (2001). Caenorhabditis elegans MES-3 is a target of GLD-1 and functions epigenetically in germline development. Genetics *159*, 1007-1017.

Yeom, K.H., Lee, Y., Han, J., Suh, M.R., and Kim, V.N. (2006). Characterization of DGCR8/Pasha, the essential cofactor for Drosha in primary miRNA processing. Nucleic Acids Res *34*, 4622-4629.

Yoo, A.S., and Greenwald, I. (2005). LIN-12/Notch activation leads to microRNA-mediated down-regulation of Vav in C. elegans. Science *310*, 1330-1333.

Zhang, C., Montgomery, T.A., Gabel, H.W., Fischer, S.E., Phillips, C.M., Fahlgren, N., Sullivan, C.M., Carrington, J.C., and Ruvkun, G. (2011). mut-16 and other mutator class genes modulate 22G and 26G siRNA pathways in Caenorhabditis elegans. Proc Natl Acad Sci U S A *108*, 1201-1208.

Zhang, C., and Ruvkun, G. (2012). New insights into siRNA amplification and RNAi. RNA Biol *9*, 1045-1049.

Zhang, F., Barboric, M., Blackwell, T.K., and Peterlin, B.M. (2003). A model of repression: CTD analogs and PIE-1 inhibit transcriptional elongation by P-TEFb. Genes Dev *17*, 748-758.

Zhong, M., Niu, W., Lu, Z.J., Sarov, M., Murray, J.I., Janette, J., Raha, D., Sheaffer, K.L., Lam, H.Y., Preston, E.*, et al.* (2010). Genome-wide identification of binding sites defines distinct

functions for Caenorhabditis elegans PHA-4/FOXA in development and environmental response. PLoS Genet *6*, e1000848.

Curriculum vitae

YINI LI

Syracuse University

Department of Biology

107 College Place, Syracuse, NY, 13244

315-751-1381

yli173@syr.edu

EDUCATION

July 2018   Ph.D. in Biology, Syracuse University, Syracuse, NY | **Advisor: Eleanor Maine**

Dissertation: The balance of poly(U) polymerase activity ensures germline identity, survival, and development in *Caenorhabditis elegans*

2012   B.S. Biology, East China University of Science and Technology, Shanghai, China

B.A. English, East China University of Science and Technology, Shanghai, China

RESEARCH EXPERIENCE

Aug 2012-   Syracuse University, Syracuse, NY, USA | **Dr. Eleanor Maine lab**

present   Investigating the regulatory mechanisms of germline development:

- The role of poly(U) polymerases in germline development (see publication)

- The small RNA and mRNA targets of poly(U) polymerases in

Caenorhabditis elegans (in progress)

Jan 2013-   Syracuse University, Syracuse, NY, USA | **Dr. Sandra Hewett lab**

Jun 2013   Rotation: the function of microRNA-26 in suppression of human/mouse/rat

glioma cell proliferation via targeting cysteine/glutamate antiporter System x_c^-

Dec 2010-   Institute Pasteur of Shanghai, Chinese Academy of Science | **Dr. Bing Li lab**

Jul 2012   Undergraduate thesis: the role of microRNA population in modulating immune

response in human immune T cells

* This study earned ECUST Outstanding Undergraduate Thesis Award

Jun 2010-   The State Key Laboratory of Microbial Metabolism, Shanghai Jiaotong

Nov 2010   University, Shanghai, China | **Dr. Hongyu Ou lab**

Independent study: sequencing and annotation of important naturally integrative

plasmids in clinical *Pseudomonas aeruginosa*

Aug 2009-   The State Key Laboratory of Bioreactor Engineering, East China University of

May 2010   Science and Technology, Shanghai, China | **Dr. Huizhan Zhang lab**

Independent study: identification of essential biosynthetic genes of antibiotic

Lincomycin

Jan 2009-   The State Key Laboratory of Bioreactor Engineering, East China University of

Jun 2009   Science and Technology, Shanghai, China | **Dr. Aiyou Sun lab**

Independent study: Cloning, expression and purification of Alkaline

phosphomonoesterase in *Escherichia coli*

*This research was supported by ECUST Undergraduate Research Program for

Outstanding Freshmen

PUBLICATIONS

Y. Li and E. M. Maine (2018) The balance of poly(U) polymerase activity ensures germline identity, survival, and development in *Caenorhabditis elegans.* Development. (in revision)

Guo, Y., B. Yang, **Y. Li**, X. Xu and E. M. Maine (2015) Enrichment of H3K9me2 on unsynapsed chromatin in *Caenorhabditis elegans* does not target de novo sites. G3 5(9): 1865-1878.

PRESENTATIONS AND CONFERENCES

<u>Y. Li</u> and E. M. Maine (2018). The balance of poly(U) polymerase activity ensures germline identity, survival, and development in *Caenorhabditis elegans,* Upstate New York *C. elegans* Meeting, NY | **Talk**

<u>Y. Li</u>, M. Snyder and E. M. Maine (2017). Investigating the role of poly(U) polymerases in germline development, 21th International *C. elegans* Meeting, LA | **Poster**

<u>Y. Li</u>, M. Snyder and E. M. Maine (2017). Investigating the role of poly(U) polymerases in germline development, Upstate New York *C. elegans* Meeting, NY | **Poster**

<u>Y. Li</u>, M. Snyder and E. M. Maine (2016). PUP-1/CDE-1 and PUP-2 poly(U) polymerases function redundantly in germline development in *C. elegans,* The Allied Genetics Conference (TAGC), FL | **Poster**

Y. Li, M. Snyder and E. M. Maine (2016). PUP-1/CDE-1 and PUP-2 poly(U) polymerases function redundantly in germline development in *C. elegans,* Upstate New York *C. elegans* Meeting, NY | **Poster**

Y. Li, M. Snyder and E. M. Maine (2015). PUP-1 and PUP-2: two redundant poly(U) polymerases regulating *C. elegans* germline development, 20th International *C. elegans* Meeting, LA | **Poster**

Y. Li, M. Snyder and E. M. Maine (2015). PUP-1 and PUP-2: two redundant poly(U) polymerases regulating *C. elegans* germline development, Upstate New York *C. elegans* Meeting, NY | **Poster**

AWARDS, GRANTS AND FUNDING

2017	Outstanding Teaching Assistant Award, Syracuse University
2016	Travel Grant, Syracuse University Department of Biology
	Travel Grant, Syracuse University Graduate Student Association
2015	Travel Grant, Syracuse University Department of Biology
2012 - present	Syracuse University Graduate Fellowship, Syracuse University, Syracuse, NY, USA (tuition)
2011	Scholarship for Excellent Academic Performance, East China University of Science and Technology, Shanghai, China
2010	Scholarship for Excellent Academic Performance, East China University of Science and Technology, Shanghai, China

SCIENCE OUTREACH

2017   Syracuse Biology Westcott Community Outreach, Syracuse, NY

- Collaborated with local community center to introduce basic science to kids in after-school program

2014   Early College High School Biology Apprentice Program, Syracuse University, Syracuse, NY

- Helped local high school students explore principles of developmental biology and assisted them with hands-on activities

2011   Volunteer, Asian Congress on Biotechnology (ACB-2011)

- Assisted conference organization

TEACHING AND MENTORING EXPERIENCE

Molecular Biotechnology Lab (2 semesters) | Teaching Assistant

Applied Biotechnology Lab (2 semesters) | Teaching Assistant

Integrative Biology Lab (2 semesters) | Teaching Assistant

Cell Biology Course (2 semesters) | Teaching Assistant

General Biology Lab (1 semester) | Teaching Assistant

Mentored undergraduate students (5 students) | Dr. Eleanor Maine lab

Mentored an undergraduate student | Dr. Sandra Hewett lab